

Dissipation and Reinforcement in Rubber
Nanocomposites
Dissertation

*zur Erlangung des Doktorgrades der Naturwissenschaften
(Dr. rer. nat.)*

der

Naturwissenschaftlichen Fakultät II
Chemie, Physik und Mathematik

der

Martin Luther Universität
Halle-Wittenberg

vorgelegt von

Sriharish Malebennur Nagaraja, M.Sc.
geboren am 06. September 1985 in Harihar, Indien.

Erstgutachter: Prof. Dr. Mario Beiner (MLU Halle-Wittenberg)

Zweitgutachter: Prof. Dr. Kay Saalwächter (MLU Halle-Wittenberg)

Drittgutachter: Prof. Dr. James Busfield (QMUL London)

Tag der öffentlichen Verteidigung: 12.11.2021

Contents

1	Introduction	1
2	Scientific background	3
2.1	Rubber compound for tire tread application	3
2.2	Reinforcement and dissipation in rubber composites	13
3	Working hypothesis and aim of the work	37
4	Materials and methods	39
4.1	Composite description and processing conditions	39
4.2	Experimental methods	45
5	Results	49
5.1	Modeling dissipation contributions in strain sweep	49
5.2	NR and NR/BR filled with carbon black	55
5.3	Influence of filler introduction method on the properties of NR/BR nanocomposites	70
5.4	BR-SBR diblock copolymer filled with silica	79
6	Discussion	83
6.1	Common origin of dissipation and reinforcement in rubber nanocomposites	83
6.2	Factors influencing reinforcement and dissipation	91
6.3	Consequences for a rational design of tire tread compounds	97
7	Conclusions	101

Bibliography	105
8 Appendix	121

Dedicated to my parents,
teachers and friends

1 Introduction

Since the accidental discovery of rubber vulcanization with sulfur in 1839 by Charles Goodyear, rubber usage is suitable for various applications.[1] The invention of the automobile in 1886 by Carl Benz [2] and the development of the first practical pneumatic tire by John Boyd Dunlop in 1890 [3] paved the way for the present days sophisticated mode of transportation. However, criticism is that this sector is having a negative impact on the environment. For instance, in the year 2010 in Europe, 33% of final energy consumption and 26% of greenhouse gas emissions are because of road transportation.[4, 5] To mitigate these negative impacts, government institutions and environmental organizations are introducing campaigns to reduce the tire's rolling resistance, which accounts for approximately 30% of fuel consumption.[6] In this regard, one of the approaches implemented in 2012 to motivate tire manufacturers and raw material producers in the EU is the tire label. [7, 8] To provide information and bring awareness among the consumers about the performance of the tire. The ambition is to produce tires with optimal dynamic properties to ensure safety on the road, improve the tire mileage, and reduce the rolling resistance.

The rubber nanocomposites used for manufacturing tires generally contain a large volume fraction of nano-sized particles to enhance the mechanical properties such as reinforcement, which leads to a parallel increase in dissipative property, as both of the phenomena are related with each other.[9–16] Although there are tremendous empirical developments over the last decades,[17] a collective understanding of enhanced mechanical properties is still missing. In

particular there is a serious lack of understanding about the molecular mechanisms causing the dissipation in rubber nanocomposites with complex internal structure used in tire treads. That is of major importance for the rolling resistance on the one side and the grip of the tire on the other side. Many research studies identify the two essential parameters filler-filler interaction and rubber filler interaction as the main reason.[18–21] However, information about the molecular origin is still lacking and a deeper understanding of the origin of reinforcement and dissipation would be a big step towards rational designing of tire composites.[22–27] To contribute to this goal was the central motivation for this PhD work, which is also very interesting from the viewpoint of fundamental research, since the topic is touching basic questions regarding the segmental dynamics of polymers,[28–31] constraints at interfaces or structure property relations in nanocomposites.[24, 32–37]

2 Scientific background

2.1 Rubber compound for tire tread application

Rubbers are one of the most versatile types of materials known for their resilient property. Usually, they can undergo large deformation under load and return almost to their original shape. This particular property facilitates them for special applications, like in the automotive tire. However, they possess low mechanical properties for such engineering applications and are often compounded with a large fraction of nanosized fillers and additives, for instance, to enhance the stiffness. The general term for the mixture of rubber, fillers, and additives is rubber composite, and the application requirements drive the designing of a composite compound. In this section the approaches towards meeting the functional requirements of the tire tread component are reviewed from rubber compound design perspective.

Requirements for tire tread compounds. A tire is the interface part between the vehicle and the road. In an operational mode of a vehicle, a tire's tread component undergoes dynamic deformations at different frequencies due to repeated rotational and braking forces. A tire's essential requirement is to carry the vehicle's load, roll forward by overcoming the retardation forces, and simultaneously maintain sufficient grip with the road.[38] Overcoming the retardation forces is related to the adhesion mechanism between the tread and road surface and is an energy-intensive process. In this respect, the stiffness of the tread compound is beneficial. On the other hand, the contrary requirement from the same tire compound is appropriate dissipative property to have sufficient

grip and ensure safety. Rolling resistance and wet grip are the two parameters quantifying the loss of mechanical energy. Former is associated with the heat production as a tire rolls a unit distance and the latter is attributed to dissipation due to deformation-induced on the tire tread's surface under braking conditions by the road surface roughness. [39–43] Generally, on a laboratory scale both the functional requirements are estimated in the frequency range of 10 to 100 Hz for rolling resistance and in the range of ≈ 1 kHz to 1 MHz for wet grip.[12, 18, 22, 44–46] Vehicle manufacturers and the regulatory bodies have expectations to reduce the rolling resistance of a tire, improve its wet grip rating, without compromising the abrasion resistance. To achieve such contrary expectations in different frequency ranges for a single tire tread compound is complicated and generally represented by a Magic triangle, as shown in the figure 2.1. [7, 42, 47–49]

This multi-parameter optimization approach involves a compromise, a fundamental task to design the rubber compound is finding most appropriate combinations of rubber and filler systems, as they are the main components of rubber composites. In this regard, continuous research to solve the complex problem has been directed toward innovative material development concepts. In the following sub-sections, recent developments are briefly summarized for rubbers and fillers.

Optimization approaches based on rubber. Traditionally in the tire tread, NR based composite is used due to its intrinsic self-reinforcement as the 100 % cis configuration of linear polyisoprene chains favor strain-induced crystallization.[50] Post first world war the usage of synthetic rubber such as cis-1,4 polybutadiene rubber (BR), Styrene-butadiene rubber (SBR) either as a single matrix or in combination by blending technique is continuing as it provides several advantages over NR. Commonly the truck's tire tread consist of NR and BR, whereas the car's tire tread is composed of SBR and BR.[51, 52] Categorically the choice

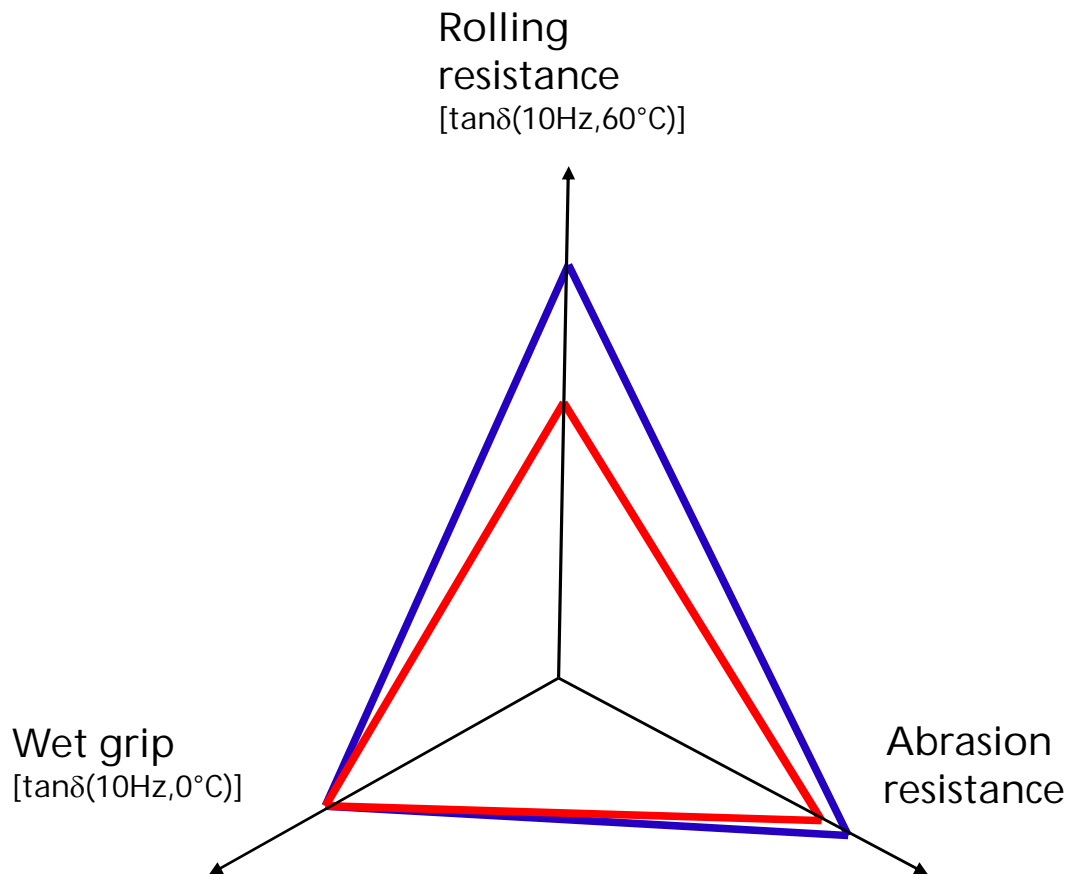


FIGURE 2.1

The three vital functional requirements of the tire tread are rolling resistance, wet grip, and abrasion resistance. The optimization approach is often a compromise, as represented by the Magic triangle. Since the involved frequencies are too high to be covered under isothermal conditions, the dynamic properties of the rubber compound are characterized at a given frequency, following the principle of time-temperature superposition equivalence. For instance, at a given frequency of 10 Hz, the rolling resistance is related to $\text{Tan}\delta$ at 60°C , and wet grip at 0°C . Understanding the microscopic origin to dissipation is crucial to optimize the properties, for instance, to achieve low rolling resistance without compromising the wet grip and abrasion resistance as represented in the red triangle in comparison with the blue triangle.

of rubber depends on the application conditions or depends on a single functional requirement. For instance, the rubber with lower dissipation value at the lower frequency regime (10 to 100 Hz) relevant in the rubbery plateau region far above the alpha relaxation process or glass transition temperature (T_g) is a preference to prepare the low rolling resistance tire tread compounds. For the case of wet grip, the expectation is contrary, higher dissipation is desired in the transition zone, as shown in the figure 2.2. [18, 22, 53]

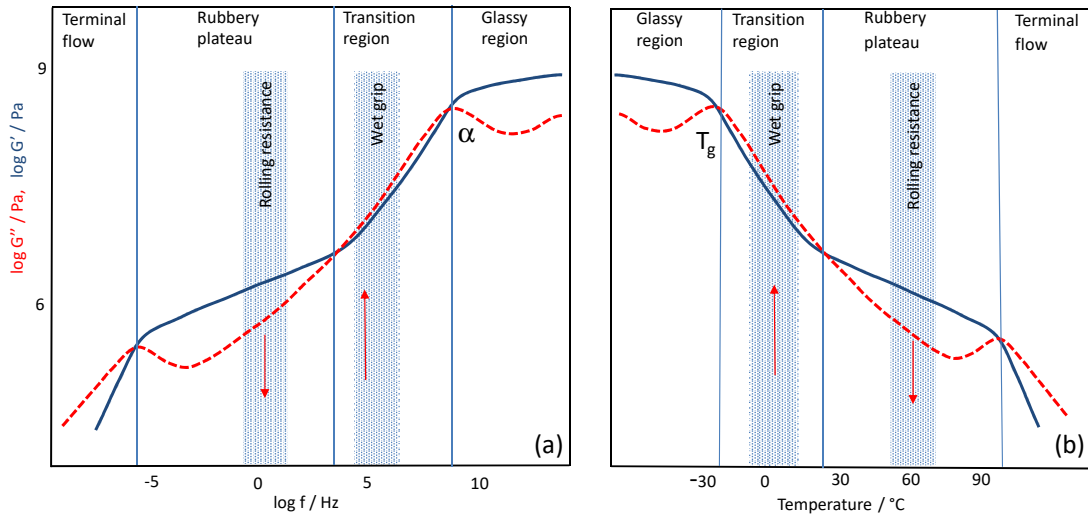


FIGURE 2.2

Schematic of dynamic shear storage modulus G' and loss modulus G'' for unfilled and uncrosslinked rubber as a function of frequency (a), the frequencies of interest are outside the limit of dynamic mechanical analysis, and the master curve construction is often complex due to the rheological complexity (particularly for filled composite). The most convenient and faster method of characterization is temperature-dependent measurement (b). The arrow shows the desired dissipation for rolling resistance and wet grip in the relevant frequencies and temperature regime.

So in this regard, generally glass transition temperature of the rubber from DSC or from relaxation spectrometers like DMA might be considered to predict the behavior of the rubber in the application relevant temperature range. However, the capability of this type of prediction is rather limited. Extensive work from Heinrich et al. focusing on wet grip rating for different kinds of rubber has clearly shown that as a rule of thumb, i.e., glassy transition temperature correlation to predict the functional requirements, is not always valid.[22, 54] For instance, T_g identified by DSC would not be appropriate, as shown in the figure 2.3. The suggestion is to consider average dissipation over the entire transition zone that would provide better correlation, as the relevant frequency range for wet grip is mostly dependent on the surface roughness of the road. The shape and width of the transition zone depend on the micro-structure and chemical composition of the rubber. In this regard, there are continuous developments related to the polymerization techniques with a special class of catalysts that facilitates to control the sequence and content of the microstructure

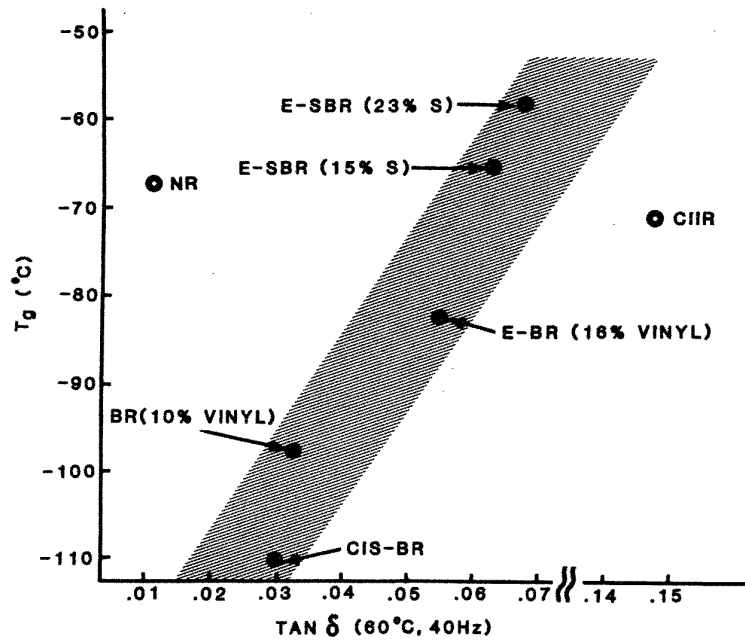


FIGURE 2.3

Glass transition temperature (T_g) and $\tan\delta$ for various vulcanized rubbers used in tired tread application, butadiene based rubbers fall in the characteristic trend that higher T_g is associated with higher $\tan\delta$, exception is the NR and CIIR, that do not fall in this trend. Figure taken from reference [51].

units of the rubber. For instance, anionic polymerization technique to produce solution SBR (S-SBR) has certain advantages to control the microstructure sequence and content over the free radical polymerization technique to produce emulsion SBR (E-SBR). Nevertheless, the choice of a single rubber does not meet the functional requirements, and a way forward to match the criterion described in figure 2.1 is by rational approaches. In the tire industry, the most popular technique is blending different kinds of rubbers in different proportions. A further aspect is to control or achieve the required morphology of the rubber matrix in composites as most of the rubber blends are immiscible, the mixing procedure could assist in tailoring the dissipation at different frequency regimes. [55] Although the blending approach is a step forward in the rational design of the rubber composites, the drawback is that their phase morphology could vary during and after the processing steps. [56] Such processing dependent changes in phase morphology are not advantageous as they can lead to

quality problems. An alternative approach to overcome the situations of the rubber blends and to achieve diverse viscoelasticity is by using block copolymers synthesized in a controlled manner to achieve specific phase morphology by varying the composition and microstructure sequence. Recent studies by Cecilia Aguiar da Silva et al. have shown the morphology of different BR-SBR block copolymers is robust and only weakly affected by the processing steps.[53]

Optimization approaches based on filler. Carbon black (CB) and silica are the most commonly used filler system to prepare rubber composites for tires. Their influence on the dynamic properties of rubber composites have been continuously investigated by many researchers.[13, 18, 47, 57–64] As shown in figure 2.4 with increase in carbon black and silica content the storage modulus G' in the rubbery plateau region is increased. Simultaneously, the loss modulus G'' is also increased, indicating that filler particles contributing to reinforcement also lead to an increase in dissipation. The situation is favorable to improve the wet grip but in contrary regarding the rolling resistance. The general consensus is that filler loading and their specifics such as surface area, size, structure, and surface activity are the parameters to consider while designing and predicting the properties of the rubber composites.[17, 18, 20, 46, 47, 65, 66] In this view, for the rational designing of the rubber compounds is to reduce the filler loading, that results in lower overall dissipation at higher temperatures above the glass transition, without compromising the mechanical properties.

The shape and structure of the filler particles as studied by electron microscopy techniques and scattering techniques specify that carbon-black particles are spheroidal in shape with typical dimensions of 10 to 90 nm, and their surface is paracrystalline.[67–69] They form aggregates with dimensions of 100 to 300 nm driven by electrostatic interactions.[70] Further during the production process they form tenuous secondary aggregates called agglomerates due to

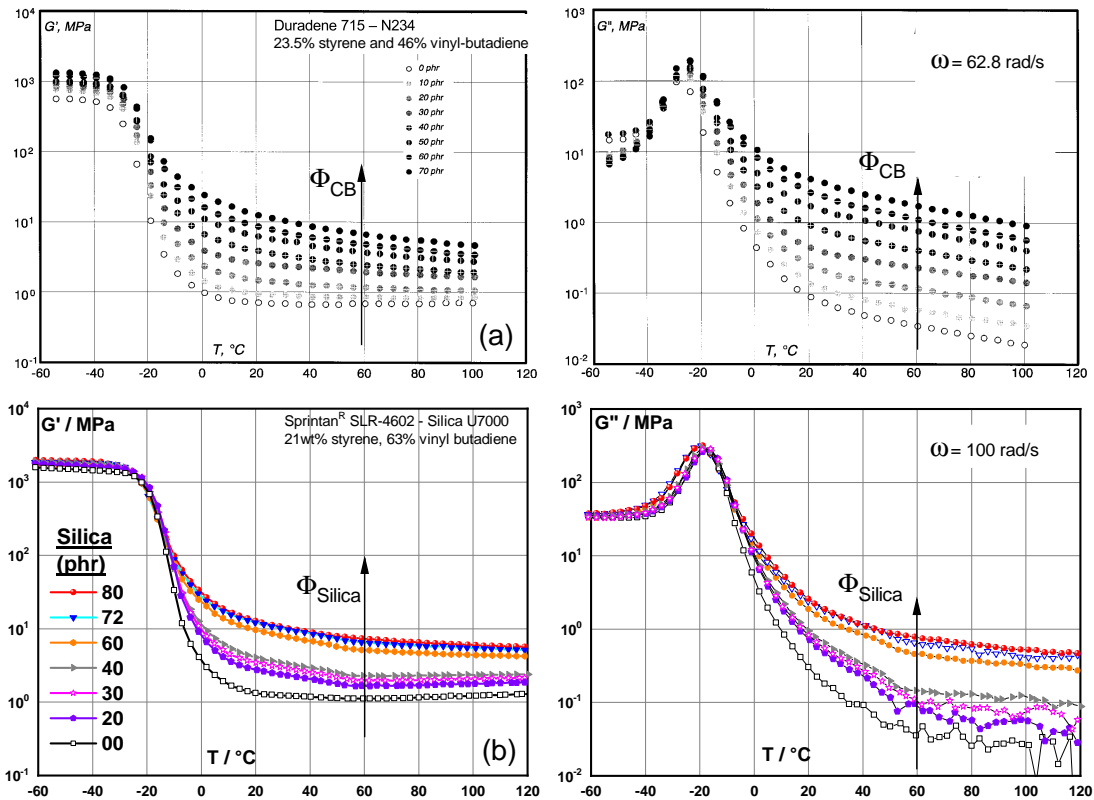


FIGURE 2.4

Temperature-dependent dynamic shear storage modulus (G') and loss modulus (G'') data for carbon black filled SSBR (a), and silica filled SSBR (b) show the dependence of dynamic properties with filler fraction. The SSBRs used in both studies have different styrene and vinyl butadiene content. However, their glassy transition temperature is almost comparable. Meanwhile, the measurement frequency is different. However, the position of glass transition is not changed due to either carbon black or silica particles for comparable silica and carbon black content. For instance, 80 Phr of filler loading at 60°C far above the glass transition temperature and relevant for rolling resistance, the G' values is almost the same for both composites, on the other hand, the G'' value is lesser for silica filled SSBR. Another interesting observation is the temperature dependence in higher filler content composites, both silica and carbon filled SSBR show decrease in G' and G'' with temperature. The dependence seems stronger for carbon black filled S-SBR. This comparison shows that multiple factors are overlapping and influencing the dynamic properties, and they depend on filler type and content and matrix composition. Figure (a) is adapted from reference [18].

Van der Waals's force of interaction.[71] Earlier studies by Medalia to characterize the structure of carbon black by the dibutyl phthalate (DBP) absorption and electron microscopy technique suggests that aggregates of carbon black are porous and anisotropic.[72, 73] Following the Medalia's work, Herd et al. based on TEM measurements described carbon black structure are self-similar objects at different length scale (fractal objects) and classified them into four

different shapes: Spheroidal, ellipsoidal, linear and branched. The scaling law, that relates an aggregate (figure 2.5) of size R to the number of particles N of size r by a mass fractal exponent F is given by $N = \alpha \left(\frac{R}{r}\right)^F$. [74, 75] Typically, F is in the range of 2.19 to 2.85 for various kinds of carbon black and α the front factor is ≈ 1 . [71]

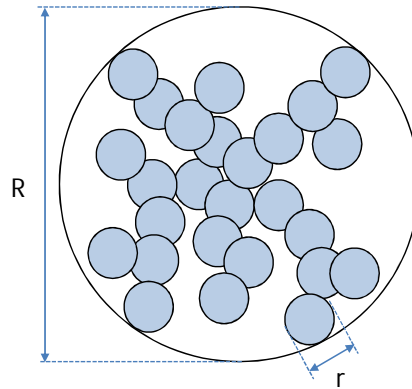


FIGURE 2.5

Schematic representing the effective filler aggregate as a spherical object.

Similar to carbon black, the manufacturing process influences the size of the silica particle. Generally, precipitated silica of dimensions 10 to 20 nm is the preferred choice in the tire manufacturing industry, and its structural hierarchy is almost similar to carbon-black particles. [15, 16, 76] Interest in silica usage, especially in tire tread compounds has largely grown after the green tire concept was introduced by tire manufacturer "Michelin". [77] In the present days, silica has almost replaced the carbon black in passenger tire tread compounds. Significant difference between silica and carbon black are the surface properties, which lead to different aggregation behavior of silica as compared to that of carbon black. The surface properties of both silica and carbon black were investigated by Wang and coworkers through the inverse gas chromatography technique, which described that surface energy of fillers γ_s constitutes of two components γ_s^d and γ_s^{sp} , where former is the dispersive component and latter is the polar component. The surface energy values would allow to understand the rubber filler interaction. [18, 78]

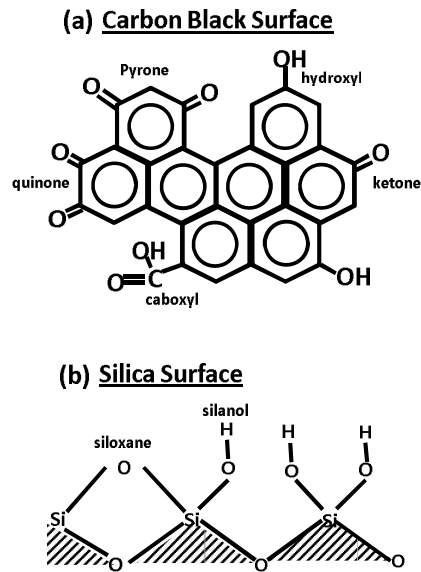


FIGURE 2.6

Schematic showing the chemical group on surface of carbon black (a) and Silica (b). Figure adapted from reference [46].

Carbon black shows a high dispersive component proportional to the accessible surface area evaluated by nitrogen or iodine absorption method. The dispersive component reported in the literature are in the range of 100 to 270 mJ/m^2 and the polar component is 120 to 60 mJ/m^2 at 150°C.[79] Whereas, commercial silica particles have a lower dispersive component in between 20 to 60 mJ/m^2 and higher polar component. [80, 81] Strong aggregation tendency and filler-filler interaction observed for silica particles is often attributed to its higher polar component. Heterogeneous surface of the carbon black consists of hydrocarbon molecules such as as carboxy, and carboxylic acid group etc., as shown in the figure 2.6, and they interact via Van der Waals force that is approximately 4 kJ/mol . [82] While silica has silanol and siloxane groups on its surface, they tend to form aggregates by strong hydrogen bond interaction forces that are approximately 20-40 kJ/mol . Apparently, the surface activity seems to define the filler-filler and filler rubber interaction. There is continuous development in this regard from methodological and materials science point of view, aimed to understand different parameters and their influence on the

dynamic properties.[21, 24, 25, 47] As most of the rubbers used in tire manufacturing are weakly or non-polar hydrocarbon rubbers, silane coupling and covering agents are used to facilitate the interaction of silica with rubber and reduce the filler-filler interaction. The most common type of coupling silane is TESPT, and the covering agent is OCTEO.[19, 20, 83, 84] Approaches towards modifying the rubber that interact better with filler particles are in progress. For instance, during S-SBR synthesis steps, functional groups like carboxyl, epoxide, hydroxyl, and alkoxy silane are attached to the rubber chains.[85–88] These attempts are basically to reduce the filler loading, as this factor along with surface area seems to directly influence the dissipative property of the compound.

Optimization approaches based on filler dispersion. Filler dispersion is another parameter that directly influences the dissipative properties of the compound. It is generally observed that poor dispersion leads to higher dissipation.[18, 89, 90] Few approaches have been developed to improve the dispersion of the filler particles by adapting different processing steps, like two-stage mixing process.[91, 92] In this method, a premixed filler particle in rubber or latex is used as masterbatch to incorporate filler in the rubber matrix.[93–95] Other methods, such as using intermeshing mixers or high-temperature mixing procedures, are used. However, there is concern about the material degradation etc.[96, 97] Recent developments are towards modifying the surface of filler during filler production. For instance, Cabot has proposed a technology to modify the surface properties of carbon black particles with silica to enhance filler dispersion.[12, 98]

The common basis for these approaches is not clear as several factors are overlapping, and there is no consensus on the question *how the filler particles influence the dynamic properties of rubber nanocomposite*, one of the reasons is lack of appropriate models describing the situation in general.

2.2 Reinforcement and dissipation in rubber composites

In the past few decades, substantial work has been focused on understanding the role of fillers and their specific properties on the performance of rubber compounds. Central aim of many studies was, in particular, to identify the reason behind the significant increase in storage modulus for compounds containing large filler fractions. Figure 2.7 highlights the general consensus about contributions to reinforcement in highly filled rubber composites.[64, 99] Although filler network is identified as the primary contribution to reinforcement, it has been impossible until today to understand the influencing factor determining its strength and to provide a clear picture on how to optimize its properties, as there are several overlapping factors at the microscopic level that are difficult to assess, isolate and quantify. Nevertheless, there are various models, and experimental approaches that discuss special aspects of reinforcement in the light of filler-filler interaction and rubber filler interaction. Conversely, models focusing on the origin of dissipation as well as experimental studies regarding the strain amplitude-dependent loss modulus are scarce although of particular importance, as understanding the mechanisms causing dissipation are of extraordinary importance for optimizing the properties of rubber composites for tire treads. The state of the art in modeling reinforcement and dissipation in rubber composites will be the focus of this section.

Hydrodynamic models describing reinforcement. In 1944, Smallwood adopted Einstein's hydrodynamic modeling of the viscosity of liquids containing suspended particles and provided a limiting law to describe the reinforcement in rubber nanocomposites being.[100, 101]

$$G' = G'_0(1 + 2.5\Phi) \quad (2.1)$$

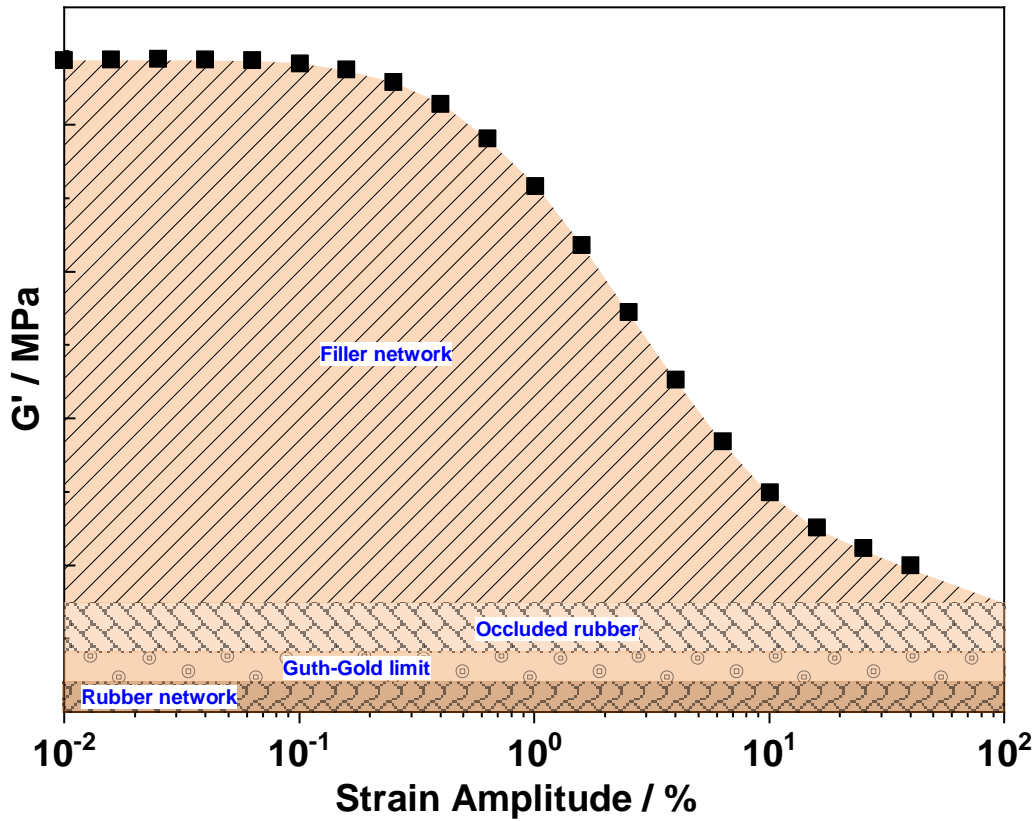


FIGURE 2.7

Schematic representation of the contributing factors to dynamic shear storage modulus of highly filled rubber composite. Through Payne effect, filler network contribution is distinguishable with other contributors that are dominant at large strain amplitudes.

where G'_0 is intrinsic modulus of the rubber and Φ is volume fraction of filler.

According to the equation 2.1, the filler particle dispersed in the rubber matrix would increase the storage modulus linearly with volume fraction of filler particles (Φ) due to hydrodynamic effects. The proposal is based on the assumption that filler particle is spherical, isolated, and is completely wetted by rubber matrix. Guth and Gold extended the Smallwood suggestion by an additional quadratic term and proposed equation 2.2 is made for the use at higher concentration of filler particles and hydrodynamic interaction between filler particles. [63, 102]

$$G' = G'_0(1 + 2.5f\Phi + 14.1f\Phi^2) \quad (2.2)$$

Further, they introduced an additional shape factor ' f ' (aspect ratio) for cases where the filler particles are not spherical, but anisotropic.

However, the prediction for G' from equation 2.2 would be much lower than the experimental data for highly filled rubber composites containing huge amounts of nanofillers. Considering the porous structure of carbon black aggregates, Medalia speculated that fraction of rubber would be captured in the voids of the aggregates and when subjected to deformations, the occluded rubber is shielded from the shear field and acts as a filler rather than part of the rubber matrix.[73] He proposed to include the effective filler volume fraction (i.e. volume fraction of filler plus the volume fraction of occluded rubber that can be calculated according to his approach by DBP absorption experiments) in the Guth Gold equation according to 2.3.[72]

$$G' = G'_0(1 + 2.5\Phi_{eff} + 14.1\Phi_{eff}^2) \quad (2.3)$$

Later, the equation have been further modified by other researchers introducing changes in prefactor, higher order contributions etc. However all the sophisticated models to describe the hydrodynamic effects in rubber composites significantly underestimate the experimentally observed reinforcement or describe only composites containing a small volume fraction of filler. The mechanisms and models developed to explain the hydrodynamic contributions depending on the filler volume fraction neglect contributions of filler network, which dominate in highly filled rubber composites. [16, 59, 103–106]

Payne effect and Kraus model. Rubber composites designed for tire tread applications, generally contain a significantly large fraction of filler particles. Such a large fraction of filler leads to the formation of a so called filler network, which

modifies the dynamic properties of the rubber composites strongly. Main feature is the non-linear dependence of the storage modulus with strain amplitude as shown in figure 2.8. Following the pioneering work by Payne, the phenomenon is famously known as the Payne effect. [9, 57, 65] He studied strain amplitude dependence of the shear modulus from dynamic measurements on different rubber nanocomposites containing varied fractions of carbon black with different surface area. The storage and loss modulus for unfilled and low filled composites showed no dependence on strain amplitude. Whereas, the composites containing a large fraction of carbon black showed a significantly different behavior. A sigmoidal decrease in storage modulus is observed as the strain amplitudes increase from small to large deformation accompanied by a peak in loss modulus at the intermediate strain amplitude. By connecting these phenomena with a filler network breakdown, Payne inferred that in highly filled rubber composites, filler aggregates are sufficiently close to each other, such that due to Van der Waals's force, the aggregates interact among themselves and form a percolating solid structure called the filler network. Similar phenomena are found in non-rubber composites such as liquid paraffin, decane, and carbon black. The magnitude of the Payne effect in storage modulus has been attributed to the filler network contribution to the reinforcement and the peak in loss modulus as energy dissipation due to continuously breaking and reforming contacts between the filler particles.

Payne proposed that

$$G_m'' = a + b(G_0' - G_\infty') \quad (2.4)$$

with G_0' being the storage modulus at small strain amplitude, G_∞' at large strain amplitude and G_m'' is the maximum in the loss modulus as seen in figure 2.8.

To further support the proposal, Payne performed time-dependent mixing

studies and observed that, with increase in mixing time the Payne effect reduced and its amplitude attained consistent for optimally dispersed compounds. In general, the Payne effect starts to appear if the filler fraction exceeds a certain filler-dependent volume fraction called percolation threshold Φ_C related to the occurrence of the first cluster of infinite size in macroscopic samples.[107]

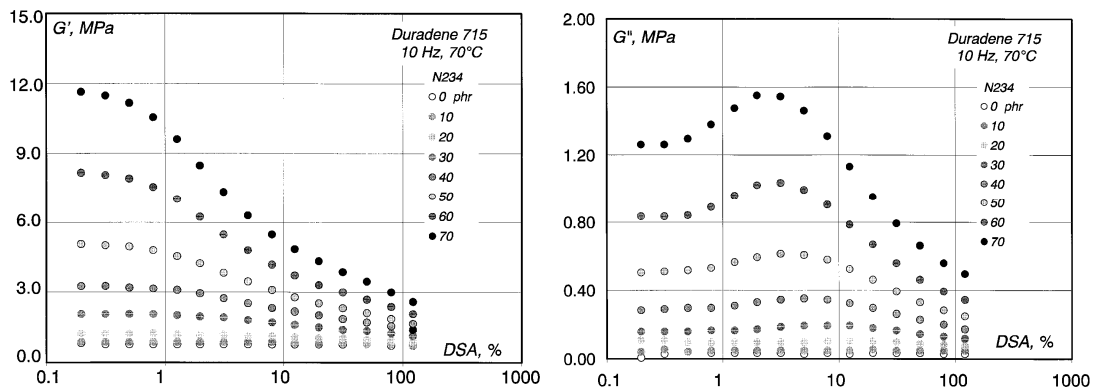


FIGURE 2.8

The storage modulus G' (a) and loss modulus G'' (b), dependence with strain amplitude and filler content. The unfilled rubber is not showing strain amplitude dependence. Likewise, the composites containing a small fraction of filler and the modulus increment would be due to hydrodynamic effects. For composites containing high loading of filler sigmoidal decrease in storage modulus and a peak in loss modulus is observed, strain amplitude dependence is known as the Payne effect. Figure adapted from reference [18]

Where, G'_0 the storage modulus at small strain amplitude, G'_∞ at large strain amplitude and G''_m identifies the peak in loss modulus in the figure 2.8.

The most frequently used approach to approximate the Payne effect is from Kraus.[108] The Kraus model is an attempt to quantify Payne's suggestion that Van der Waals interaction between the filler particles as a source of energy storage in the filler network. The model considers, soft spheres, as filler particles positioned to each other in equilibrium such that a small displacement from their positions results in interacting forces (repulsive and attraction) similar to the Lennard-Jones potential. Further, to describe the strain amplitude dependence of dynamic properties, the mechanism of deagglomeration and agglomeration is considered. The rate constants of these phenomena are related

to potential change due to the soft sphere's displacement from their equilibrium position and, consequently, softening of the filler network is projected. The detailed derivation given below establishes a relation between the strain amplitude dependence of G'_γ and G''_γ and the number of effective contacts between the filler particles.

Basic assumption is that the rate of filler contact breakage (deagglomeration) R_b is proportional to strain amplitude γ_0 and the number of surviving contacts N according to

$$R_b = k_b \gamma_0^m N, \quad (2.5)$$

where k_b is rate constant of deagglomeration, m is an exponent that describes the amplitude dependence.

On the other hand rate of filler contact formation (reagglomeration) R_m is proportional to the broken number of contacts $N_0 - N$ and strain amplitude powered by negative m , i.e.

$$R_m = k_m \gamma_0^{-m} (N_0 - N) \quad (2.6)$$

It is further postulated that at equilibrium both the rate of filler contact breakage and formation are equal ($R_b = R_m$). At the critical strain amplitude $\gamma_c = (k_m/k_b)^{2m}$ the number of surviving contacts is then given by

$$N = \frac{k_m \gamma_0^{-m} N_0}{k_b \gamma_0^m + k_m \gamma_0^{-m}} = \frac{N_0}{1 + \left(\frac{\gamma_0}{\gamma_c}\right)^{2m}}. \quad (2.7)$$

Further, by relating the excess modulus, i.e. the contributions from the filler

network, at any given strain amplitude to the number of existing contacts between the filler particles. The equation 2.7 can be written in terms of the storage modulus as.

$$G'(\gamma_0) = \frac{G'_0 - G'_\infty}{1 + \left(\frac{\gamma_0}{\gamma_c}\right)^{2m}} - G'_\infty \quad (2.8)$$

For dissipation, Kraus has accounted for excess frictional forces between the particles or between the particles and rubber matrix as contacts are broken. By considering the basis for equation and the point made by Medalia, the filler contact breakdown and reformation occur at all strain amplitudes during a deformation cycle.[58] If the steady-state population of elastically effective contacts is small, then the rate of reformation and breaking of such contacts may be large, i.e., deagglomeration and reagglomeration process are deemed to dissipate energy in addition to the energy dissipated by straining the rubber. Then the excess loss modulus is assumed to be proportional to the rate of deagglomeration process, giving the equation.

$$G''(\gamma_0) - G''_\infty = ck_b \gamma_0^m N \quad (2.9)$$

Where c is a constant of proportionality, substituting for N from equation 2.7 and approximating $G'(\gamma_0) - G'_\infty \propto N_0$.

$$G''(\gamma_0) - G''_\infty = \frac{C\gamma_0^m(G'(\gamma_0) - G'_\infty)}{1 + \left(\frac{\gamma_0}{\gamma_c}\right)^{2m}} \quad (2.10)$$

The function 2.10 has a maximum value G''_m when $\gamma_0 = \gamma_c$. So,

$$G''_m = G''_\infty + \frac{C\gamma_c^m(G'(\gamma_0) - G'_\infty)}{1 + \left(\frac{\gamma_c}{\gamma_c}\right)^{2m}} \quad (2.11)$$

Which gives constant C,

$$C = 2 \frac{(G_m'' - G_\infty'')}{(G'(\gamma_0) - G_\infty') \gamma_c^m} \quad (2.12)$$

Substitution of C in equation 2.11 gives

$$\frac{G''(\gamma_0) - G_\infty''}{G_m'' - G_\infty''} = \frac{2 \left(\frac{\gamma_0}{\gamma_c}\right)^m}{1 + \left(\frac{\gamma_0}{\gamma_c}\right)^{2m}} \quad (2.13)$$

By Validating the Payne data by above equation 2.8 and 2.13 for storage and loss modulus respectively. Kraus suggests that the parameters m , γ_c , and the ratio of rate constants are independent of rubber, filler type, and extent of dispersion.

Payne demonstrated that at constant carbon black loading and optimal mixing time, the modulus at small strain amplitude and the Payne effect magnitude increases with a surface area of the carbon black. [9] This seems reasonable through Kraus equation, as the number of contacts would also depend on a surface area of the filler particles. Payne also suggested that adhesion between the rubber and filler could be one of the contributors to reinforcement. However, its consideration in Kraus attempt to describe the dynamic properties is unclear as the nature of contacts between the filler particles or between the rubber filler is not specified and clear.

Kraus model is extensively used to approximate the experimental results as it gives a good description of the Payne effect, especially for storage modulus. The loss modulus is more seldomly considered and the equation for loss modulus fails to approximate the dissipation at a small strain amplitude. Ulmer assessed the Kraus equations with different rubber nanocomposites and highlighted the poor fitting competence of the equation 2.13 and proposed

different modifications with an additional component to hold the Kraus approach of the deagglomeration and agglomeration process of filler contacts. [109] These attempt were, however, unsuccessful as the fitting parameters (m and γ_c) deviate largely with fitting parameters of storage modulus. Finally, Ulmer suggested to use the equation 2.14.[110]

$$G''(\gamma_0) - G''_\infty = \frac{2\left(\frac{\gamma_0}{\gamma_c}\right)^m (G''_m - G''_\infty)}{1 + \left(\frac{\gamma_0}{\gamma_c}\right)^{2m}} + \Delta G''_2 e\left(\frac{-\gamma}{\gamma_2}\right) \quad (2.14)$$

With an empirical extra-term $\Delta G''_2$ decaying exponentially with a different critical strain γ_2 that is not associated with the filler network but related to the used rubber type. The model proposed by Kraus is phenomenological and is formulated with two empirical parameters γ_c and m . The exponent m is found to be independent of temperature, frequency, filler type, and content for ($\Phi > \Phi_C$), i.e., it is determined to be approximately 0.6 for various rubber composites by many authors. Even γ_c is often found to be a constant and depends basically on the investigated rubber composite.[13, 110–112]

Although the Kraus model provides qualitative correlations to Payne's discussion for strain amplitude dependence of storage modulus, the drawback of this model is that it fails to explain the temperature dependence of small strain amplitude modulus G'_0 . Kraus disregarded the Payne speculations that adhesion between the filler and rubber as one of the contributor reinforcement. Nevertheless, the Kraus approach strongly convinced that increasing the filler fraction above the percolation threshold leads to an increase in reinforcement at small strain amplitudes and dissipation at the intermediate strain amplitudes.

More recent approaches to model reinforcement and dissipation. Huber and Vilgis [113] have attempted to describe the Payne effect by considering the fractal feature of carbon-black aggregates, which scale up with connectivity exponent C to form a filler network for loading above the percolation threshold. In this

regard, the Zener model is used to evaluate the excess energy stored by the filler network at a small strain amplitude, and an exponent C to capture the amplitude dependence of stored energy above 1% deformation. The value of exponent estimated through the model is approximately 1.625, allowing them to connect the strain amplitude dependence exponent and fractal network connectivity exponent C . Following this proposal, the Payne effect's description is that the filler network extent reduces by disintegrating into smaller entities for strain amplitude above 1% deformation, and consideration for large strain amplitude is that the rubber matrix supports the deformation. The approach is similar to the Kraus equation for storage modulus, shape fitting parameter m in the equation is interpreted as a geometric parameter that tells about the filler networks fractal nature through connectivity exponent C . As the value of m is universal in different kinds of rubber composite systems, the conclusion is that the filler network structure is basically independent on the specific filler type.

The filler particles fractal nature is also considered in Heinrich and Klüppel's [13, 71, 114] attempt to understand the filler network formation through the kinetic cluster-cluster aggregation (CCA) model. It is proposed that filler particles embedded in the rubber matrix after the optimal mixing period flocculate from their mean position to form clusters termed as primary structures, for filler loading below the percolation threshold Φ_C , i.e., assigned as gel point in this model, the primary structures are well separated, represented by the shaded circles in figure 2.9a. In this situation, the applied deformations are considered to be carried by the rubber matrix surrounding the clusters. Further, for filler loading above the percolation threshold ($\Phi > \Phi_C$), the flocculated clusters form a tenuous infinite cluster called the filler network, as shown in figure 2.9b, due to space-filling conditions that hinder the earlier situation driven by diffusion. By approximating several experimental results, the

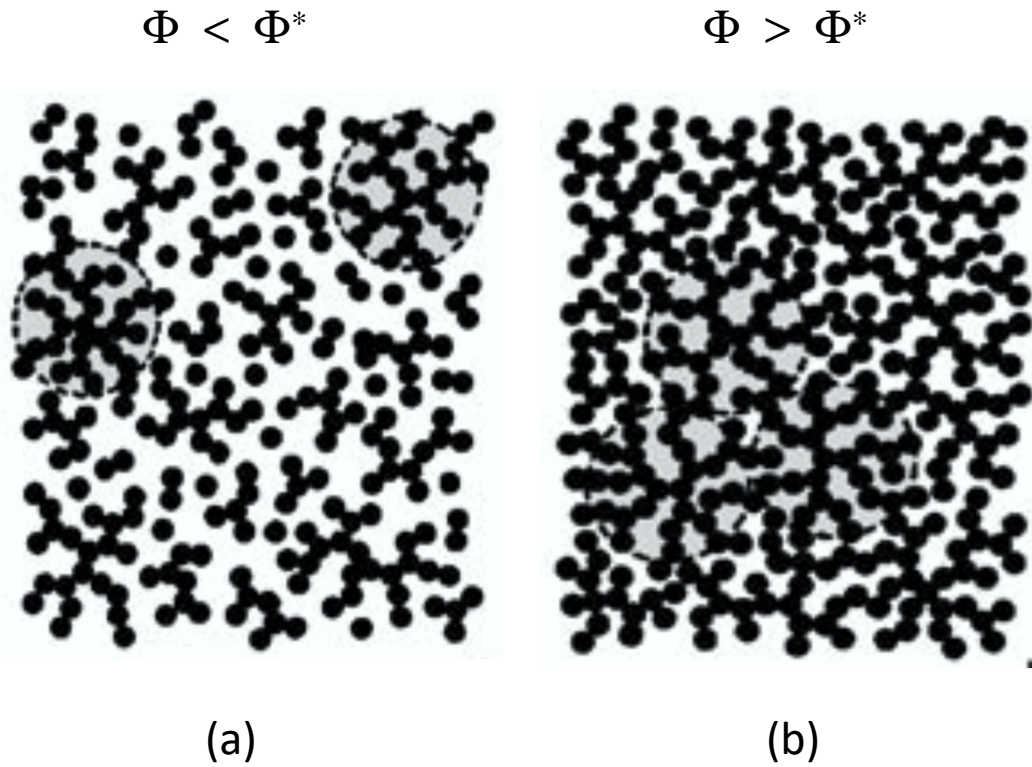


FIGURE 2.9

The shaded circles in figure (a) and (b) indicate cluster formed due to flocculation process, for filler loading above the gel point Φ^* the clusters are connected to each other forming filler network (b). Figure taken with permission from reference [[13]. Copyright (2002) Springer.

trend in storage modulus increment at small strain amplitudes for filler fraction above the percolation threshold is suggested to be universal, as the model predicts ($G'_0 \approx \Phi^{3.5}$). Through this observation, the proposal is that clusters connectivity path defines the modulus, and the values can be estimated based on the elastically stored energy at the connecting points between the clusters. The approach further specifies that the Payne effect is the consequence of the dislocation of clusters from the network configuration and predicts that

$$G'(\gamma_0) = G'_\infty + (G'_0 - G'_\infty) \left[1 + \left(\frac{\gamma_0}{\gamma_c} \right)^{2m} \right]^{-\tau}, \quad (2.15)$$

where γ_c is the critical strain amplitude that defines the stability of the filler network against cyclic deformations. It is discussed that γ_c is probably related

to rubber filler interaction and τ is constant $\cong 3.6$ for various rubber composites.

In the equation 2.15, the strain amplitude dependence is similar to that of the Kraus approach, and the only difference is an exponent that signifies the fractal feature of the filler network. The excess energy stored ($G'_0 - G'_\infty$) is related in this approach to the filler-filler bonds that lead to the formation of a filler network formed due to flocculation. The parameter γ_c , is associated with the stability of the filler network by considering the dynamics of flocculation that depend for e.g. on the molecular weight and vulcanization temperature. The proposal is that filler-filler bond formation is by squeezing out the bound rubber (i.e., a fraction of rubber not extractable from unvulcanized rubber compound by a suitable solvent of the matrix). The filler-filler contact strength supposedly depends on gap size and is considered to be high for composites containing high molecular weight matrix, and fillers with small particle size, that interact weakly among themselves, but strongly with the rubber matrix. Further, the fraction of the rubber confined at the contact point is claimed to be immobilized rubber, which is in the glassy state. To validate the hypothesis, the activation energy obtained from the vertical shift factors used for frequency-dependent measurement to construct a smooth storage modulus master curve at a low-frequency regime is related to the stiffness of the intact cluster-cluster contact, and the same obtained from loss modulus shifting is related to damaged soft cluster-cluster contacts. [36, 115] This idea is developed referring also to Vieweg's work and related studies,[34, 116, 117] that showed earlier that the glassy bridges undergo sequential softening several 10K above the rubber matrix glass transition temperature. The fundamental proposal from Heinrich and Klüppel work is that in the regime of lower frequencies or higher temperature above the alpha relaxation, the filler-filler bonds formed due to flocculation disappear to a state similar to the dislocation

of filler network at large strain amplitudes. Consequently, it is expected that the rubber compound at this state shows rubber elasticity phenomena, which are common for unfilled or low filled rubbers.

The flocculation phenomenon is considered by many researchers to describe the formation of filler network.[61, 118–121] A famous work in this line is from Meng-Jiao Wang.[18, 79, 81, 122] Measuring various rubber composites containing conventional carbon black grades, graphitized carbon black, surface modified, and non-modified silica by the dynamic mechanical analysis. He highlighted that filler network formation is related to filler-filler and rubber-filler interactions from thermodynamic and kinetic points of view. The interpretation is supported by inverse gas chromatography results that provide information about filler surface activity and bound rubber measurement results that tell about the rubber filler interactions. Through these studies, the recognition is that the Payne effect is due to multiple overlapping mechanisms that depend on the molecular weight of the rubber matrix before vulcanisation and its interaction with the filler. Further, to describe the mechanism, rubber shell and joint shell model is proposed. In the rubber shell model, the bound rubber fraction around the filler is shown and is related to the rubber filler interaction parameter. The joint shell model represents the filler particles with rubber shell are connected to form a filler network due to the flocculation process (figure 2.10). The presumption is that during the flocculation process, a fraction of rubber gets trapped in the filler network and eventually acts as a filler by losing its identity, and thus leading to increased storage and loss modulus at small strain amplitude regime due to hydrodynamic effects. The Payne effect is associated with the disruption of joint shells in the filler network. The amplification of storage modulus and loss modulus at small strain amplitude is related to the hydrodynamic effects, a sigmoidal decrease of the former is related to the release of the trapped rubber, and the peak in loss modulus is

related to internal friction caused by the deagglomeration and agglomeration of joint shells in the filler network as described by Kraus.[108] Within the joint shell model for the temperature dependence of the Payne effect, the discussion is that at a temperature well above the rubber glass transition temperature, the modulus of the rubber in the junction of the joint shell is equivalent to the bulk rubber modulus, that the filler network is less rigid leading to reduced contribution to absolute modulus values.

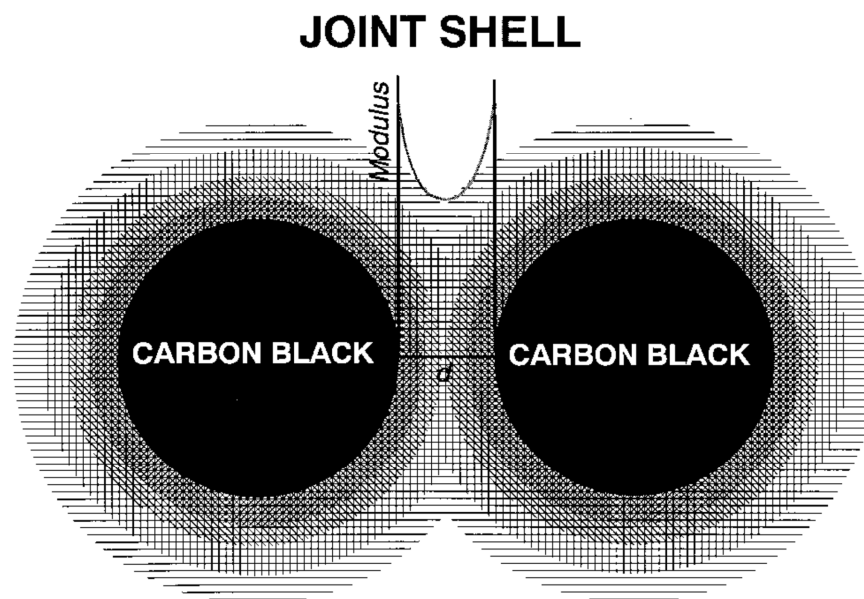


FIGURE 2.10

The joint shell model by Wang, The schematic describes the change in modulus away from the filler surface and the modulus at the center of the joint shell is smaller is less, indicating that the filler network is soft due to joint shell. Figure taken from reference [18]

The junction gap in the joint shell model, i.e., distance between the filler aggregates, denoted by δ in Figure 2.10, is deduced by considering the random spatial arrangement. The argument is that δ value depends on the filler content, and it would reach a minimum or critical value for filler loading equivalent to loading at which the small strain amplitude modulus deviates from the Guth-Gold approximation. As the δ value is related to filler size

or surface area but not to its structure in highly filled rubber composites, this study proposes to hinder the formation of filler network in order to reduce dissipation at higher temperatures or lower frequency. Some of the ideas proposed to inhibit the flocculation process based on thermodynamic, and kinetic (processing) approaches are as follows,

Thermodynamic approaches:

- Reduce the differences in surface characteristics, especially in surface energy, between rubber and filler by filler surface modification and rubber modification.
- Increase filler-rubber interaction and compatibility by filler surface modification, rubber modification, by chemical or physical coupling agents.

Kinetic approaches:

- Improve the initial filler dispersion in the compound.
- Increase the mean surface-to-surface distance between aggregates by changing filler morphology.
- Increase bound rubber to increase the effective aggregate size and the viscosity of the rubber matrix.

Although the Payne effect is generally seen as a consequence of filler networking, there are various ideas about filler networking. Depending on the approach it is related to filler-filler interactions or rubber-filler interaction or both.[123, 124] It remains challenging to identify the microscopic origins related to nano-sized fillers since neither filler-filler interaction nor filler rubber interaction can be neglected. Some authors have explicitly claimed that the primary mechanism of the Payne effect is not the filler-filler interaction or percolation but, instead due to rubber filler interactions. [125–130] Sterstein and Zhu [125] propose that the primary mechanism of the Payne effect is not the

filler-filler interaction or percolation, but it is due to rubber filler interaction by observing the Payne effect in composites containing a small fraction of filler particles. Reinforcement in this case is related to trapped rubber chains in the vicinity of filler surfaces that are physically entangled and show near field restriction on the bulk rubber as they are not behaving like a Gaussian chain. Further, reduction in reinforcement due to disentanglement of the trapped chains from the filler surface under applied strain amplitudes and loss of energy during the process is suggested to be influencing the dissipative property of the composites.

A famous approach that also considers the rubber attachment on the filler surface due to adsorption and detachment due to desorption is from Maier and Göritz.[127] This model assumes that rubbers chains on the filler surface have a probability to form stable and unstable contact points. In accordance with the model the detachment of rubber chains from unstable contact points under deformation results in reduced reinforcement seen as the Payne effect.

A similar kind of approach is the network junction model by Ouyang [129] developed on the suggestions made by Wang et al.[18, 79, 81, 122] The junction rubber that connects the filler aggregates is considered to describe the dissipation. It is hypothesized that inward and outward movement of rubber chains from the junction region due to applied deformations induce friction between the rubber chains that results in loss of energy through the Payne effect. The rubber filler interactions are mostly physical in nature, due to rubber chains physical adsorption on the filler surface. Exceptions are found when chemical interactions are induced, for instance, in silica-filled rubber composites in which silane is used as a coupling agent. The adsorption should then depend on the surface activity of the fillers. The fraction of rubber is assumed to have restricted mobility and is in this case generally termed as bound rubber.

Unfortunately, there is much confusion in the literature about the terminology as a uniform definition is lacking. The quantification of the bound rubber is often done by solvent extraction method,[131] which is no measure for the mobility restriction. This is one of the severe misunderstandings while correlating the bound rubber content with mechanical properties.[20, 132]

Dannenber [\[133\]](#) has shown that multiple factors influence the volume of bound rubber formation like filler specifics(surface activity, particle size, and structure), rubber specifics (chemical composition), additives used in the compound formulation, and processing conditions like temperature, time, equipment, and also the extent of dispersion. With the lack of correlations with the mechanical properties, he raised a dilemma, whether the filler network and bound rubber actually exist in vulcanizate or whether it is merely a test method dependent on known reinforcement factors! An additional question raised from this work are whether bound rubber is indicative or operative? By invoking this dilemma, Litvinov et al. [\[132\]](#) has studied the EPDM compound containing carbon-black particles through 1H NMR to answer the rubber chain molecular mobility questions in filler's vicinity. By analyzing the T_2 relaxation experiments, bound rubber is distinguished into two rubber fractions with different chain mobility. Immobilized rubber and the loosely bound rubber, the former fraction is substantially smaller compared to the latter, and its formation is due to the strong physical adsorption on the filler's surface. The role of immobilized rubber is to act as a junction between the filler surface and loosely bound rubber that interconnects the carbon-black particles and glues them to the rubber matrix. At small deformations regime in strain amplitude measurement, the loosely bound rubber is speculated to distribute the applied strain. With higher strain amplitudes, the junction chains slipping from the filler surface is discussed as the source for dissipation,[\[134\]](#) and eventually

seen as reason for the reduction of the storage modulus observed as Payne effect. Although the heterogeneity in the mobility of different rubber fractions is mentioned, it is explicitly pointed out that immobilized rubber fraction is independent on temperature. The lack of temperature dependence is speculated to be due to adsorption, and desorption equilibrium as the surface energy of carbon- black particle is heterogeneous.[135] Further, the immobilized rubber fraction volume is assessed with filler surface area to provide information about the layer thickness, approximately being $1nm$. However, the possible discrepancies in the estimated thickness value are directed to questions about filler particles microdispersion.

The spatial arrangement of the filler particles in the rubber matrix at the microscopic scale is one of the most critical parameters that could influence the rubber composite mechanical properties, as they directly influence the surface available for rubber filler interaction.[90, 136–138]

Unfortunately, there is no standard technique to evaluate the microdispersion. Commonly used techniques are the TEM, USAXS, SANS.[37, 139–141] However, the data evaluation is complex, and no model or theory is available to quantify the complex situation completely. There are open questions about how to evaluate the data as well as methodical limitations. Especially in the case of TEM image analysis, the quality of the image and the extractable information depend very much on the preparation method.[140]

Baeza et al. [139, 142] have provided an approach to understanding the results from USAXS measurements. They have shown through a series of uncrosslinked SBR-Silica composites that type and concentration of the silane do influence the silica particle microdispersion. Conclusion is that the silane agents alter the aggregate size and interaggregate interactions. Further, the hypothesis is proven by studying model composites prepared by grafting small molecules of different lengths on the silica particle surface. Very recently,

Musino et al. has highlighted that small molecule additive, which are used in rubber compounding do also influence the microdispersion of silica particles.[143] This has been concluded from studies on SBR-Silica composites with silanes of different chain lengths together with Diphenylguanidine (DPG) and without DPG. The extent of silanization is quantified through bound rubber content. Note that this method is seen critical by other authors as there are much harder challenges due to chemistry involved in the silanization process and it is already known to fail for in carbon-black filled composites. There are competing results in the literature.[16, 20]

For instance, Ramier et al. [20, 144] in his early studies on SBR filled with silane treated silica particles correlations between bound rubber, Payne effect and filler dispersion evaluated by TEM and USAXS. The results show no significant influence of silane type and concentration on the dispersion of silica particles. Nevertheless, the Payne effect measurement results showed dependence on silane concentration. The Payne effect's magnitude decreased with an increase in the concentration of reactive silane up to specific coverage and then showed an inverse trend.

Another example comes from Litvinov et al. 1H NMR investigations on natural rubber filled with hydrophilic silica.[145] The fraction of immobilized rubber quantified based on mobility for the untreated silica-containing composite was relatively higher than that for silane treated silica-containing composites. Understanding the physical state of the immobilized rubber is crucial to distinguish it from the bound rubber. The terminology immobilized refers to a fraction of rubber that is strongly adsorbed on the surface and has a segmental dynamics that is significantly slowed down compared to that in the bulk fraction of the rubber a few nanometers away from the filler surface.[25, 26] The immobilized fraction certainly depends on the type of filler system, but its occurrence seems to be common although competing information is present

in the literature. A few representative studies are referred below. Vieweg et al. [146] has shown the existence of immobilized rubber in SBR filled with different hard polymeric filler particles with sizes ranging from 25 to 75 nm. The fraction of immobilized rubber is quantified based on reduced mobility as criterion using DSC measurements. Delta C_p values of composites containing different amounts of polymer fillers are evaluated. The thickness of immobilized rubber layers on filler surfaces is deduced to be in the range of 1.5 nm. Pissis and Klonas et al. [147, 148] observed similar values for different types of composites containing surface treated and untreated filler particles. It is shown through DSC measurements that the fraction of immobilized rubber is varying with filler fraction and its slow segmental dynamics is evaluated by dielectric spectroscopy. An increase of the relaxation times by 2 to 3 orders of magnitude in comparison to the bulk fraction is reported. The immobilized rubber on the filler particle surface is suggested to be in glassy and rigid form relative to the bulk fraction and is termed rigid amorphous fraction (RAF) in the recent publications in certain analogy to immobilized material close to crystal surfaces.

Long et al. [34, 149] has developed a micromechanical model to describe the reinforcement in nanocomposites by considering interfacial material on the filler surfaces, which is physically in a glassy state due to confinement effects. The idea in the model is that when filler aggregates are sufficiently close to each other, the glassy interfacial material could overlap and act as a bridge that connects the filler aggregates to form a filler network. It is highlighted that glassy bridges are the primary components that contribute to the reinforcement at small strain amplitudes in Payne effect measurements. At higher strain amplitudes yielding of glassy bridges is considered as a reason for the Payne effect. However, the thickness of the glassy bridges computed through this model is few ten times more than that quantified by experimental studies indicating commonly 1-3 nm under ambient conditions. Much larger fractions of

glassy rubber in composites seem to be inconsistent with various experimental results in particular from DSC and NMR. The Long model has been further used to evaluate data for model composites filled with polymer-modified silica particles. The existence of the glassy fraction is supported by analyzing the FID from NMR measurements.[150, 151] The temperature-dependent measurements suggest that glassy bridges thickness reduces sequentially. Papon et al.[138] have supported the model proposed by Long through her extensive studies for understanding the phenomena of reinforcement. In these studies, NMR spectroscopy is used to evaluate the polymer-filler interactions in terms of immobilized rubber, and SANS is used to describe the dispersion of the filler particles in the matrix. The proposal is that the immobilized rubber layer is 7 to 10 nm thick and contains two components with a different degree of mobility: (1) glassy immobilized rubber and (2) intermediate mobility immobilized rubber. By analyzing SANS data, she suggests that the number of glassy bridges in the percolated filler network defines the Payne effect's amplitude, and is independent on rubber filler interaction microdispersion, filler size, and content.

A similar two component picture for the immobilized rubber is also discussed by Litonov et al.[132] However, he suggests that the dynamics of second component that is having intermediate mobility is not much different than the bulk rubber.

Gusev et al.[152] have shown through FEM simulations that enhanced reinforcement and dissipative properties of the rubber composites can be realized by a tiny fraction of immobilized rubber acting as bridges between the filler particles in a percolated filler network. Nevertheless, the existence of immobilized rubber is not generally accepted and strongly criticized by many other researchers.[61, 66, 153–156] The reason behind this is often wrong interpretation, misunderstanding and confusion with the terminology.[157] Finally, one should note that the existence of a homogenous immobilized layer on filler

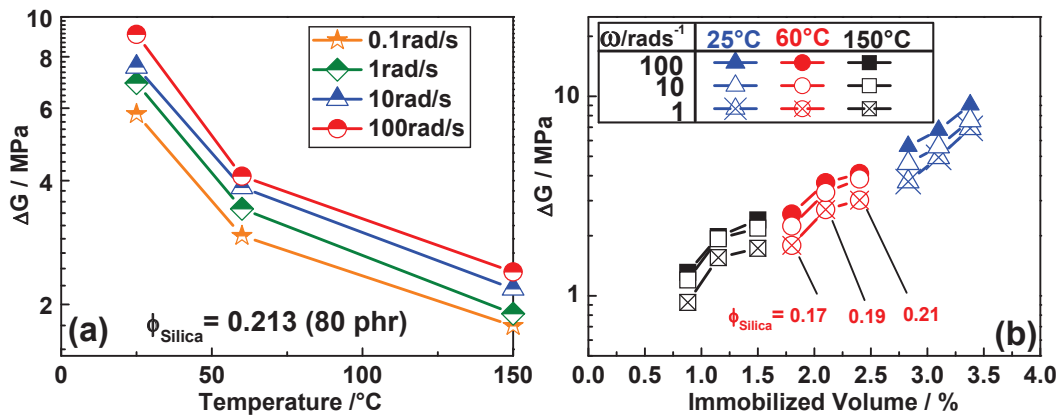


FIGURE 2.11

Viscoelastic nature of the filler network is demonstrated: Strength of the filler network at different frequencies with respect to temperature dependence for SSBR containing 21 vol% of silica show (a), Strength of the filler network from temperature and frequency dependent measurements for varied fraction of silica above the percolation threshold is plotted with respect to fraction of immobilized rubber evaluated by NMR (b). Figure taken from reference [46]

surfaces seems to be unlikely due to distance dependence of surface-induced interactions. Hence, a uniform relaxation dynamics of the immobilized rubber layer is not expected. Instead, the relaxation spectrum should be broadened and softening should occur over a wide temperature range due to the gradient in mobility, which could be related to structural inhomogeneities. The extent of broadening could be influenced by different factors, such as the microstructure of rubber and its interaction with the filler.[158] In addition it is crucial to understand that bound rubber is different from immobilized rubber. Bound rubber is a fraction of rubber occurring in filled composites and is dependent on different factors such as processing conditions, the molecular weight of the rubber etc. In contrast, the immobilized rubber is a fraction which is probably much smaller than the fraction of bound rubber and is formed due to adsorption on the surface. From the view point considered in this work its segmental dynamics is mostly influenced, and it should show a broad softening behavior such as density gradients on the nanoscale. Results which are consistent with this idea has been reported recently by Mujataba et al.[25, 26] Figure 2.11 shows data from strain sweeps performed at different temperatures

and frequencies on SBR-silica composites demonstrating a clear dependence of the filler network strength $\Delta G'$ on these parameters like expected for glassy bridges softening sequentially depending on the distance from the filler surface. Additional low field NMR experiments showed that these tremendous changes in the dynamics are caused by a immobilized rubber fraction of about 1-3 % decreasing with increasing temperature. Unfortunately, more direct information about the features of immobilized rubber is still lacking so far due to limitations of existing experimental techniques providing the most important quantities directly.[141, 154] Hence, experimental methods giving only indirect information have to be further used in order to deepen the knowledge. Even more important is in this situation to combine the results for different rubber composites with systematically varied properties to come to new insights.

3 Working hypothesis and aim of the work

The starting point of this work is a continuation of the previous study that showed the significant reinforcement property observed in highly filled rubber composites is due to a tiny fraction of immobilized rubber. It is proposed that immobilized rubber is a part of the filler network, and it acts as a bridge connecting the filler particles.[26] Due to its glassy state, the viscoelastic nature is induced to the solid filler network. Based on temperature-dependent double quantum NMR measurements, the volume of immobilized rubber is observed to be decreasing with increasing temperature. When correlated with the strain sweep measurements, it shows that glassy bridges are the load-carrying units in the filler network, and strength of filler network reduces either with an increase in temperature or decreasing frequency as a consequence of sequentially softening of the glassy bridges. Filler surface to volume of immobilized rubber provides the thickness of the glassy layer to be around 2 nm, and the estimated modulus is in the range of GPa. If this tiny fraction of immobilized rubber is contributing to reinforcement significantly, then it could also have a significant influence on the dissipative properties of the rubber nanocomposites. The central part of this work is to know the contributions to dissipation and visualize the possible parameters that would define the dissipative and reinforcement properties of the rubber composites and to look for general trends that mirror the correlation between reinforcement and dissipation through the proposed physical picture 3.1.[159] For this purpose, a methodical approach is instigated by DMA to evaluate the reinforcement and dissipative properties depending on temperature and strain amplitude for different kinds of rubber composites.

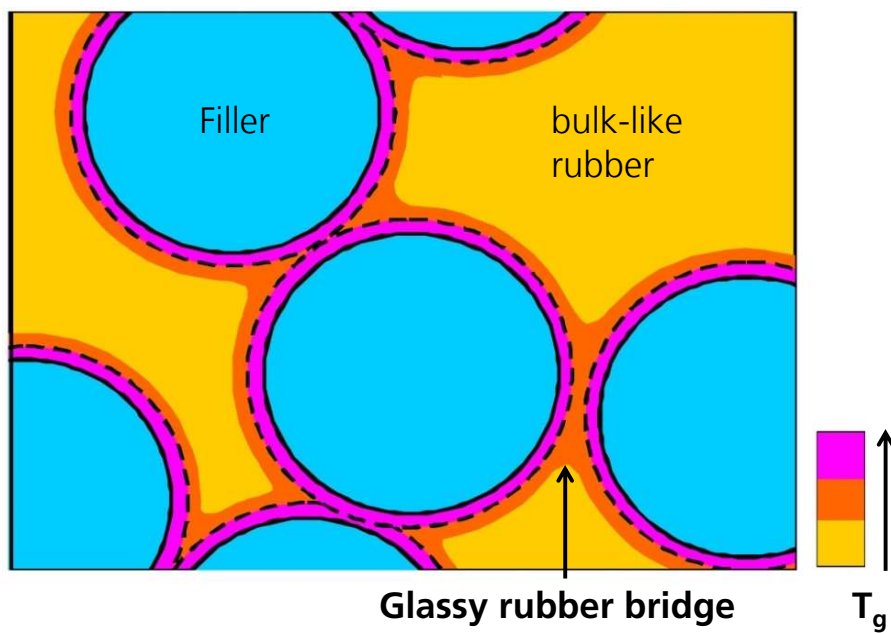


FIGURE 3.1

Schematic representation of the viscoelastic filler network. The filler particles are in contact with each other through glassy rubber bridges, different colored layers represent the sequential softening behavior of the glassy bridges at temperatures higher than the bulk rubber glassy transition temperature. Figure taken with permission from reference [159]. Copyright (2017) Elsevier

4 Materials and methods

4.1 Composite description and processing conditions

In this section, a detailed description of the rubber nanocomposites studied in this work is provided. Intending to isolate and understand the parameters that influence the reinforcement and dissipation, the composite series are designed systematically by varying specific parameters.

Natural rubber and its blend with polybutadiene rubber filled with carbon black. Series of natural rubber (standard Vietnamese rubber – SVR 10) based nanocomposites (NR-CB) are prepared by introducing different fractions of carbon black (N234 – STSA surface area $113 \text{ m}^2/\text{g}$). The volume fraction of the carbon black (Φ_{CB}) ranges from 0 to 21 vol%. The crosslinking system contains sulfur (Carl Roth GmbH) along with N-Cyclohexyl-2-benzothiazylsulphenamide (Rheogran CBS – 80, Rhein Chemie Additives) and diphenylguanidine (Rhenogran DPG, Rhein Chemie Additives) as accelerators, together with zinc oxide (purity 99%, Carl Roth GmbH) and stearic acid (purity 98%, Carl Roth GmbH) as activators. The volume fraction of vulcanizing additives is constant for all the NR-CB composites.

To evaluate the influence of matrix composition, in a second composite series, 30 mass fraction of SVR 10 is replaced by cis1,4 polybutadiene (Trinseo Deutschland GmbH Schkopau with the trade name of BUNATM cis 132) to prepare 70:30 natural rubber / polybutadiene rubber (NR/BR) blend nanocomposites. The grade of carbon black N234 and vulcanization system are the same

as those used for the to composites of the NR-CB series.

Both NR-CB and NR/BR-CB composites are prepared under identical conditions. The mixing process is done in two steps. The first step involves the incorporation of carbon black into the rubber matrix along with additives (Zinc oxide and Stearic acid) except for vulcanizing agents. The kneader equipment used for mixing rubber and carbon black is HAAKE PolyLab kneaderTM, the mixing chamber volume is 78 cm³ and it is equipped with a pair of Banbury rotors. The entire mixing unit is heated up to initial mixing temperature of 80°C with electricity. The mass of rubber, carbon black and other additives are weighed corresponding to fill 68% of the chamber. First, the rubber is introduced into the chamber and masticated for 1 min as the Banbury rotors rotate at 75 rpm. Next, the carbon black is introduced in two steps at different time. 3/4 of the carbon black is added right after the mastication process, followed by 1/4 of carbon black together with zinc oxide (5 phr) and stearic acid (3 phr). The temperature increases due to high shear forces involved during the mixing process, during the complete mixing process of 10 mins, the torque is monitored, which is almost steady after 6 to 7 mins depending on carbon black content. The dumped compound is allowed to cool down, and vulcanizing additives, sulphur (2.25 phr) and TBBS (0.7 phr) are added in the second step of mixing on a two-roll open mill at a temperature lower than 80°C for 2 to 3 mins. The vulcanizing time is measured using MDR (Mooney disk rheometer) at iso temperature of 150°C. The samples are pressed into a rectangle plate of thickness approximately 2 mm, in hydraulic pressing equipment at 150°C to determine T_{95} that corresponds to curing time obtained from MDR.

Variation of carbon black introduction method in NR/BR blends. To evaluate the influence of filler incorporation method on dynamic properties, natural / polybutadiene rubber blend (NR : BR ratio is 70 : 30) nanocomposites (NR/BR-CB) are prepared not only conventionally but also by using masterbatches of

carbon black (N234 with STSA surface area $113 \text{ m}^2/\text{g}$). Two types of masterbatch, carbon black premixed in NR matrix and BR matrix denoted by NR-MB and BR-MB respectively are used to prepare composites containing varied volume fractions ($5\% \leq \Phi_{CB} \leq 15\%$) of carbon black. The reference composites are prepared by conventional method of carbon black incorporation with same filler content as that of composites belonging to 100 NR-CB and 50 NR/BR-CB prepared by NR-MB and BR-MB. The number in the prefix represent the proportion of NR-MB used, i.e. 100 NR-CB composites are prepared by 100% of NR-MB and 50 NR/BR-CB composites contain 50% of NR-MB and 50% of BR-MB. The method of filler incorporation is varied with an intention to influence the dissipation and reinforcement of the produced NR/BR composites without changing the recipe. NR-MB and BR-MB contain 36 wt% of carbon black and their proportion is adjusted to achieve a defined volume fraction of carbon black and to maintain the blend ratio of 70 NR/ 30 BR. The average molecular weight of NR (SVR 10) is 2.200 kg/mol and for BR (BUNATM cis132-Schkopau) is 650 kg/mol. The glass transition temperature measured by DSC is -67°C for NR and -107°C for BR (1,4 cis % of 95). Other additives used to in the formulation are again zinc oxide (3phr), stearic acid (2phr), sulphur (1.5phr) and TBBS (1.5phr). Two step mixing procedure is followed. In the first step carbon black was added directly or through masterbatch into the rubber and curatives were added on a open mill in the second step. The mixing machine used is HAAKE PolyLab kneaderTM a volume of 379 cm^3 and with Banbury rotors. The processing parameters used for reference composites and masterbatch based composites (100 NR-CB and NR/BR-CB) are identical. The fill factor used is 0.68, rotor speed 75rpm, the initial set temperature is 80°C and the mixing time 10 mins. The second step is to introduce accelerators and vulcanizing agents, and this process is done in a two-roll mill at a temperature lower than 80°C for 3 to 5 mins. The crosslinking of all the composites is done at 160°C and time corresponding to t_{95} as obtained from cure curves measured in moving disc

rheometer (MDR).

polybutadiene - styrene butadiene rubber diblock copolymers filled with silica. A BR-SBR (polybutadiene - styrene butadiene rubber) diblock copolymer containing 46 vol% SBR blocks with a styrene content of 45 mol% are filled with different amounts of silica. The total molecular weight of the block copolymer is $M_W=210$ kg/mol and 1,2 vinyl contents are low ($\approx 8,3$ mol% in BR and ≈ 15 mol%). The sample has been synthesized by Cecilia Aguiar da Silva at the Fraunhofer PAZ.[53] Further details are reported in refs and as reference a SBR-BR blend with (50 vol% solution SBR SE 6233 (S-SBR, SUMITOMO-JAPAN) and 50 vol% polybutadiene BUD 1207 (GDYR-CHEM-BEAUMONT)) is filled with variable volume fractions silica ($\phi_{silica} = 0.082, 0.152, 0.212$ and 0.264) corresponding to 20 to 80 phr using a three step mixing procedure. The machine used for processing the rubber composites was an internal mixer (Brabender Plasticorder) of 83cm^3 volume. In the first stage, the initial mixing temperature was set to 80°C with a rotor speed of 19 rpm. Here, rubber strips, silica (Zeosil 1165MP from Solvay with surface area of $165\text{ m}^2/\text{g}$), anti-oxidant (0.75 phr, 6-PPD), oil (TDAE oil) and silane (Si 266 from EVONIK) were mixed. For the diblock copolymers, the oil to silica and silane to silica ratios used were 0.25 and 0.08 phr per 1 phr filler, respectively. On the other hand, for the SBR-BR blend the oil to silica ratios used were 0.94, 0.47, 0.31 and 0.29 per 1 phr filler, respectively. Since the commercial SBR samples is oil 37.5 phr oil extended, it was not possible to keep the oil/filler ratio constant for the different sample composites. Upon complete filler and additives incorporation, the temperature rose to about 110°C . After that, the rotor speed was increased to 40 rpm for 2 min until the temperature reached about 130°C . Consecutively, the rotation was increased to 60 rpm and consequently an increase in temperature up to few Kelvins was observed depending on the silica loading. Afterwards, the rotor speed was set to 80 rpm for 1 min and finally to 100 rpm for more 1 min. In this

last step the mixing temperature was approximately 150 °C at which silanization reaction takes place. Thereafter, the mixed batch was discharged and a relaxation time of about 1.5h was given prior to the second non-productive stage. This batch was further mixed at comparable conditions. Later, the curatives were added zinc oxide (2.5 phr), stearic acid (2 phr), sulphur (1.4 phr), CBS (2 phr), DPG (1.5 phr). In this mixing step, temperature was not higher than 110 °C in order to avoid pre-mature vulcanization. Thereafter, the mixed batch was discharged and taken to the mill. It was passed through the roll mill four times with the back and front rotor speeds of 21 and 25 rpm, respectively, and a gap between them of 1.65 mm. Temperature in the roll mill was 50 °C. The milled sheet was vulcanized into a 2mm thick sheets at 150 °C applying a hydraulic pressure for 32 min. The chosen cure time was for all crosslinked samples larger than t_{95} .

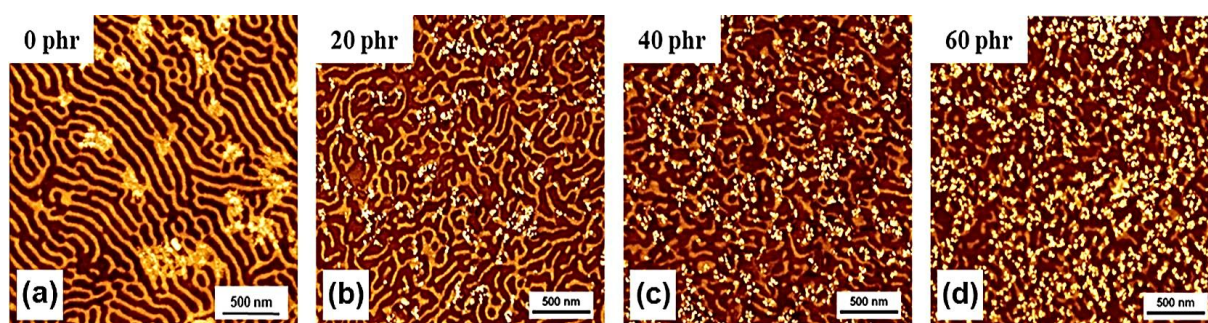


FIGURE 4.1

AFM images of BR-SBR diblock copolymer samples showing a lamellar morphology in vulcanized state. Unfilled sample (a) and samples filled with 20 phr (b), 40 phr (c) and 60 phr (d) silica particles are compared. The silica particles appear white and are mostly in the styrene rich phase (orange). The dark brown regions in the image corresponds to BR phase. Reprinted with permission from reference [160]. Copyright (2018) American Chemical Society.

Lamellar morphology expected due to nearly symmetric architecture of block copolymer is confirmed by SAXS and AFM. AFM images in figure 4.1 display lamellar morphology of the diblock copolymer and also demonstrate that silica particles preference for the SBR phase. The AFM images indicate that average SBR lamellae thickness is not altered significantly for filled composites in comparison with unfilled SBR-BR block copolymer. SAXS data reported in

Ref. support this finding. Periodicity in the range 77 to 80 nm are obtained by SAXS and FFT from AFM images for all investigated composites. Remarkable is that the phase morphology of the self-assembled block copolymer is neither destroyed by crosslinking nor by the processing steps needed to incorporate the silica particles. However, the long-range order is obviously reduced with increasing filler content.[160]

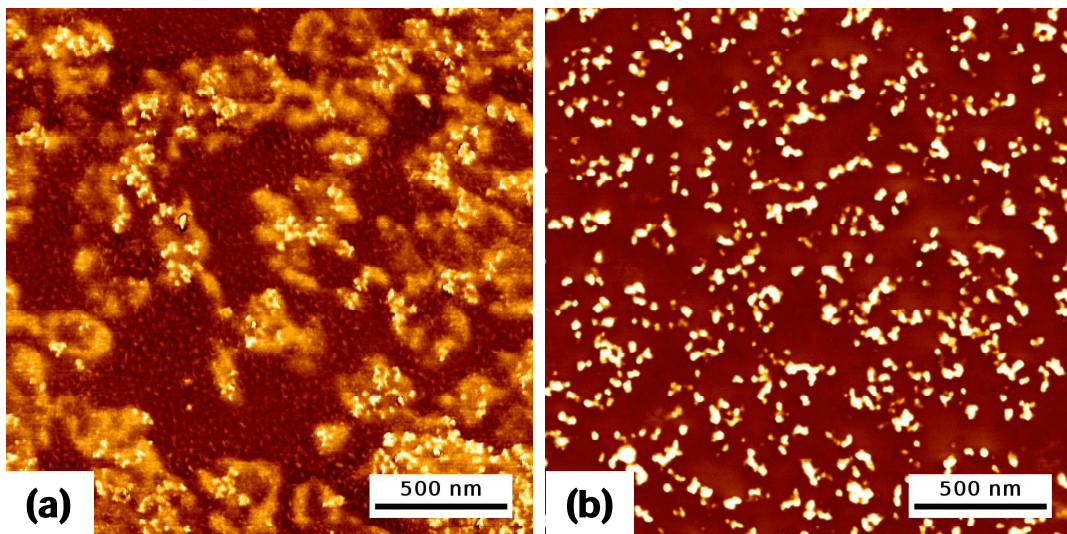


FIGURE 4.2

AFM phase images for SBR-BR blends filled with 20 phr (a) and 60 phr (b) silica. In (a) the BR domains appear in brown and SBR domains in orange and silica appear in white color. In (b) both the phases of SBR and BR are not distinguishable, due to limited differences in the mechanical properties. Reprinted with permission from reference [160]. Copyright (2018) American Chemical Society.

Composites based on BR-SBR blends incorporated in this work show as expected a much coarser morphology as seen in figure 4.2. Typical SBR domain sizes are larger than 250 nm in this cases. Selective incorporation of the silica particles in the SBR phase is also indicated in case of blends and the macrodispersion seems to be uniform.

4.2 Experimental methods

In this work, the mechanical properties are evaluated for different rubber nanocomposites by Dynamic Mechanical Analysis. In this technique, the response of the specimen to the applied perturbations is analyzed. Generally, deformations in the form of sinusoidal strain or stress are applied, and the response is sinusoidal stress or strain, which is out of phase due to the viscoelastic characteristic of the rubber. As shown in the figure 4.1 (e), the response to the applied sinusoidal strain is stress with phase lag δ .

$$\gamma = \gamma_0 \sin \omega t \quad (4.1)$$

$$\sigma = \sigma_0 \sin(\omega t + \delta) \quad (4.2)$$

where, γ_0 and σ_0 are the strain and stress amplitudes, respectively.

Deconvoluting the response function into in-phase and out of phase components with applied strain, we get,

$$\sigma = \sigma_0(\sin \omega t \cos \delta + \cos \omega t \sin \delta) \quad (4.3)$$

Further one can express the equation in terms of dynamic shear storage modulus G' and loss modulus G'' corresponding to the in-phase component $(\sigma_0/\gamma_0) \cos \delta$ and out of phase component $(\sigma_0/\gamma_0) \sin \delta$, respectively. One gets

$$\sigma = \gamma_0 G' \sin \omega t + \gamma_0 G'' \cos \omega t. \quad (4.4)$$

The energy loss per cycle of induced deformation can be calculated by

$$\Delta E = \int \sigma d\gamma = \int_0^{2\pi/\omega} \frac{d\sigma}{dt} dt. \quad (4.5)$$

Further substituting equation 4.1 and 4.4 into 4.5 we get

$$\Delta E = \omega \gamma_0^2 \int_0^{2\pi/\omega} (G' \sin \omega t \cos \omega t + G'' \cos^2 \omega t) dt = \pi \gamma_0^2 G'' \quad (4.6)$$

At a given strain amplitude (γ_0), the energy loss (ΔE) over a deformation cycle is directly proportional to the dissipative component, i.e., loss modulus (G'').

Temperature sweep. Temperature-dependent mechanical properties in the linear response region are measured using Rheometrics dynamic analyzer ARES equipped with FRTN (Force rebalance transducer with normal force). The specimens of about $2 \times 8 \times 30 \text{ mm}^3$ clamped in a torsional tool were first cooled down below the glassy transition temperature by liquid nitrogen, and the specimen was heated up to the temperature range of interest with a temperature step of 3°C . At each temperature step, the specimen was equilibrated for 60 sec, and oscillatory deformation of 0.1% was applied at three different angular frequencies ($\omega = 1, 10, 100 \text{ rads}^{-1}$). The measurements were set and controlled using Orchestra Software, and the obtained data points were plotted and analyzed using Origin software.

Strain sweep. Dynamic shear measurements with variable strain amplitude were done using an Anton Paar MCR501 Twin-Drive rheometer. Rectangular specimen of dimension $2 * 8 * 30 \text{ mm}^3$ were stamped out of rubber composite sheets and clamped with approximate length of 20 mm in the rheometer tools. Strain amplitude was increased logarithmically from 0.001 to 40 % at a fixed angular frequency (ω) of 10 rad/s. The normal force was maintained close to zero during the soak time of 600 sec before the measurement. Note, that for each measurement temperature $T = 0, 25, 60^\circ\text{C}$ a new specimen is used. Storage modulus $G'(\gamma)$ and loss modulus $G''(\gamma)$ are measured depending on strain amplitude and used afterward to quantify the different contributions to reinforcement and dissipation.

For morphological characterization of the rubber composites and to evaluate the micro and nano-dispersion Transmission Electron Microscopy (TEM) is used.

Transmission electron microscopy. TEM studies were performed by means of a FEI Tecnai G2 TEM operated at 200 kV and the cell^F software (Olympus Soft Imaging Solutions GmbH) and Image J was used for image processing and evaluation. Ultrathin sections having a thickness of approximately 60 nm were prepared by cryo-ultramicrotomy using a RMC Power Tome with CRX cryo chamber equipped with a Diatome diamond knife.

5 Results

This section presents the results from dynamic mechanical measurements, in conjugation with morphological information obtained by microscopic image techniques for selected samples. As the main aim of this study is to isolate different contributions to dissipation. At first, the approach developed by modifying the Kraus equation for loss modulus depending on strain amplitude is described. Further, the approach is validated based on strain sweeps measured at different temperatures for various rubber composites. Additionally, the filler network related contribution to the storage modulus is studied and evaluated by Kraus equation to develop a common understanding of the molecular origin to dissipation and reinforcement. The results are compared between the relevant series of composites in order to find important factors influencing dissipation and reinforcement.

5.1 Modeling dissipation contributions in strain sweep

A sigmoidal decrease in storage modulus G' and simultaneously occurring peak in loss modulus G'' with strain amplitude γ are indicators for the existence of filler network in a rubber composite that forms for filler fractions (Φ) above the percolation threshold (Φ_c). It has been demonstrated that its contribution to reinforcement, i.e., the load-carrying capacity of the filler network ($\Delta G' = G'_0 - G'_\infty$), can be approximated by the Kraus equation 5.1 for storage modulus.[108]

$$G'_\gamma = \frac{G'_0 - G'_\infty}{1 + \left(\frac{\gamma}{\gamma_c}\right)^{2m}} + G'_\infty \quad (5.1)$$

with, G'_0 is the storage moduli at small ($\gamma \rightarrow 0$) and G'_∞ at very large ($\gamma \rightarrow \infty$) strain amplitudes. The difference $\Delta G' = G'_0 - G'_\infty$ determines the overall filler network contribution to reinforcement corresponding to the load carrying capacity of the filler network. Other parameters are the critical strain amplitude γ_c and the exponent m describing the shape of the sigmoidal decrease in $G'(\gamma)$.

The Kraus model is considering agglomeration and deagglomeration phenomena and it approximates the storage modulus data over the complete strain amplitude range quite well (8.1).[46, 161, 162] This applies also to the rubber composites investigated in this work at different temperatures. An analogous derivation leads the loss modulus to equation 5.2.

$$G''_\gamma = \frac{2(G''_m - G''_\infty)\left(\frac{\gamma}{\gamma_c}\right)^m}{1 + \left(\frac{\gamma}{\gamma_c}\right)^{2m}} + G''_\infty \quad (5.2)$$

A fit of loss modulus data over the complete strain amplitude range based on equation 5.2 is given by the black line in figure 5.1. It is clearly visible that the approximation fails. Although equation 5.2 describes the peak at G''_m relatively well, it is not taking into account that the plateaus at small and large strain amplitudes are different.

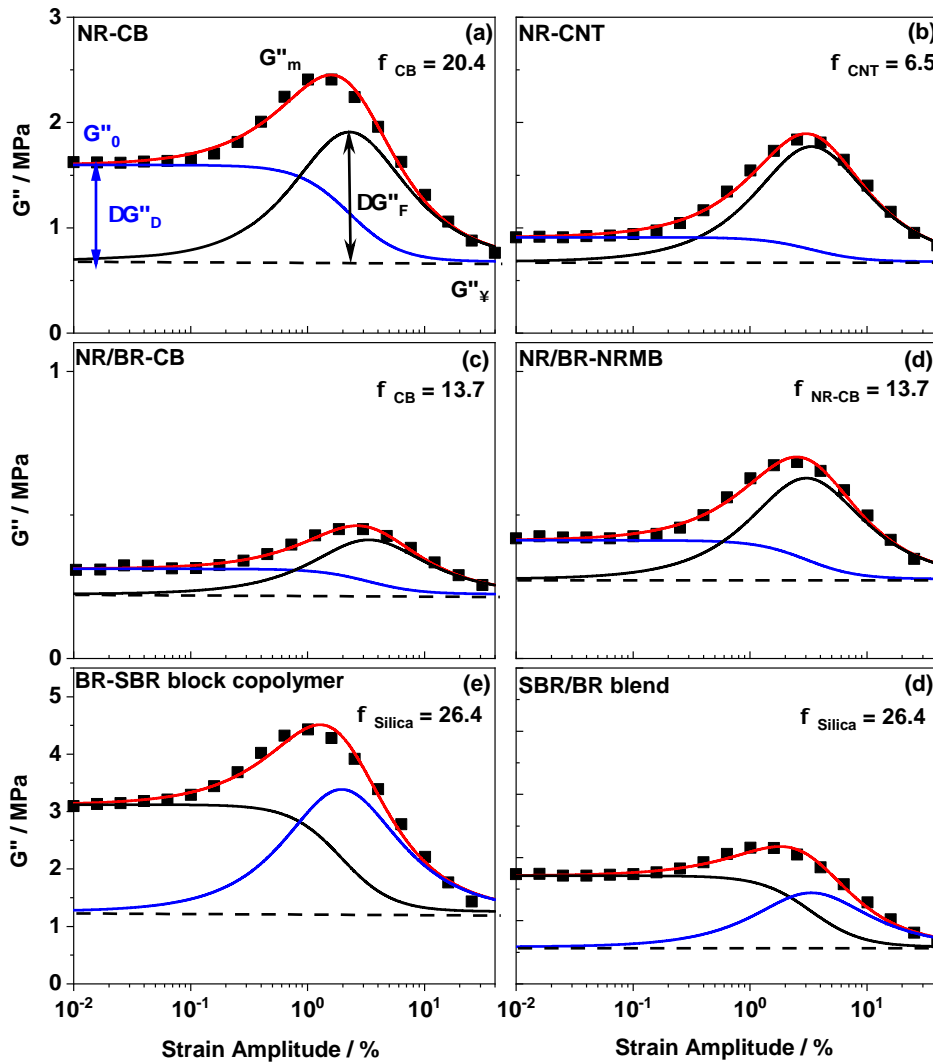


FIGURE 5.1

Strain amplitude dependent dynamic shear loss modulus $G''(\gamma)$ measured at ($T=25^\circ\text{C}$ and $\omega=10\text{ rad s}^{-1}$) for (a) NR containing 20.4 Vol% of CB, (b) NR with 6.5 vol% CNT, (c) NR/BR blend filled with 13.7 Vol% CB, (d) NR/BR blend with 13.7 Vol% CB introduced via master batch, (e) a BR-SBR block copolymer filled with 26.4 vol% silica as well as (f) a SBR-BR blend containing 26.4 vol% silica. Further details about these samples are discussed later in this section. The data fitting of $G''(\gamma)$ by equation 5.2 according to the Kraus model, are represented as black lines. The modified Kraus fitting through equation 5.3 is shown as red line. The blue line represent the additional sigmoidal term $\widehat{G}''_{\gamma,D}$ addition factor introduced in 5.3.

The drawback indicates that the origin of dissipation is not only due to the breaking down of the filler network. Instead, there is obviously another important contribution that amplifies the dissipation at small strain amplitudes, which is significantly higher than that at large strain amplitudes. In this respect, an additional sigmoidal contribution has to be introduced in the original Kraus equation 5.2, represented by blue line in the figure 5.1. Equation 5.3 is a modified Kraus equation represented by the red line, providing a good approximation to the experimental results over the complete strain amplitude range.

$$G''_{\gamma} = \frac{G''_0 - G''_{\infty}}{1 + \left(\frac{\gamma}{\gamma_c}\right)^{2m}} + \frac{2(G''_m - G''_{\infty})\left(\frac{\gamma}{\gamma_c}\right)^m}{1 + \left(\frac{\gamma}{\gamma_c}\right)^{2m}} + G''_{\infty} \quad (5.3)$$

$$G''_{\gamma} = \widetilde{G}''_{\gamma,D} + \widetilde{G}''_{\gamma,F} + G''_{\infty} \quad (5.4)$$

This equation 5.3 discriminates between the dissipation G''_0 at small strain amplitudes where the filler network is intact and the dissipation G''_{∞} at large strain amplitudes where the filler network is totally broken. The equation 5.4 is the generalized form of modified kraus equation 5.3 distinguishing between two types of contributions to dissipation that are related to the filler network $\widetilde{G}''_{\gamma,D}$ and $\widetilde{G}''_{\gamma,F}$ and an extra term G''_{∞} being physically of different nature. From our point of view these three terms have the following molecular origins:

1. The dissipation $\widetilde{G}''_{\gamma,D}$ is due to oscillatory deformation induced by the intact part of the filler network, i.e. intact glassy bridges between filler particles, and reduces sigmoidally as the strain amplitude increases.
2. The dissipation $\widetilde{G}''_{\gamma,F}$ in the form of a peak occurring simultaneously at the intermediate strain amplitudes is related to dissipative mechanisms occurring due to fracture of glassy bridges connecting filler particles.

3. The term G''_{∞} represents contributions which are not related to filler network, i.e. induced in particular by parts of the rubber matrix far away from filler particles behaving more or less bulk-like.

Note that by estimating the step height $\Delta G''_D = G''_0 - G''_{\infty}$ and the peak height $\Delta G''_F = G''_m - G''_{\infty}$, filler network related contributions can be quantified. Although both contributions, $\widetilde{G''}_{\gamma,D}$ and $\widetilde{G''}_{\gamma,F}$, should be according to the proposed physical picture proportional to the number of intact bridges in the filler network (N_0) their magnitude can vary since the individual average contribution to dissipation per bridge will depend on the nature of the glassy bridge. The dissipation quantum q_F occurring if a glassy bridge breaks is different for each rubber composite and the same is true for the dissipation quantum q_D related to each intact glassy bridge due to the fact that dissipation during oscillatory deformation of a glassy rubber bridge is commonly higher as compared to the dissipation caused by a rubber.

There are seven parameters in equations 5.1 and 5.3. In this work, the approximations of the experimental results are made by fixing the m parameter to be 0.6. Under this condition the characteristic strain amplitude (γ_c) shows commonly only a small difference between fits from equations 5.1 and 5.3 (table 5.1 and 5.2). Earlier, Ulmer [109] proposed an equation similar to equation 5.3. However, he disclaimed its usage as the validation was not satisfactory. His approximation showed a discrepancy in m and γ_c values for his own and Payne's experimental result. Hence he rejected such an approach possibly due to quality of experimental data and missing understanding of the molecular origin of dissipation at small strain amplitudes.

From figure 5.1 it is clear that modified Kraus equation 5.4 enables us to quantify filler network contributions to dissipation in different kind of rubber composites. It seems that filler network contributions are system dependent as indicated, for instance, by data for differently filled NR composite with CB

TABLE 5.1: Kraus Parameters for storage modulus from figure 8.1

	G'_0 MPa	G'_∞ MPa	m	γ_c	$\Delta G'$ MPa
NR-CB	21.9	4.63	0.6	1.6	17.27
NR - CNT	22.26	4.42	0.6	2.68	17.85
NR/BR-CB	5.56	2.86	0.6	2.08	2.69
NR/BR-NRMB	7.91	2.69	0.6	2.31	5.22
PB / SBR copolymer	27.34	4.68	0.6	1.61	22.66
SBR/BR blend	12.37	2.66	0.6	2.40	9.71

TABLE 5.2: Modified Kraus Parameters for loss modulus from figure 5.1

	G''_0 MPa	G''_∞ MPa	G''_m MPa	m	γ_c	$\Delta G''_D$ MPa	$\Delta G''_F$ MPa
NR-CB	1.60	0.68	2.27	0.6	1.76	0.92	1.59
NR - CNT	0.91	0.68	2.09	0.6	2.60	0.23	1.41
NR/BR-CB	0.31	0.22	0.47	0.6	2.58	0.09	0.24
NR/BR-NRMB	0.41	0.28	0.73	0.6	2.35	0.13	0.45
BR-SBR block copolymer	3.12	1.26	4.01	0.6	1.51	1.86	2.75
SBR/BR blend	1.71	0.58	1.69	0.6	2.59	1.13	1.11

and CNT. The strength of the filler network $\Delta G'$ is almost identical, (table 5.1). However, the dissipation at small strain amplitudes $\Delta G''_D$ and at intermediate strain amplitudes $\Delta G''_F$ are quite different, (table 5.2). To come to a detailed understanding of both filler network related contributions to dissipation, $\widetilde{G}''_{\gamma,F}$ and $\widetilde{G}''_{\gamma,D}$ the approach presented above is further used in this study to quantify dissipation and reinforcement dependent on temperature and filler fraction in different rubber composites.

5.2 NR and NR/BR filled with carbon black

In this section results for a series of NR composites and NR/BR blends filled with different amounts of carbon black are presented and compared.

Natural rubber filled with carbon black. Temperature dependent shear modulus data for $G'(T)$ and $G''(T)$ measured at an angular frequency (ω) of 10 rads^{-1} are shown in figure 5.2. At lower temperatures the values for $G'(T)$ and $G''(T)$ are almost identical, as the rubber in unfilled and filled NR-CB composites is in a glassy state. At a characteristic temperature, $G'(T)$ decreases significantly, and simultaneously with a peak occurring at -57°C is observed in $G''(T)$ since NR undergoes its dynamic glassy transition (α relaxation). In the rubbery plateau region (at temperatures well above the α relaxation process), the changes in the $G'(T)$ value due to presence of filler particles is visible. As expected the G' values for unfilled natural rubber is approximately 10^6 Pa and its value shows a weak increase with temperature as a consequence of entropic elasticity.[163] On the other hand, for filled composites the $G'(T)$ values in the rubber plateau range are increasing systematically with carbon black content. For highly filled composites containing carbon black $\Phi_{CB} \geq 10$ vol% a unique trend is observed. $G'(T)$ is decreasing continuously with temperature (inset of figure 5.2(a)). This indicate the existence of a situation where filler related effects dominate over entropic elasticity.

Similarly, the loss modulus $G''(T)$ for filled composites show systematic increase in the rubber plateau regime with carbon black content. Clearly a systematic increment in the dissipation is visible in inset of figure 5.2(b). The effect is significantly more pronounced above the percolation threshold of $\Phi_{CB} \geq 10$ vol%. The overall temperature dependence is similar to that of storage modulus, i.e. the dissipation is reducing with increasing temperature for highly

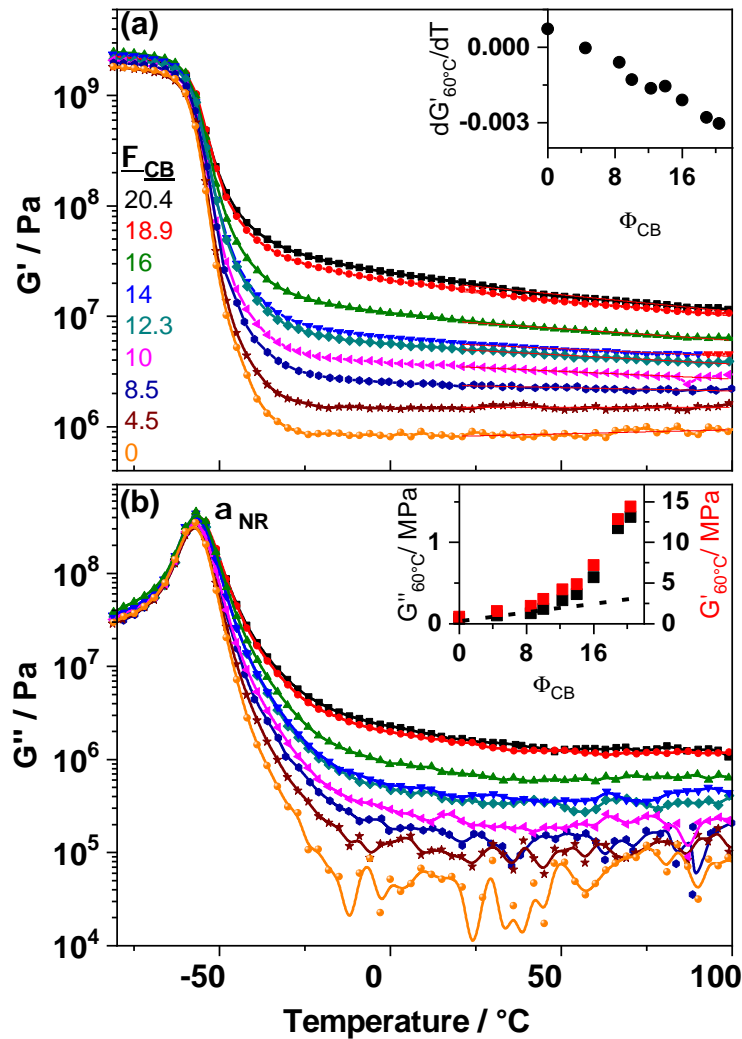


FIGURE 5.2

Temperature dependence of (a) storage modulus $G'(T)$ and (b) loss modulus $G''(T)$ measured at 10 rad s^{-1} for unfilled and filled NR-CB composites containing different volume fractions of carbon black (Φ_{CB}) as given in the legend. The α_{NR} indicate the dynamic glass transition of natural rubber. Inset in (a) shows the average slope of $G'(T)$ in the temperature range from 20° to 100°C , inset in (b) gives $G'(T)$ and $G''(T)$ at 60° obtained by averaging over 5 data points (from 54° to 66°C).

filled composites. These trends are expected and well documented in literature since carbon black particles are known to form a filler network for loading above a percolation threshold (ϕ_C), i.e. they contribute significantly to reinforcement and dissipative properties of the rubber nanocomposites.[13, 25, 36]

While models explaining the origin of reinforcement due to filler network are

broadly considered, the molecular origin of dissipation at small deformations amplitudes (0.1% in the linear response range are used here) was basically not or only very seldom discussed.[13, 110] A standard technique to resolve the filler network related contributions to reinforcement and dissipation is to perform measurements where the strain amplitude varied under isothermal conditions at fixed frequency. Usually room temperature is used in combination with a single frequency in the range 1 to 10 Hz. A special approach in this study is to incorporate always strain sweeps at different temperature between 0°C and 60°C in order to investigate systematically the influence of temperature on dissipation and reinforcement. In special cases also frequency dependent experiments are performed and is shown in appendix figure 8.2

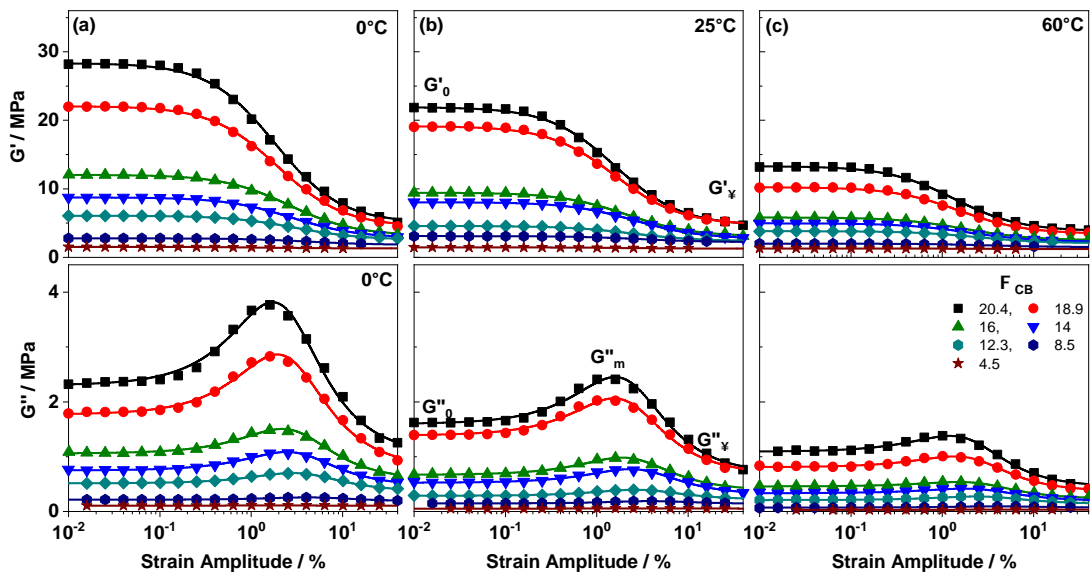


FIGURE 5.3

Strain amplitude dependent (top) storage modulus $G'(\gamma)$ and (bottom) loss modulus $G''(\gamma)$ measured at 10 rads^{-1} for natural rubber composites containing different fraction of carbon black (Φ_{CB}) at three different temperature (a) 0°C, (b) 25°C and (c) 60°C. The data points are approximated by the Kraus equation 5.1 for the storage modulus $G'(\gamma)$ and by the modified Kraus equation 5.3 for the loss modulus $G''(\gamma)$

The data obtained by deforming the specimen from small strain to large strain amplitude (γ from 0.001% to 40%) at a fixed angular frequency (ω) of 10 rads^{-1} at three different temperatures 0°, 25° and 60°C are presented in figure 5.3.

Note that the preferred temperatures fall in the regime of rubber plateau (figure 5.2). Commonly the storage modulus $G'(\gamma)$ is increasing with carbon black content, but the magnitude is dependent on filler volume fraction (Φ_{CB}), measurement temperature and strain amplitude regime. The increment of $G'(\gamma)$ is relatively weak for composites containing small volume fraction of carbon black and it shows no dependence with strain amplitude from small strain amplitude ($\gamma < 1\%$) to large strain amplitude (γ up to 40%). The situation is different for composites containing $\Phi_{CB} \geq 10 \text{ vol\%}$. For such filler contents the storage modulus value G'_0 at small strain amplitude shows a strong dependence on filler content. In addition sigmoidal decrease of $G'(\gamma)$ with the strain amplitude is observed. The feature is generally observed in composites containing a filler network, that forms for filler loading above the percolation threshold (ϕ_C).

The phenomenon of sigmoidal decrease in storage modulus with strain amplitude is well known as Payne effect and is related to a filler network breakdown.[9] The storage modulus G'_0 is strongly increasing with increasing the filler loading above ϕ_C , whereas at large strain amplitude ($\gamma \approx > 25\%$) the modulus G'_∞ estimating the reinforcement contributions due to occluded rubber and rubber network is weakly dependent on filler volume fraction.[25] Similar behavior is seen commonly for rubber composites containing high loading of nano particles. Temperature dependent measurements are seldomly reported in literature. G'_0 value for a given filler content above percolation threshold (ϕ_C) show strong dependence on temperature. The G'_0 value systematically reduces with increasing the temperature, while G'_∞ is weakly influenced by temperature and filler loading. This feature indicates that filler network contributions to the storage modulus G' are reduced systematically as the temperature is increased.

The loss modulus $G''(\gamma)$ is nearly featureless and independent on strain amplitude, similar to $G'(\gamma)$ for composites containing carbon black loading significantly below the percolation threshold (ϕ_C). In these composites values corresponding to small G''_0 and large strain amplitude G''_∞ are almost same. However, for composites containing carbon black loading $\Phi_{CB} \geq 10$ vol%, the loss modulus show a different behavior depending on strain amplitude. A peak labeled with G''_m is observed at intermediate strain amplitude. This feature is also related to Payne effect and commonly seen in composites containing a filler network. [9, 108]

Most interestingly, G''_0 is showing similar decreasing trend with carbon black content and temperature as seen in G'_0 for composites containing percolated filler network. Similarly, the peak intensity G''_m is also increasing with carbon black content and decreasing with temperature, while G''_∞ is only weakly changing under identical conditions. In general, the strain sweep in figure 5.3 demonstrate clearly that filler network formed by carbon black particles in NR matrix is influenced strongly by temperature and that in particular reinforcement and dissipation in the rubbery plateau region are at least for high filler loadings and temperatures between 0° and 60°C dominated by filler network related contributions.

NR/BR filled with carbon black. Temperature dependent data for shear storage modulus $G'(T)$ and loss modulus $G''(T)$ for rubbers containing 70 wt% NR and 30 wt% BR together with different amounts of carbon black are presented in figure 5.4. As expected, NR and BR is immiscible and show two independent α relaxation processes. The peak in G'' at approximately -99°C corresponds to α relaxation of polybutadiene rubber, the other peak at approximately at -57°C is related to natural rubber. The latter peak position is similar to the one observed earlier in NR-CB composites and is unaffected due to BR fraction. The occurrence of both α relaxation processes results in a step-wise softening process observed clearly in $G'(T)$. In the temperature range between both α relaxations the storage modulus is still in the GPa range and only weakly dependent on filler content. Only at temperatures significantly above -57°C , where the majority NR fraction softens, the typical rubber plateau region is observed. The position of both α relaxation processes is practically identical in unfilled rubber and rubber composites containing different volume fractions of carbon black. Pronounced changes due to the presence of carbon black particles are evident in the rubbery plateau region. The $G'(T)$ and $G''(T)$ values in this region increase systematically with increasing carbon black content. However, the increment in $G''(T)$ with filler fraction is not as ideal like in NR-CB composites (inset of Figure 5.4(b)) since above the percolation threshold, the increase in $G''(T)$ is broadened. Possibly this has to do with the preferential filler distribution in both rubber phases, it is known that carbon black prefers BR phase.[95, 164] Temperature dependence in the rubbery plateau regime is similar to that of highly filled NR-CB composites, both $G'(T)$ and $G''(T)$ are decreasing with increase in temperature and the relevant slope dG'/dT decreases with increasing filler content (inset Figure 5.4(a)).

The results from strain sweep measurements in figure 5.5 show the $G'(\gamma)$ dependence on carbon black content. A sigmoidal decrease in $G'(\gamma)$ and a peak

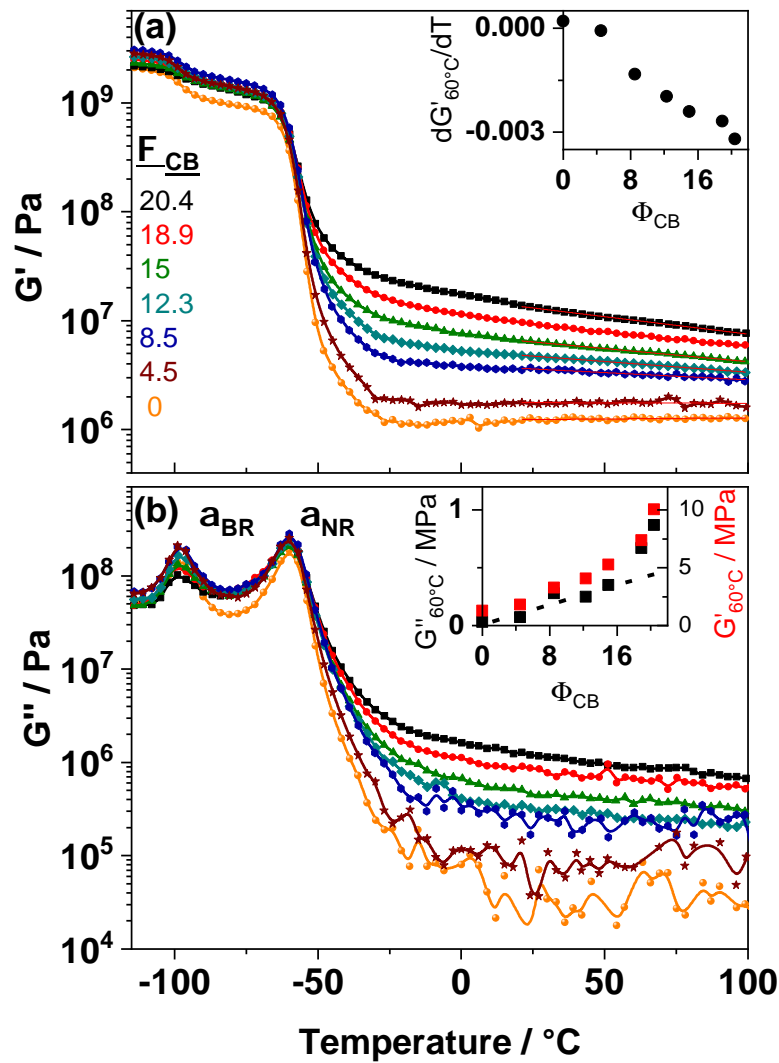


FIGURE 5.4

Temperature dependence of (a) storage modulus G' and (b) loss modulus G'' measured at 10 rads^{-1} for unfilled and filled natural and polybutadiene rubber blends (NR/BR-CB) containing different fraction of carbon black (Φ_{CB}). Distinct α_{NR} and α_{BR} indicate that both the components in the composite are immiscible. Inset in (a) gives the slope of $G'(T)$ in the temperature range from 20° to 100°C , inset in (b) gives the $G'(T)$ and $G''(T)$ values at 60° obtained by averaging over 5 data points (from 54° to 66°C).

in $G''(\gamma)$ demonstrate the existence of the Payne effect in highly filled composites. G'_0 and G''_0 values are strongly increasing, for carbon black content $\Phi_{CB} \geq 12.3 \text{ vol}\%$. The temperature dependence is similar to that of highly filled NR-CB composites, the sigmoidal step in $G'(\gamma)$ and peak intensity G''_m show a

decrease with increasing temperature. The results indicate that the filler network contributions to reinforcement and dissipation in blend composite behave qualitatively similar to that of single matrix composites. Although, the carbon black grade and processing conditions are identical for both NR-CB and NR/BR-CB composites, differences exist in the absolute values of reinforcement and dissipation at a given carbon black content and temperature. Hence, it is interesting to cross compare the absolute values in order to see the effect of replacing 30% of NR by BR rubber.

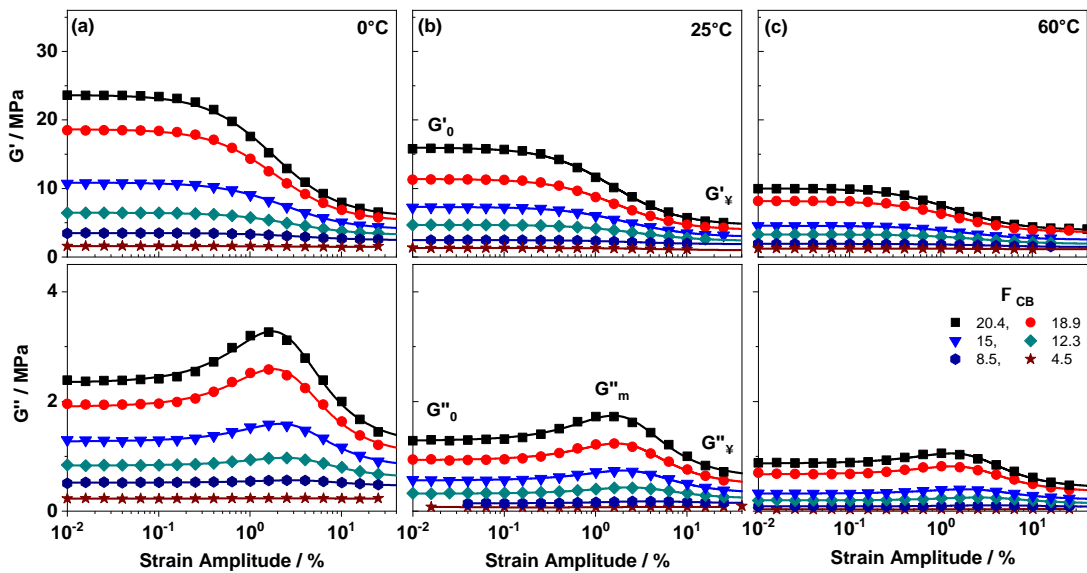


FIGURE 5.5

Strain amplitude dependent (Top) storage modulus $G'(\gamma)$ and (bottom) loss modulus $G''(\gamma)$ measured at 10 rad s^{-1} for NR/BR-CB composite blends containing different fraction of carbon black (Φ_{CB}) at three different temperatures (a) 0°C , (b) 25°C and (c) 60°C . The data points are approximated by Kraus equation 5.1 for the storage modulus $G'(\gamma)$ and by modified Kraus equation 5.3 for the loss modulus $G''(\gamma)$.

Comparison between NR-CB and NR/BR-CB. Qualitatively, the results from strain sweeps show that the Payne effect features identified by sigmoidal decrease in $G'(\gamma)$ and a peak in $G''(\gamma)$ is common for highly filled NR-CB and NR/BR-CB based composites. This confirms clearly that the filler network formed by carbon black particles above the percolation threshold, which is seemingly quite independent on the rubber matrix, significantly influences the dynamic mechanical properties of the rubber composites. Further, strain amplitude measurements show that filler network contributions to reinforcement and dissipation are strongly temperature dependent. Moreover, the intensity of Payne effect seems to be different at given carbon black content and measurement temperature for both NR-CB and NR/BR-CB composites. Comparing the fit parameters obtained from approximating the $G'(\gamma)$ and $G''(\gamma)$ based on equations 5.1 and 5.3 provides additional information about the influence of matrix composition.

In figure 5.6, the storage modulus G'_0 and G'_∞ , corresponding to two limiting strain amplitudes are plotted with respect to carbon black loading. The data clearly show the strong dependence of G'_0 on carbon black loading, specifically for loading above the percolation threshold which is approximately ($\Phi_{CB} \cong 10$ vol%) for both NR-CB and NR/BR-CB composites. On the other hand, G'_∞ show weak dependence with carbon black loading for both composite series. At a comparable temperature, the values of G'_0 are consistently higher above the percolation threshold for NR-CB composites in comparison with those for NR/BR-CB composites. Interestingly, the G'_∞ values for both NR and NR/BR composites is almost equal, indicating that contributions due to occluded rubber, hydrodynamic reinforcement and rubber matrix are not influenced (as the processing conditions and carbon black grade are identical). The influence of measurement temperature is also clear. While the filler network is intact

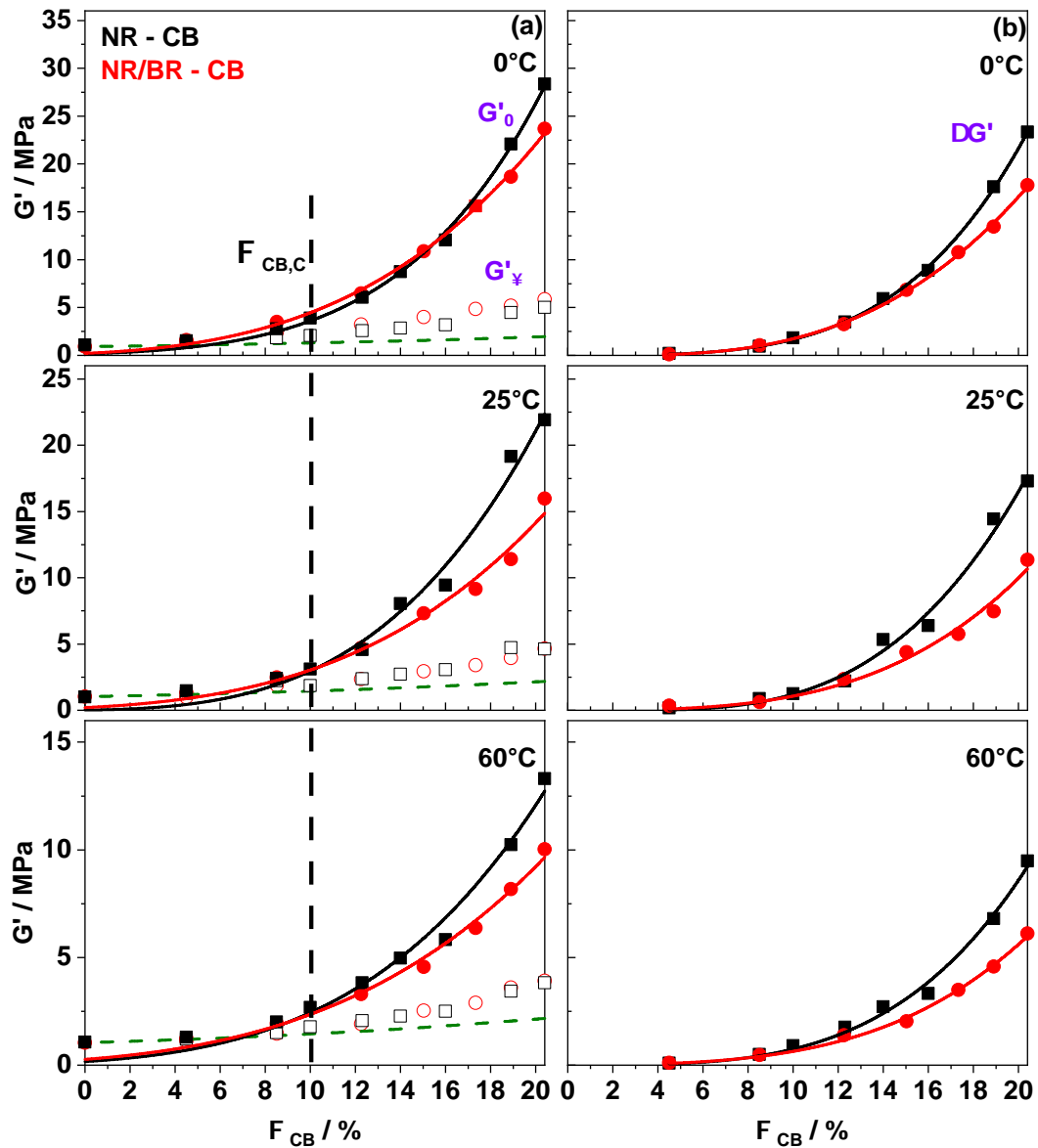


FIGURE 5.6

Temperature and filler fraction Φ_{CB} dependence of (a) G'_0 (filled) and G'_∞ (open) being Kraus fitting parameters for NR-CB (black square) and NR/BR-CB (red circle) composites, black dotted vertical line represents the estimated percolation threshold $\Phi_{C,CB}$ and green dotted line is hydrodynamic reinforcement predictions according to Guth-Gold [102]. (b) Strength of filler network $\Delta G' = G'_0 - G'_\infty$ with respect to carbon black filler volume fraction Φ_{CB} for NR and NR/BR based composites, lines connecting the points are a guides to the eye.

the measured storage modulus values G'_0 above the percolation threshold decrease with temperature, whereas G'_∞ values show a very weak dependence on temperature. The difference between both the limiting modulus values $\Delta G'$ plotted with respect to carbon black loading at three temperatures in figure

5.7 b confirms that the filler network formed by carbon black particles in NR-CB composites contribute slightly stronger to reinforcement in comparison to filler network formed in NR/BR-CB composites. The temperature dependence of $\Delta G'$ shows that the temperature-dependent softening behavior of the filler network is common for both NR-CB and NR/BR-CB composites and indicate that composition of the rubber matrix has a significant influence on filler network contribution to reinforcement.

The parameters obtained by approximating the loss modulus $G''(\gamma)$ by the modified Kraus equation 5.3 are plotted for both NR-CB and NR/BR-CB composites with respect to carbon black loading in figure 5.7. The filler network contributions $\Delta G''_D$ and $\Delta G''_F$, related to dissipation at small strain amplitudes while the filler network is intact and peak intensity at the intermediate strain amplitude show systematic dependence on carbon black loading. Both the contributions are strongly increasing with increase in carbon black loading above the percolation threshold confirming the dominance of filler network related contributions to dissipation in highly filled composites. Additionally, the decreasing trend of both $\Delta G''_D$ and $\Delta G''_F$ with increase in temperature indicate that the softening of filler network influences strongly the dissipation in highly filled composites. At large deformations, the magnitude of absolute G''_∞ values is low in comparison with filler network related contributions to dissipation. Comparing the absolute $\Delta G''_D$ and $\Delta G''_F$ values for NR-CB and NR/BR-CB composites, the trends are similar to those obtained for the filler network contribution to reinforcement, i.e. $\Delta G''_D$ and $\Delta G''_F$ are commonly higher for NR-CB composites. Finally, this clearly indicates that the filler network formed by carbon black in a NR matrix is showing different mechanical properties in comparison to that in a NR/BR matrix. This is an interesting finding and the reasons for the observed differences has forced further investigations. Hence, imaging methods have been applied in order to learn more about the filler

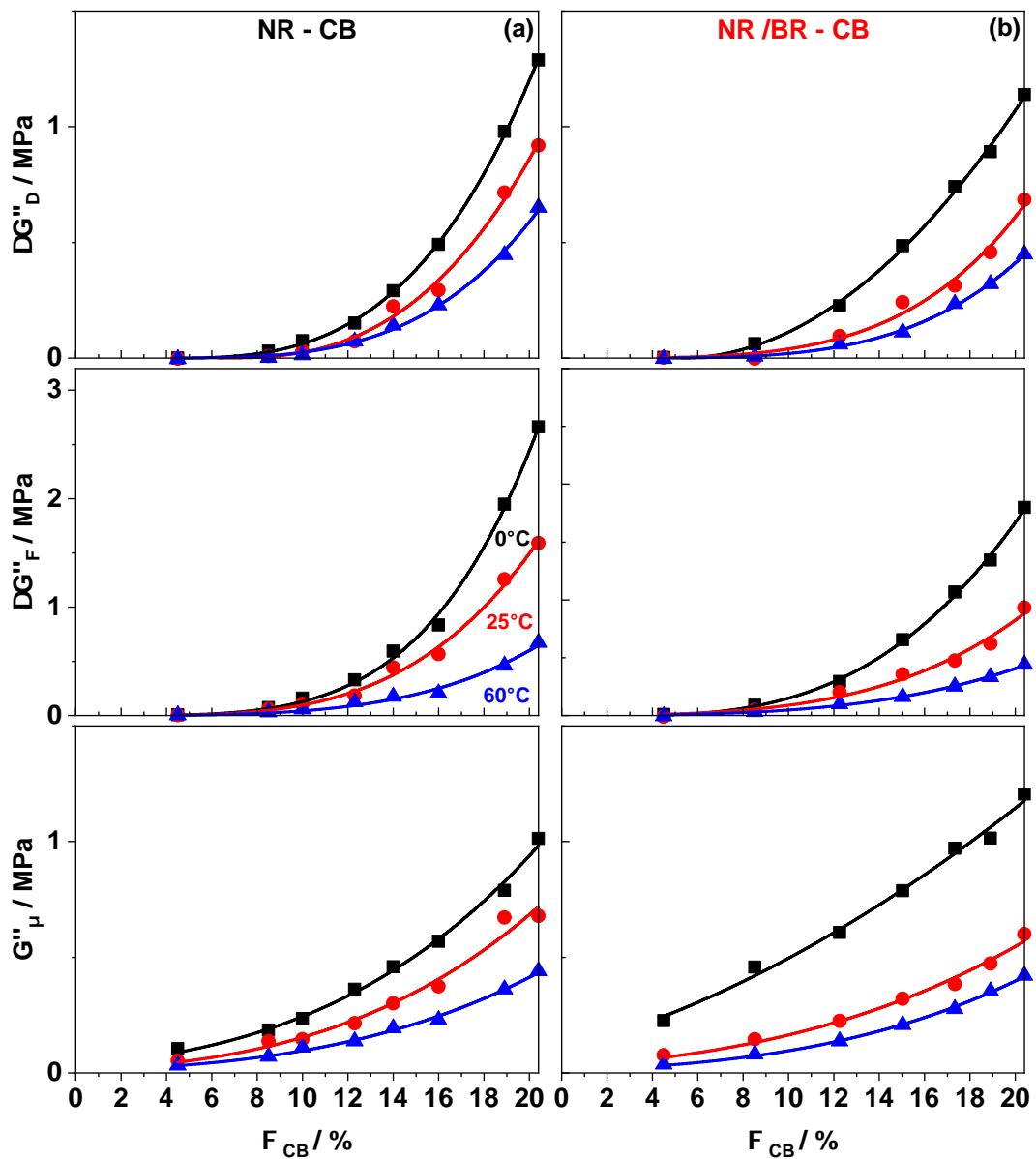


FIGURE 5.7

Values for $\Delta G''_D$, $\Delta G''_F$ and G''_μ as obtained from fits based on equation 5.3 with respect to carbon black loading Φ_{CB} for (a) NR-CB and (b) NR/BR-CB composites measured at three different temperatures 0°C (squares), 25°C (circles) and 60°C (triangles). The line connecting the points is a guide to the eye.

rubber phase morphology and filler dispersion.

The representative TEM images of NR-CB and NR/BR-CB composite containing carbon black Φ_{CB} fractions less than and greater than $\Phi_{C,CB}$ are shown in figure 5.8. In case of composites containing $\Phi_{CB} = 4.5$ vol%, as the filler content is well below the percolation threshold in both NR-CB and NR/BR-CB

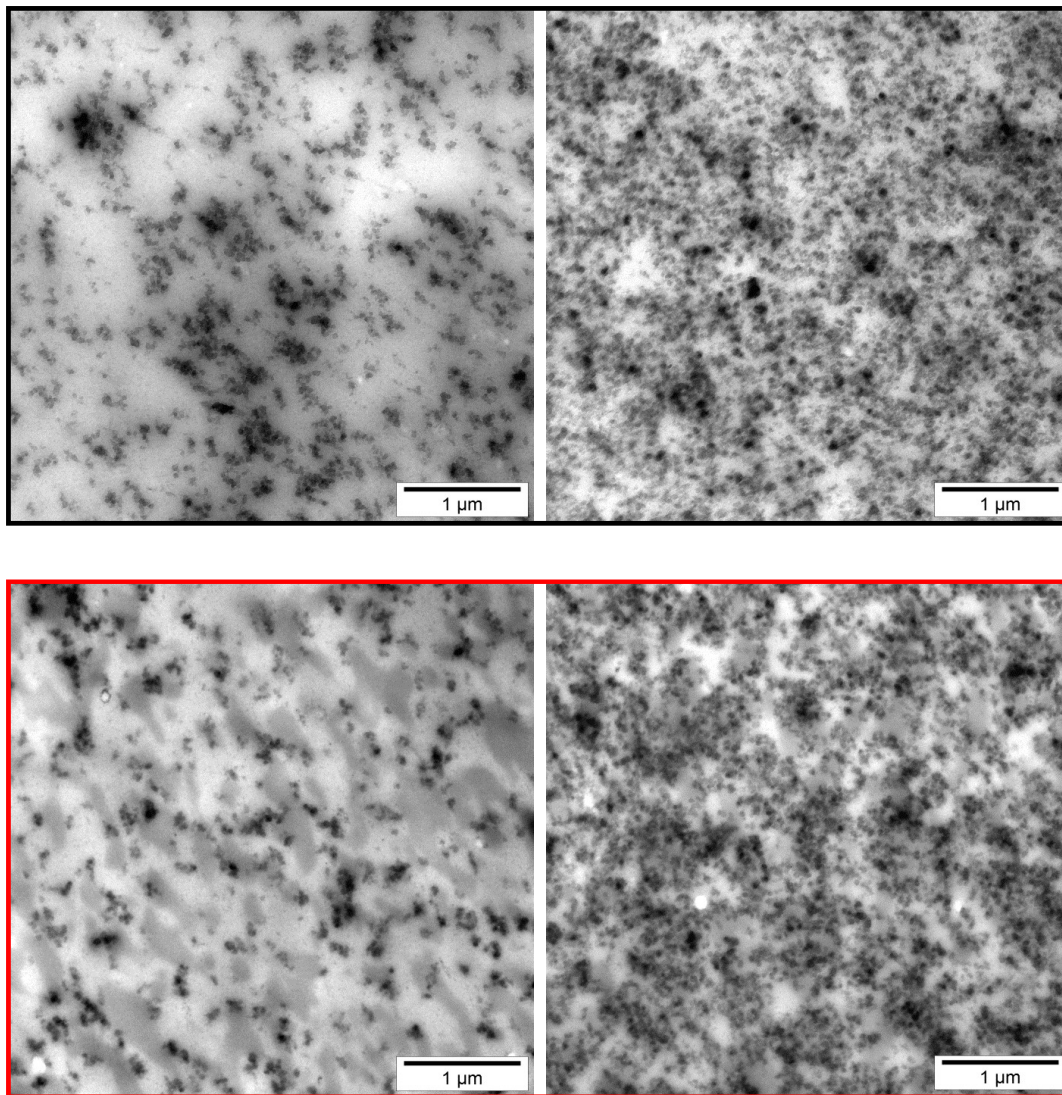


FIGURE 5.8

TEM micrographs for (Top) NR filled with Φ_{CB} : (left) 4.5, (right) 16 vol% and (bottom) NR/BR blend filled with Φ_{CB} : (left) 4.5, (right) 15 vol%, dark gray domains are BR dispersed in light gray NR matrix.

composites, the TEM micrographs enables to identify the filler aggregates that are well dispersed throughout the matrix and are isolated from each other. As expected, NR/BR based composite show a blend morphology, where isolated BR domains are distributed uniformly in NR matrix. Interestingly, the dispersion of the filler particles is quasi identical and the shape of the filler clusters (branched) seems to be preserved in both single and blend system. Although, the filler fraction is well below the percolation threshold, a quantification of the filler localization based on TEM images in both rubber phases seems to be

complicated. The intrinsic problems of this method for that propose (limited phase contrast, superposition of particles in different depth etc) Here alternative methods like AFM have to be considered. In case of composites containing 16 and 15 vol% i.e. filler fractions above the percolation threshold in both NR and NR/BR blend respectively, even a quantitative description of filler dispersion is complicated, as the filler clusters overlap and connect to each other to form a percolating filler network. Nevertheless, an attempt is made to compare the filler dispersion in both single and blend composites. In this attempt the area of unfilled regions, i.e. the regions in the TEM image that obviously do not contain any filler particles, is identified and measured by drawing polygons representing the circumference of such regions. The processed image is shown in figure 5.9 and the histogram of unfilled areas is used to quantify filler dispersion and to compare the situation in NR and NR/BR based composites.

Histograms in figure 5.9(b,d) clearly shows that distribution of unfilled areas in NR composites is not too different from that in NR/BR based composites. The statistical average size obtained from an analysis based on 374 and 328 unfilled areas is 13931 nm^2 and 17843 nm^2 for NR-CB and NR/BR-CB composites, respectively. Another parameter that can be compared is the peak position in both histograms, which seems to be similar for both NR and NR/BR composite. These observations are understood as an indication for an almost identical filler network topology in both the composites above the percolation threshold and a minor influence of the rubber matrix composition on filler network topology in case of NR and NR/BR composites filled with CB.

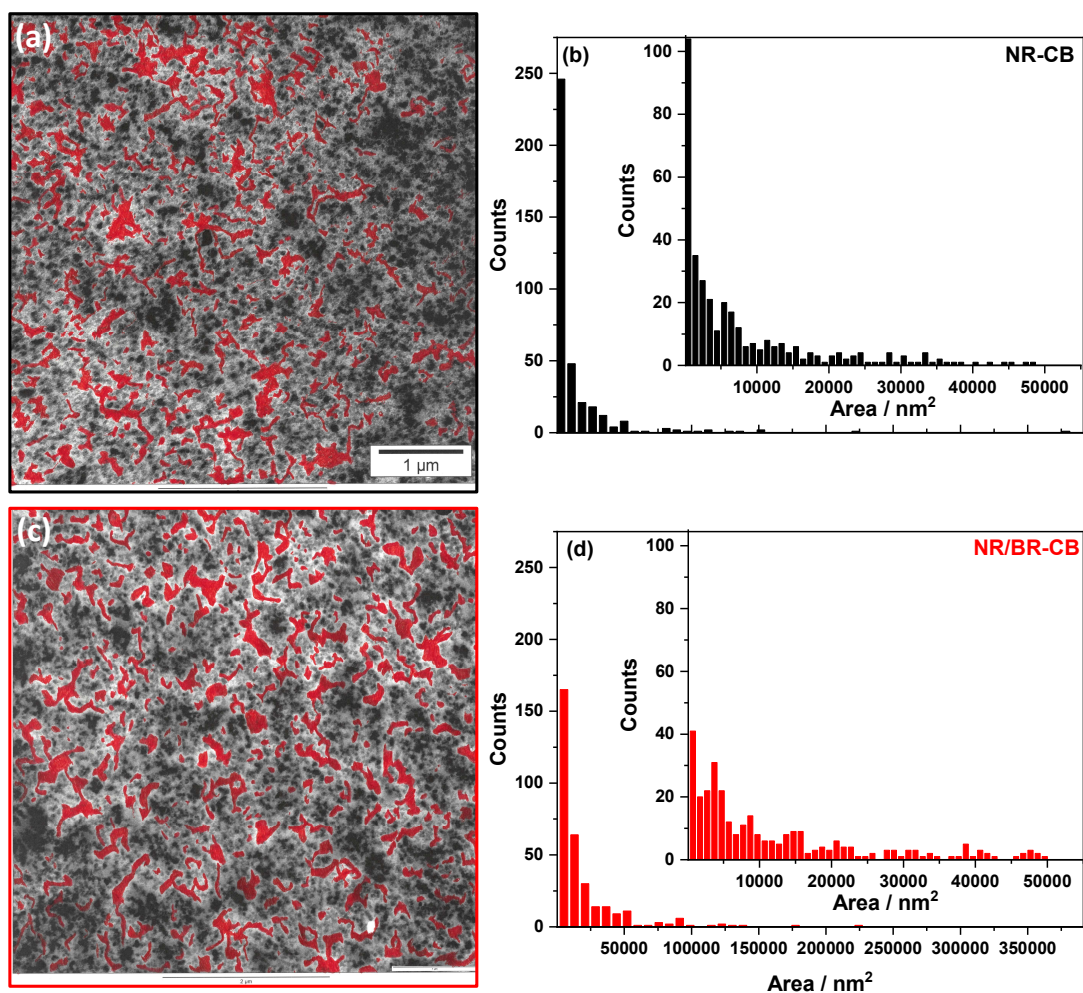


FIGURE 5.9

The unfilled regions in TEM images are filled with red color for (a) NR-CB and (c) NR/BR-CB containing 16 and 15 vol% CB, their areas are estimated by ImageJ software. Histogram (b,d) representing the frequency of unfilled areas in the investigated images (a,c) is constructed by binning the unfilled areas between 100 to 391451 nm^2 into 50 bins (bin size = 7827 nm^2), inset in each histogram is a zoom constructed similarly as the main histogram with bin size = 998 for unfilled areas between 100 to 50000 nm^2 .

5.3 Influence of filler introduction method on the properties of NR/BR nanocomposites

In this section the mechanical properties of NR/BR blends filled with different amounts of carbon black are reported. The rubber matrix of all investigated rubber nanocomposites contains 70 wt% NR and 30 wt% BR. The filler fraction is varied between 0 and 13.7 vol% carbon black N234. Special point of this study is that the method of carbon black incorporation is varied for different series of nanocomposites. The filler is either (i) freshly mixed to the rubber matrix as commonly done in conventional mixing procedure or (ii) introduced first with high concentration in a single rubber producing a so called masterbatch, which is subsequently mixed with all other components to a nanocomposite.

The temperature dependent storage modulus $G'(T)$ and loss modulus $G''(T)$ data show the influence of carbon-black particles on dynamic properties of NR/BR-CB nanocomposites is shown in figure 5.10. The dynamic glass transition temperatures of both NR ($\alpha_{NR} \approx -52$ °C) and BR ($\alpha_{BR} \approx -91$ °C) components of unfilled rubber blend is negligibly influenced for composites containing low (5 vol%) and high fraction (13.7 vol%) of carbon-black. The weak step in $G'(T)$ at about -20°C might be related to melting of a certain crystalline BR fraction,[95] which is quite prominent in data for unfilled rubber samples. In the rubbery plateau region ($T > 0$ °C), both reinforcement ($G'(T)$) and dissipation ($G''(T)$) are almost a decade higher for composites containing $\Phi_{CB} = 13.7\%$ in comparison with composites containing $\Phi_{CB} = 5\%$ and unfilled rubber. Additionally, the temperature dependence of $G'(T)$ for composites containing $\Phi_{CB} = 13.7\%$ is also different than that of composites containing $\Phi_{CB} = 5\%$ and unfilled rubber. A clear decrease of $G'(T)$ with temperature

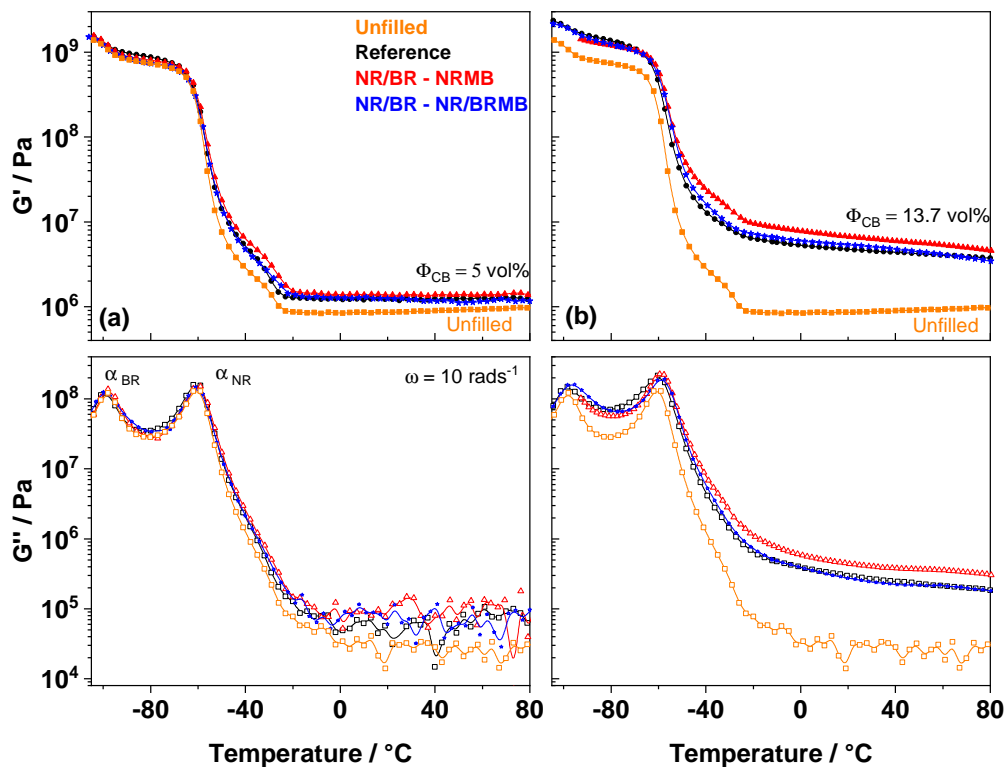


FIGURE 5.10

Dynamic shear storage modulus G' and loss modulus G'' as a function of temperature for differently prepared NR/BR composites (cf. legend). Data for (a) unfilled and composites containing $\Phi_{CB} = 5\%$ as well as (b) unfilled and composites containing $\Phi_{CB} = 13.7\%$ are compared.

is observed like discussed already for other highly filled nanocomposites indicating sequential softening of small rubber fractions. Note that the method of carbon-black incorporation and apparently the proportion of different carbon black masterbatch also significantly influences the degree of reinforcement and dissipation in highly filled composite containing $\Phi_{CB} = 13.7\%$. Higher reinforcement is for NR/BR-NRMB composite prepared solely by NR masterbatch, followed by NR/BR-NR/BRMB composite prepared by replacing 50% NR masterbatch by 50% BR masterbatch. The least reinforcement is observed for reference composite prepared by conventional method of carbon-black incorporation. Qualitatively, the loss modulus data in the rubber plateau range behave similarly. These trends provide a hint that filler network formed at

filler loading above percolation threshold would be different and its contribution to reinforcement and dissipation is significantly dependent on the method of carbon black incorporation.

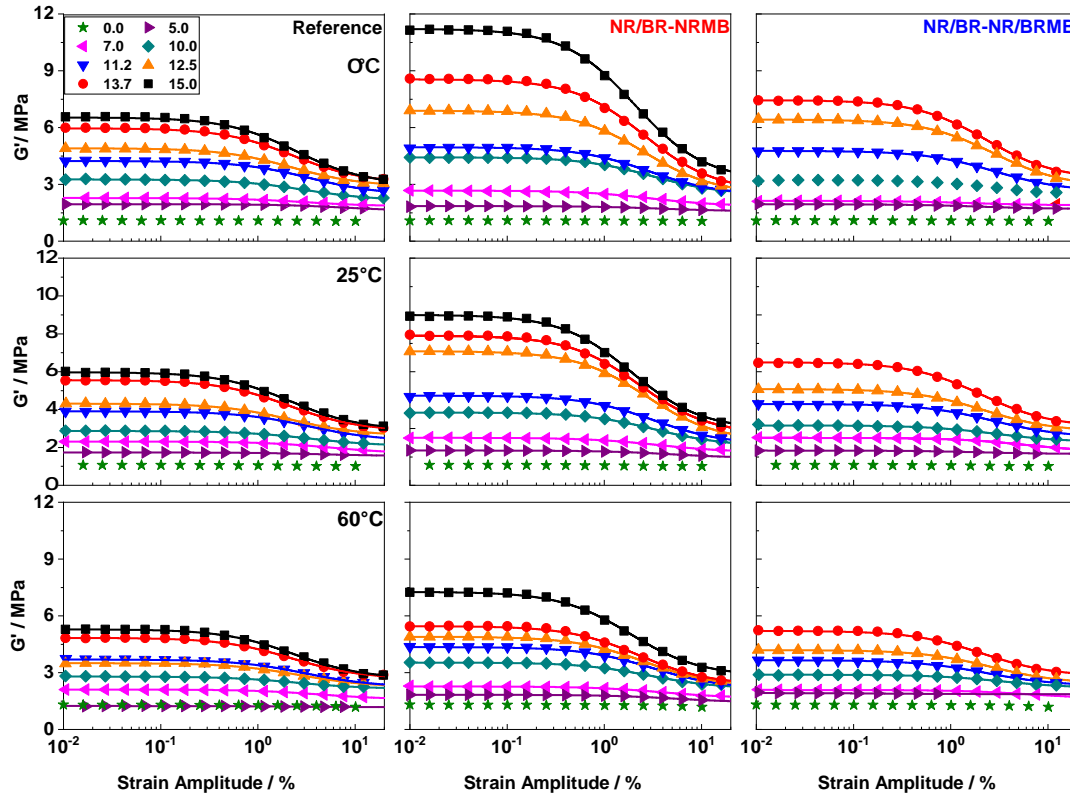


FIGURE 5.11

Dynamic storage modulus G' as a function of shear strain amplitude γ (Payne effect) for NR/BR matrix filled with varied fraction of carbon black Φ_{CB} , (Left) reference, (middle) NR/BR-NRMB and (right) NR/BR-NR/BRMB. All measurements are done at 10 rad/s and temperatures of (top) 0°C, (middle) 25°C and (bottom) 60 °C, while the lines over the data points are fits based on the Kraus equation Eq.5.1.

Strain sweep measurements at different temperatures ($T = 0, 25, 60$ °C) shown in figure 5.11 elucidate the apparent differences between the composites prepared by carbon black masterbatches and conventional method of carbon-black incorporation. As expected, irrespective of carbon-black incorporation method, the initial modulus G'_0 is increasing with carbon black loading and the Payne effect is observed for highly filled composites, indicating the presence of a filler network. At small strain amplitude, the temperature dependence of highly filled composites are similar to that seen in figure 5.10, G'_0 is decreasing

systematically with increase in temperature from 0°C to 60°C. The intensity of Payne effect is showing temperature dependence as G'_∞ is weakly influenced by increasing temperature. In addition, the magnitude of G'_0 in composites containing large fraction of carbon-black is strongly dependent on method of carbon black incorporation and temperature.

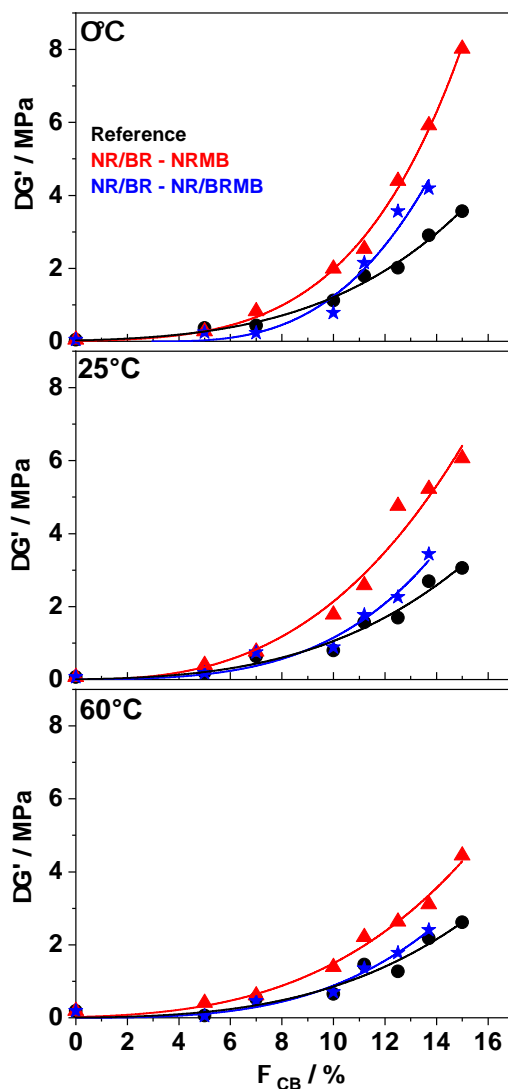


FIGURE 5.12

Strength of filler network with respect to carbon black filler volume fraction Φ_{CB} compared between (circle)Reference, (triangle) NR/BR-NRMB and (star) NR/BR-NR/BRMB at three different temperatures. Lines connecting the points are a guides to the eye.

The difference $\Delta G' = G'_0 - G'_\infty$ (estimated based on fits to equation 5.1) quantifies the carbon-black network contribution to reinforcement and underlines the

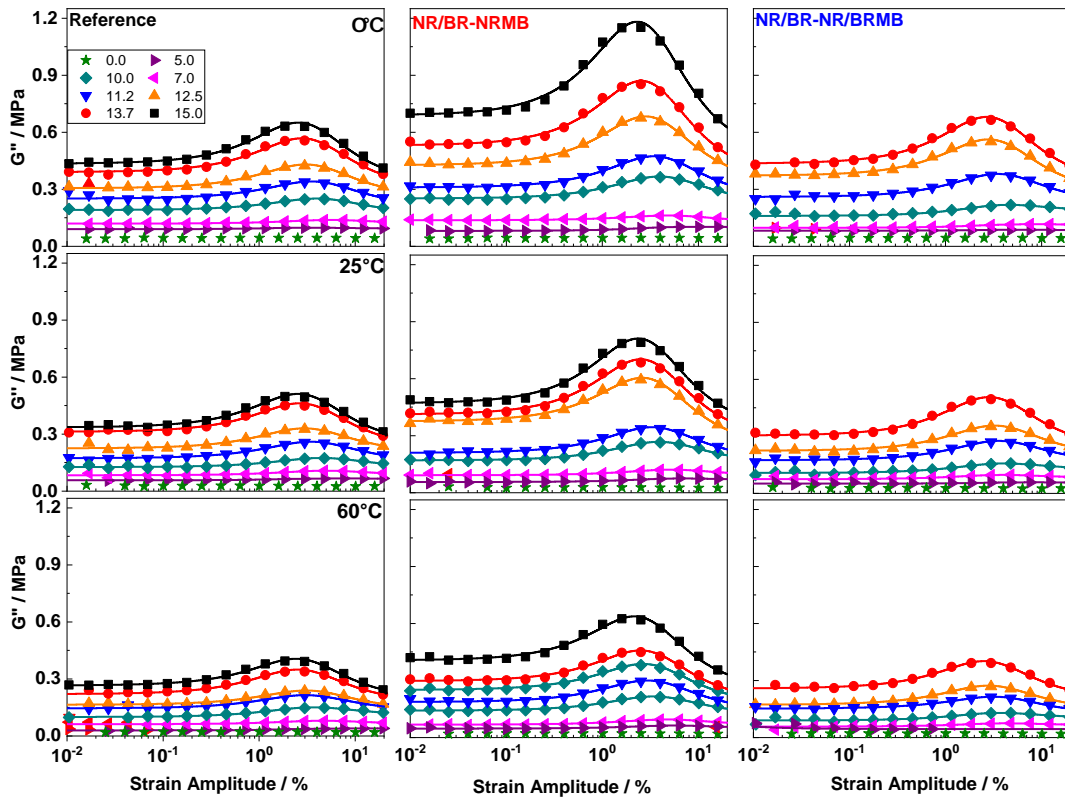


FIGURE 5.13

Dynamic shear loss modulus G'' as a function of shear strain amplitude γ for NR/BR rubbers filled with varied fraction of carbon black Φ_{CB} : (Left) Reference, (middle) NR/BR-NRMB and (right) NR/BR-NR/BRMB. All measurements are done at 10 rad/s and temperatures of (top) 0°C, (middle) 25°C and (bottom) 60 °C. The lines are fits based on the modified Kraus equation 5.3

above mentioned trends figure 5.12. In comparison with reference composites prepared by conventional method of carbon black incorporation the strength of filler network $\Delta G'$ is consistently higher for NR/BR-NRMB composites that are prepared by natural rubber master batch. Followed by NR/BR-NR/BRMB composites that are prepared by 50:50 combination of NR and BR carbon black masterbatches. This confirms that the method of carbon-black incorporation has serious influence on filler network contribution to reinforcement.

The data for dissipation $G''(\gamma)$ measured for the three of NR/BR-CB nanocomposites series at temperatures $T = 0^\circ, 25^\circ, 60^\circ \text{C}$ are shown in figure 5.13. In general, dissipation is increasing with carbon-black content. For composites

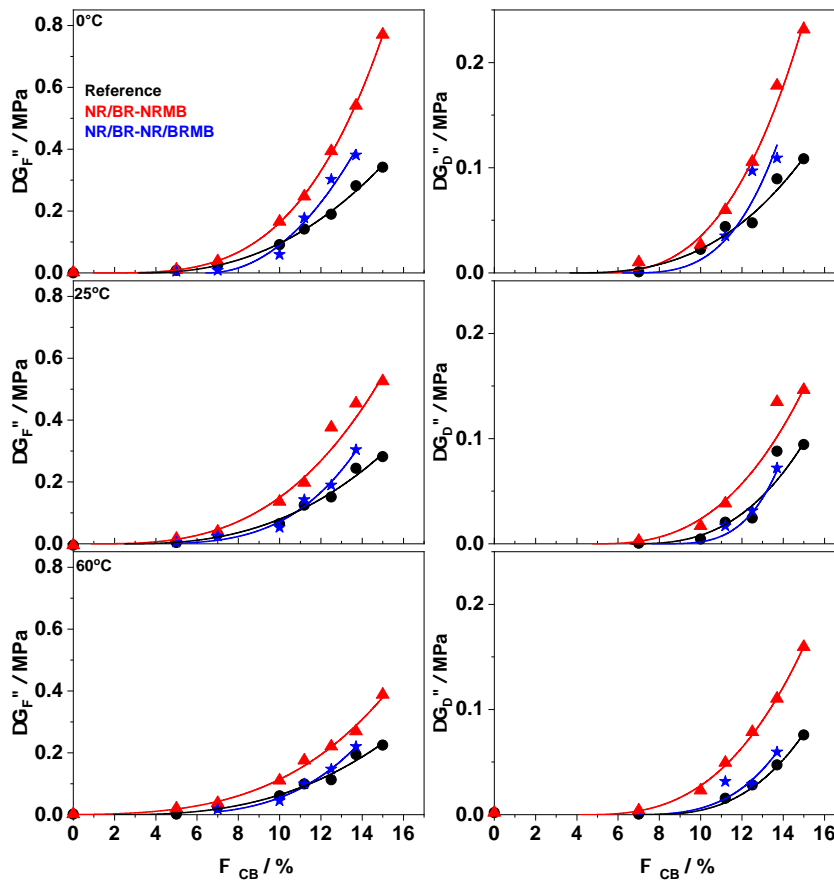


FIGURE 5.14

Fit parameters $\Delta G_F''$ (top) and $\Delta G_D''$ (bottom) as function of carbon black loading Φ_{CB} for NR/BR based composites, where different filler incorporation methods are used. Data for rubber composites, where standard method (circle), NR masterbatch (triangle) and NR/BR masterbatches (star) are used, are compared at three temperatures: (top) 0°C, (middle) 25°C and (bottom) 60 °C. The lines connecting the points are a guides to the eye.

containing large fraction of carbon-black a pronounced Payne effect is observed indicated by a peak at intermediate strain amplitudes. Similar to G_0' , the dissipation at small strain amplitude, G_0'' is increasing with carbon black loading and decreasing with temperature. For highly filled composites, the height of the characteristic peak G_m'' at intermediate strain amplitude is also showing similar trends, while G_∞' shows a weak dependence on temperature and carbon black content as the filler network is broken. Most interestingly, peak heights as well as G_0' are quite different for different filler incorporation methods corresponding to the findings in case of the storage modulus $G'(\gamma)$.

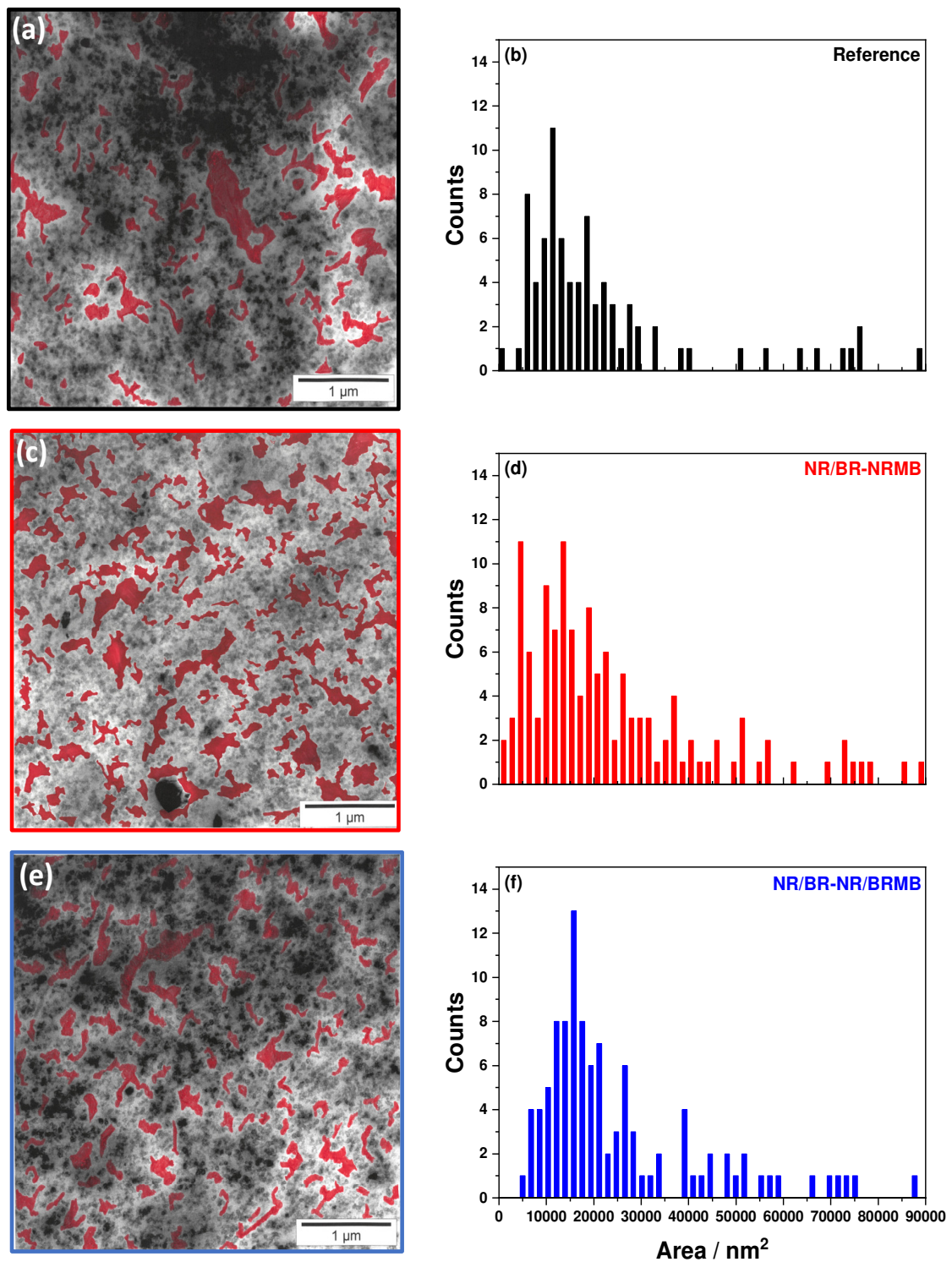


FIGURE 5.15

The unfilled regions are red colored in TEM micrograph for NR/BR composites filled with $\Phi_{CB} = 13.7\%$ carbon black, prepared by (a) conventional mixing, (c) NR masterbatch and (e) NR/BR masterbatches. The unfilled areas estimated by ImageJ software are binned into 50 bins with a bin size of 1798 nm^2 and represented by histograms (b,d,f), respectively.

In order to quantify different filler network contributions to dissipation all data presented in figure 5.13 are fitted to equation 5.3. The obtained parameters $\Delta G''_D$ and $\Delta G''_F$, are plotted in figure 5.14. The absolute values of $\Delta G''_D$ and $\Delta G''_F$ are increasing non-linearly with increasing carbon black content and decreasing with increasing temperature. The composites belonging to NR/BR-NRMB show the highest values, whereas the lowest values are observed for composites that are prepared by conventional method of carbon black incorporation. NR/BR-NR/BRMB composites prepared by 50% of NR-CB and BR-CB masterbatch fall between NR/BR-NRMB and reference composites. Strain amplitude measurements evidence that the filler network contributions to reinforcement and dissipation are dependent on temperature and it varies also with the method of carbon black incorporation method as already indicated in temperature dependent measurements in the linear response range..

Images from TEM for three composites containing $\Phi_{CB} = 13.7\%$ in figure 5.15 reveal the existence of percolated filler network indicated by Payne effect in figures 5.11 and 5.13, respectively. The high carbon-black concentration complicates the evaluation of dispersion and it is difficult to describe the topology of the filler network. In order to come to a quantitative estimate, the area of unfilled regions is analyzed giving a more or less direct information about the level of micro and nano dispersion. Indirectly, this method assists in distinguishing the topology of carbon-black network depending on the method of carbon-black incorporation.

In figure 5.15 histograms quantifying the distribution of unfilled areas are shown. The overall shape of the distributions is seemingly only weakly influenced by the filler incorporation method, despite of the fact that the smaller areas are more populated in case of NR/BR-NRMB composite. The average size of unfilled areas for the composites prepared by masterbatches is only

about 2 and 10% different with respect to the reference NR/BR-CB composite (reference = 29756.44, NR/BR-NRMB = 29006.37 and NR/BR-NR/BRMB = 26680). Note that the integrated area of the unfilled regions is changing a bit more depending on the filler incorporation method. Considering the fraction of unfilled areas in the TEM images one get 10.1% for NR/BR-CB, 15,6% for NR/BR-NRMB and 11.2% for NR/BR-NR/BRMB. However, one should keep in mind that this is only a local snapshot and a statistics on that length scale is requiring an analysis of various TEM images which is at the moment missing (Note that a certain thickness variations in ultra microtomed films can exist). In general, the data seem to indicate that the topology of the carbon-black network is not much influenced by the method of carbon-black incorporation and by the masterbatches uses (NRMB and BRMB masterbatche.)

5.4 BR-SBR diblock copolymer filled with silica

The AFM images of BR-SBR diblock copolymer shown in figure 4.1 clearly indicate the lamellar morphology at the nanoscale is not fundamentally changed due to high shear forces involved during incorporation of silica particles through mechanical mixing process. Only prominent effect of an increasing filler fraction seems to be a reduced long range order. In contrary, the reference composite prepared by SBR/BR blend do not display the defined morphology as seen in diblock copolymer. Interestingly, the silica particles have preferred the styrene rich phase of the investigated BR-SBR diblock copolymer resulting in an architecture of filler network guided by the phase morphology of the block copolymer. For SBR/BR blend based composites though the silica particles show a weak tendency to prefer the SBR phase the dispersion of silica particles seems to be random. As seen in Figure 4.1, this can be explained by the absence of a self-assembled morphology characteristic for the investigated block copolymers as well as much bigger domains and better miscibility in case of the investigated SBR/BR blends.

To identify the influence of filler dispersion on mechanical properties, strain sweep measurements are done at three temperatures (0° , 25° and 60°C) for both block copolymer and blend based composite containing different volume fraction of silica particles. The results for silica filled block copolymers are shown in figure 5.16. The storage modulus at small strain amplitude G'_0 show strong dependence on silica content and it is increasing with increasing the filler content at all the measured temperatures. This increasing the amplitude of the Payne effect, which commonly observed in the strain sweeps related to filler network breakdown. Since G'_∞ at large strain amplitudes is showing a weak dependence with silica content. Note that as a consequence of glass transition temperature of SBR block ($T_g \approx -8^\circ\text{C}$) a Payne effect like features is observed for unfilled block copolymer at 0° . This is indicating that the

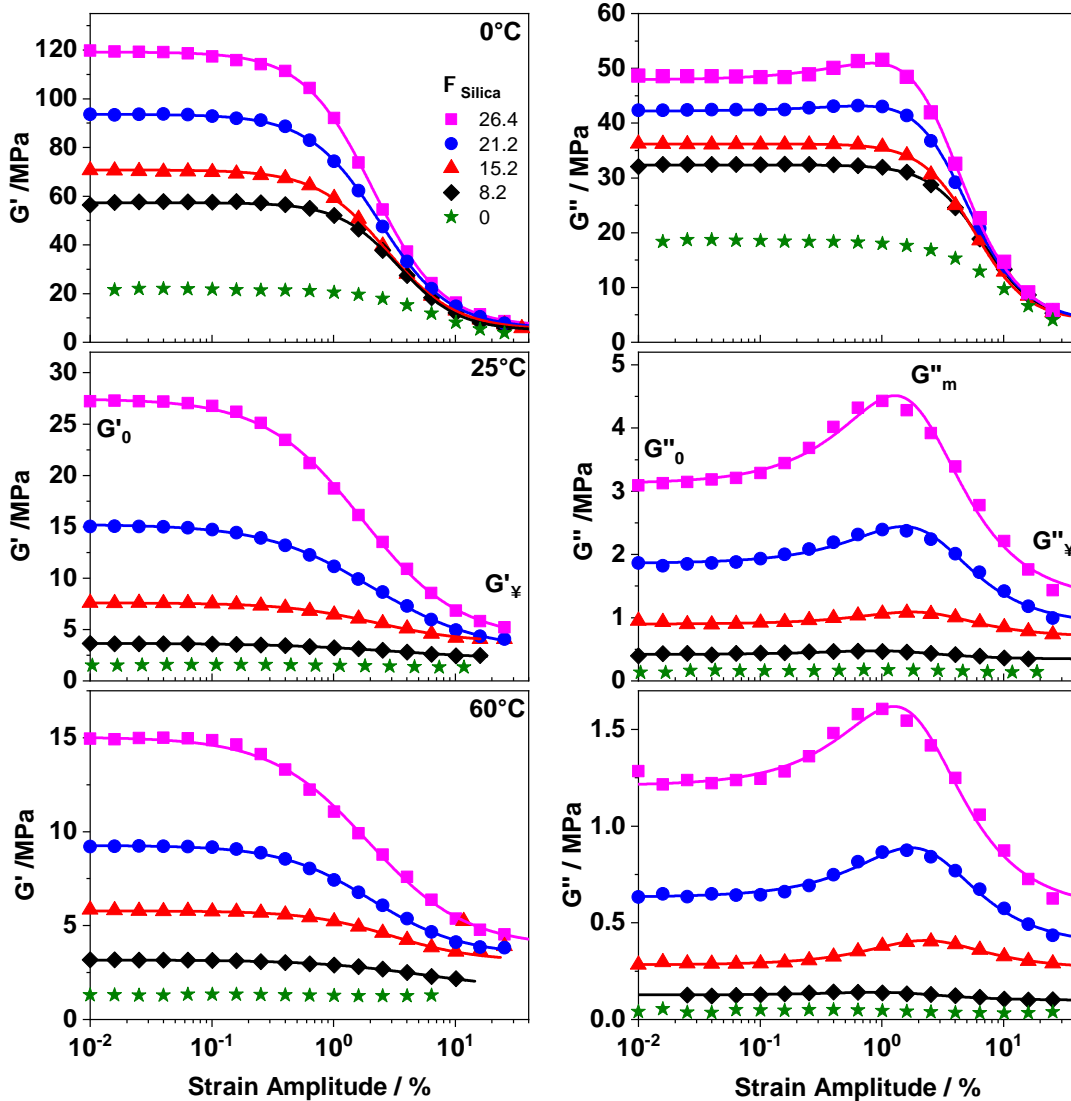


FIGURE 5.16

(left) Storage modulus and (right) loss modulus of the dynamic shear modulus as a function of shear strain amplitude γ for a BR-SBR block copolymer filled with different amounts of silica Φ_{Silica} . All measurements are performed at 10 rad/s and temperatures of (top) 0°C, (middle) 25°C and (bottom) 60°C, while the lines are fits based on equations 5.1 and 5.3.

SBR phase is percolated and accordingly the absolute values of G'_0 for filled composites at 0°C are quite high. At 25°C and 60°C the Payne effect is absent for unfilled BR-SBR diblock copolymer while G'_0 and the amplitude of Payne effect for silica filled composites is significantly reduced as G'_∞ is not only showing a weak dependence on filler content but also on the temperature. Similar to G'_0 , the loss modulus at small strain amplitude G''_0 shows a strong dependence on silica content and temperature. As the strain amplitude is increasing,

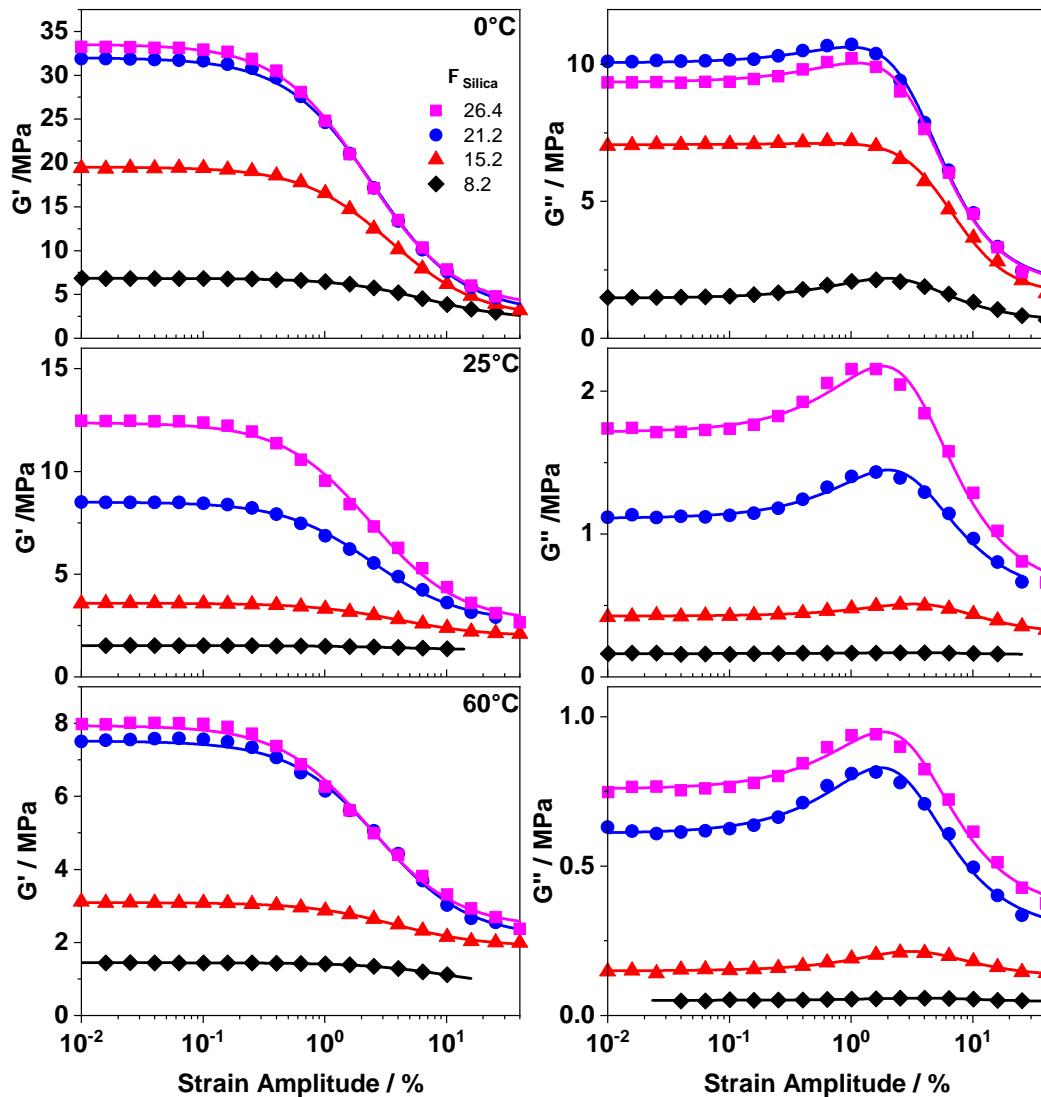


FIGURE 5.17

(left) Storage modulus and (right) loss modulus of the dynamic shear modulus as a function of shear strain amplitude γ for SBR/BR blend based composites filled with different amounts of silica Φ_{Silica} . All measurements are performed at 10 rad/s and temperatures of (top) 0°C, (middle) 25°C and (bottom) 60°C, while the lines are fits based on equations 5.1 and 5.3.

a simoidal decrease in G'_0 is accompanied by the peak characterized by the height G''_m reflecting the Payne effect. As in case of G'_∞ , the loss modulus at large strain amplitude G''_∞ is weakly dependent on filler fraction as well temperature. The temperature dependence of G'_0 and G''_m is qualitatively similar to that observed in G'_0 , with increase in temperature all the values are reducing for all the composites. Note that Payne effect-like features are also found in $G''(\gamma)$ at 0°C for the unfilled block copolymer supporting the interpretation

that the percolating SBR phase is already partly glassy under these conditions. Strain amplitude dependent storage and loss modulus data for SBR/BR blend based composites are shown in figure 5.17. The Payne effect is observed for these composites at all the measured temperatures except the SBR/BR blend containing 20 Phr silica at higher temperatures ($\geq 25^\circ\text{C}$). In general, all trends seen in BR-SBR block copolymer-based composites are preserved. In particular, a significant reduction of the Payne effect in $G'(\gamma)$ and $G''(\gamma)$ is seen with increasing filler content and decreasing silica fraction like in other cases. A clear difference compared to BR-SBR-based composites is that the amplitude of the Payne effect in G' and G'' is obviously smaller for all filler contents at temperatures below 60°C .

Strength of the filler network $\Delta G'$ as well as filler network related contributions to dissipation $\Delta G''_D$ and $\Delta G''_F$ taken from equations 5.1 and 5.3 for silica filled BR-SBR block copolymers and SBR/BR blends are compared in figures 8.3 and 8.4. Consistently, the values are higher for block copolymers in comparison with the SBR/BR blend composites with identical silica contents if lower temperatures ($T < 60^\circ\text{C}$) are considered.

6 Discussion

6.1 Common origin of dissipation and reinforcement in rubber nanocomposites

Viscoelastic filler-network. It is well known that incorporating nanosized particles in the rubber matrix changes the composite's mechanical properties by altering the viscoelastic properties.[18] For instance, 20.4 vol% of carbon-black incorporation into the NR increases the shear loss modulus G'' and storage modulus G' at ambient temperature, in the rubbery plateau region by a factor of 54 and 23, respectively (figure 5.2). Due to the lack of an appropriate approach, detailed understanding at the molecular level about the origin of such a significant change in mechanical properties is limited.[154, 158] Common understanding in application relevant rubber nanocomposites containing a large fraction of filler particles is that filler network contributions to reinforcement are much larger than the hydrodynamic effects.[13, 25] This underlines that the filler network related to a percolating solid phase above the percolation threshold is of major importance for the performance of rubber composites. While early models assume that the filler network is caused by filler-filler interaction [9, 10, 108] more recently glassy rubber bridges interconnecting filler particle have been discussed.[25, 117, 151, 152] Common assumption of different approaches is that immobilized rubber layer with a thickness of 1-3 nm exist on the surface of filler particles.[46, 90, 132] Studies focusing on the temperature and frequency dependence of filler network related contributions

to reinforcement in rubber composites show that immobilized rubber in the filler's vicinity has molecular dynamics different from bulk rubber and is speculated to be of importance as it connects the filler particles in the percolated filler network softens sequentially with increasing temperature and decreasing frequency.[46] This immobilized fraction has to be clearly distinguished from bound rubber.[157] The major difference between both types is that immobilized rubber fraction is relatively small, around 1 to 3 % depending on the filler content, specific surface area of the filler and measurement temperature. It is supposedly in a glassy state but heterogeneous showing a gradient in density and resulting in unusual softening behavior occurring at lower frequencies or higher temperatures. Contrary, the bound rubber is a fraction, which cannot be extracted by a good solvent, and its volume depends on different parameters such as filler matrix interaction and molecular weight of the used rubber. Its volume is generally much higher than that of immobilized rubber.

Several studies have demonstrated the difference between bound rubber and immobilized rubber by techniques that give information about molecular dynamics like DSC, NMR, DMA, Dielectric, and SANS.[117, 132, 138, 147, 148, 151, 157] However, even within these studies different interpretations have been chosen. Few studies have distinguished immobilized rubber fraction into layers with intermediate molecular mobility and glassy layer. Such approaches lead to immobilized rubber layer thickness estimations from few to several nanometers depending on the assumptions made.[37] In several cases it is not clearly defined what type of mobility is really considered and which length scales are relevant for the underlying motions.

Recently, Mujtaba et al. have studied SSBR filled with silica particles combining strain sweep at various temperatures by of DMA and a special solid

state NMR spectroscopy method giving quantitative information about immobilized rubber fractions with the intention to recognize filler network contributions to reinforcement.[25] The conclusion of this studies is that the filler network, which is originally described as an infinite path of solid particles, indeed incorporates viscoelastic elements. It is proposed that immobilized rubber fractions on the filler surface are formed resulting in glassy rubber bridges connecting the filler particles and being part of the filler network. This glassy rubber fraction exhibits a gradient in the glass temperature (T_g) explaining sequential softening and viscoelastic behavior of the filler network. The volume fraction of immobilized rubber quantified in this study is in the range of 1 to 3 vol% depending on temperature and filler fraction.

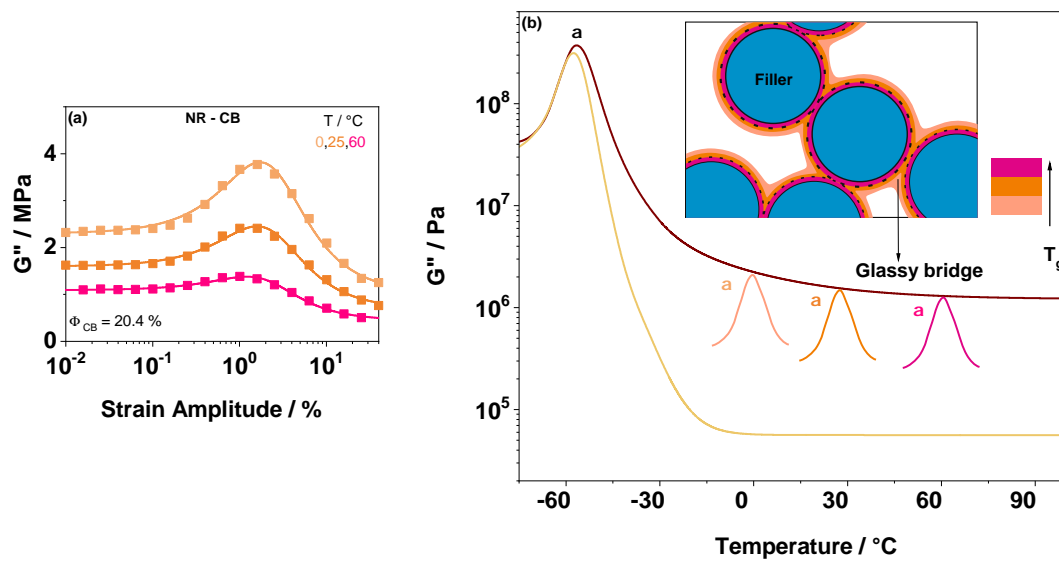


FIGURE 6.1

(a) Strain amplitude dependent loss modulus $G''(\gamma)$ at three different temperatures for NR filled with 20.4 vol% of CB and (b) a schematic showing a temperature dependence of loss modulus $G''(T)$ for unfilled and highly filled composite. The inset scheme shows the viscoelastic filler network. For the visualization purpose, the gradient in the glass transition temperatures of the glassy bridges is represented by three colors that corresponds to three T_g and relevant with strain amplitude dependent measurement temperatures.

A sketch showing the possible localization of this tiny fraction of immobilized rubber within the filler network is shown in the inset of the figure 6.1.[159] Its

formation may be attributed to physical adsorption phenomena. A potential explanation is that rubber chain segments very close to the filler surface pack different from the bulk situation and are densified due to strong interactions between rubber and filler. In this regard, the volume of immobilized rubber or the number of glassy bridges would increase with the filler loading or with available surface area. The physical picture highlights the specific importance of the glassy bridges, which soften sequentially at temperatures of several 10K higher than the bulk rubber's glass transition.

The reinforcement data obtained for different rubber composites in this work strongly supports the physical picture described above. In highly filled rubber composites, the temperature dependence of $\Delta G'$ is due to variation in immobilized rubber fraction in the glassy bridge. The glassy bridge's cross-section would increase with a decrease in temperature. Accordingly, the filler network's load-carrying capacity increases. The glassy rubber bridges break for shear strain significantly larger than 1%, resulting in the Payne effect, as they are the weakest component of the filler network.

A question that remained basically open in earlier studies is that for the molecular origin of different dissipative contributions seen in the strain amplitude dependent loss modulus (G''_{γ}). For the first time in this work, filler network-related contributions to dissipation are isolated and quantified by a modified Kraus equation for loss modulus and associated to specific molecular mechanisms by considering their temperature dependence.

Quantification and understanding of different contributions to dissipation. A central result of this work is the observation that the modified Kraus equation 5.4 is required to approximate the loss modulus (G''_{γ}), since the original equation 5.2 proposed by Kraus fails to approximate the amplified dissipation at small strain amplitudes for composites containing a large volume fraction of filler particles. The finding is that the sigmoidal term $\widetilde{G''}_{\gamma,D}$ and the peak-like

term $\widetilde{G''}_{\gamma,F}$ capture the filler network contributions to dissipation. The experimental results accumulated in this work strongly suggest that the origin for both the contributions are physically different although both are dependent on filler fraction and measurement temperature. An interpretation for both filler network-related contributions to dissipation in accordance with the viscoelastic nature of the filler network is given below:

- $\widetilde{G''}_{\gamma,D}$: Dissipation due to oscillatory deformation of intact glassy rubber bridges in the filler network (dominates at $\gamma < 0.1\%$)
- $\widetilde{G''}_{\gamma,F}$: Dissipation due to fracture of glassy rubber bridges.

In addition an extra contribution to dissipation is commonly observed and related to

- G''_{∞} : Dissipation independent from the filler network.

From this point of view, the amplified dissipation, G''_0 is due to oscillatory deformations of all initially intact glassy bridges (N_0) in the percolated filler network. For strain amplitudes more than approximately 1% the number of glassy bridges (N_0) decreases sigmoidally, as proposed by the Kraus, explaining the sigmoidal decrease in the storage modulus (G'_γ). Consequently, a similar sigmoidal contribution in G''_γ related to $\widetilde{G''}_{\gamma,D}$ occurs in addition to the peak related to $\widetilde{G''}_{\gamma,F}$ arising due to the heat dissipated during the breakage of glassy bridges. Note that also the peak height G''_m of the latter contribution should be proportional to the number of initially intact bridges N_0 , i.e. depending on filler fraction and temperature.

In this regard, an increase in loss modulus (G'') in the rubbery plateau region for the filled rubber composite compared with the unfilled rubber seen in linear response measurements with small strain amplitude can be discussed. For instance, in figure 6.1(b) the amplified dissipation in rubber plateau region for composite containing a percolated filler network can be rationalized by the

physical picture assuming glassy rubber bridges connecting the filler particles. The dissipation that decreases over broad temperature range well above the bulk α relaxation temperature of the rubber matrix for the filled composite is understood as a consequence of sequential softening of small immobilized rubber fractions. In the linear response regime, a step like decrease in G' shall result in a peak like contribution in G'' resulting in the amplified dissipation. If sequential softening of small fractions with different T_g appears within immobilized rubber fractions forming glassy rubber bridges. Then, the findings in $G^*(T)$ for highly filled composites measured using small strain amplitudes can be related to a reduction in the glassy rubber bridge volume with the temperature.

The temperature dependence of initial dissipation G''_0 in the figure 6.1(a) can be understood through the same physical picture. The behavior results from a reduction in the volume of the immobilized rubber in the glassy rubber bridges. As a consequence, not only the dissipation due to the deformation of the glassy bridge ($\widetilde{G''}_{\gamma,D}$) reduces, the heat released due to the breakage of the glassy bridge ($\widetilde{G''}_{\gamma,F}$) should also reduce. In particular a prediction is that the step height $\Delta G''_D = G''_0 - G''_\infty$ and peak height $\Delta G''_F = G''_m - G''_\infty$ should increase with filler fraction and decrease with temperature, respectively. The results accumulated for different kinds of rubber composites studied in this work support qualitatively the proposed picture without exception.

A prediction of the proposed approach, which can be used for a quantitative check, is that both $\Delta G''_D$ and $\Delta G''_F$ are proportional to the initial number of relevant bridges (N_0), where the filler network is intact, as the number of glassy bridges at large strain amplitudes is considered to be zero. In this respect, one can conclude that the total number of glassy bridges (N_0) that amplify the dissipation at small strain amplitudes are the number of glassy bridges that break at deformations larger than $\approx 1\%$ and contribute to dissipation

as heat due to breakage of glassy bridges. The plot of $\Delta G_D''$ vs $\Delta G_F''$ in figure 6.2 evidence that both the contributors to dissipation are proportional to each other supporting that the used picture is applicable.

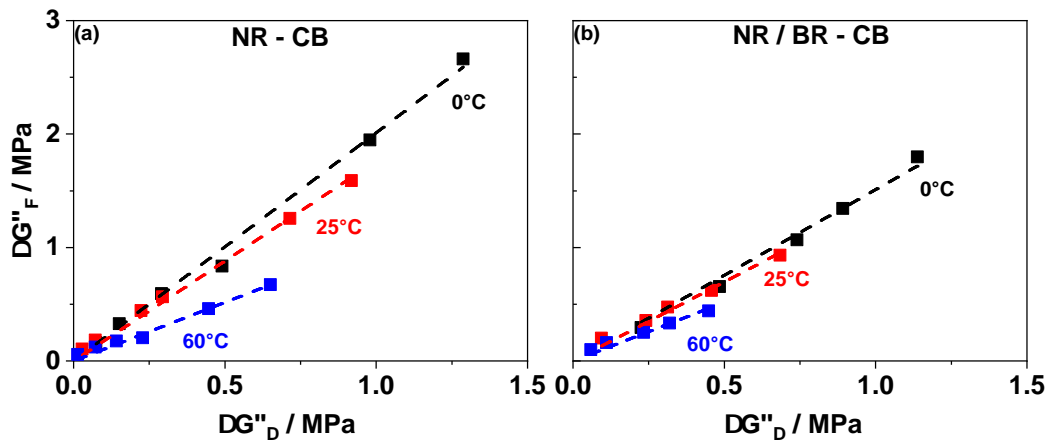


FIGURE 6.2

$\Delta G_F''$ vs. $\Delta G_D''$ for (a) NR-CB and (b) NR/BR-CB composites at three temperatures: 0°C (black), 25°C (red) and 60 °C (blue).

In summary one can conclude that the results from this work for different kinds of rubber composites containing different types of matrix and filler support the suggested interpretation. Although the glassy bridges are the source for both filler network related contributions to dissipation and both are proportional to the initial number of intact bridges, the physical origin of $\Delta G_D''$ and $\Delta G_F''$ is different. Despite of this proportionality both quantities are different since the heat needed for breaking glassy bridge q_F and dissipation due to deformation of a glassy bridge q_D are independent quantities which are also different for different composites and measurement conditions.

Relation between dissipation and reinforcement. Following the proposed interpretation, reinforcement and dissipation can be quantified using the modified Kraus model and their molecular origin is understandable through a common picture. Figure 6.3 shows the proportionality between filler network-related contributions to dissipation and strength of the filler network. Commonly an increase in dissipation and reinforcement with an increase in filler

fraction can be related to the number of glassy bridges (N_0), while their temperature dependence can be related to the sequential softening of the immobilized rubber fraction. The results consistently show that the filler network contribution to the reinforcement in $\Delta G'$ rubber composite is closely connected with both dissipative contributions related to the filler network, $\Delta G_D''$ and $\Delta G_F''$. All three quantities increase with increasing the filler content and decreasing temperature.

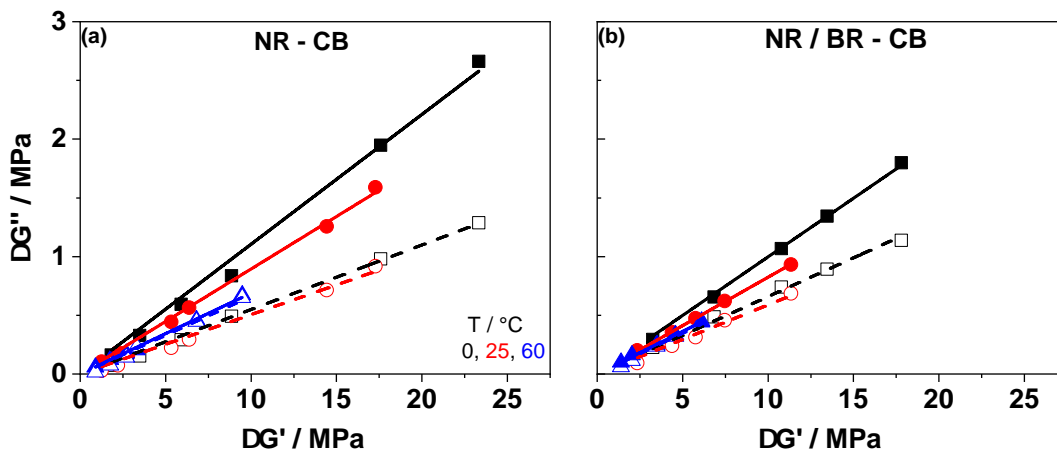


FIGURE 6.3

$\Delta G''$ vs. $\Delta G'$ for (a) NR-CB and (b) NR/BR-CB composites at three temperatures: 0°C (black), 25°C (red) and 60°C (blue). Closed symbols represent $\Delta G_F''$ and open symbols represent $\Delta G_D''$.

The details are dependent on the investigated composite since the individual prefactors depend on specific properties like filler surface area, shape of filler aggregates, filler-rubber interaction, dissipation in the glassy state etc. Within the proposed physical picture, there is a common origin of reinforcement strength and dissipation caused by the filler network. Glassy rubber bridges that carry the load as long they are intact, and dissipate energy during small oscillatory deformation as well as if they break at large deformations.

6.2 Factors influencing reinforcement and dissipation

An interesting advantage of this work is that composites series are studied where the influence of different factors can be systematically assessed. An important finding is that the viscoelastic filler-network related contributions to dissipation and reinforcement can be quantified by a common model. An arising question is, however, how to explain specific differences between the different types of composites depending on the types of filler, rubber matrix, and processing conditions. These aspects are in the focus of the following part of the discussion. The hypothesis which is considered here, is that there are commonly two main reasons for differences in the mechanical properties of the filler network in different rubber composites: (1) chemical composition of the glassy rubber bridges and (2) filler network topology.

Influence of the rubber matrix. Clear differences in the filler network contributions to reinforcement and dissipation are seen in the comparative plots (figures 5.6 and 5.7), for NR-CB and NR/BR-CB composites. The result indicate that filler network in bi-phasic rubber composite is different from that in a single rubber composite. Considering the glassy rubber bridges as very important part of the filler network, and the fact that the filler dispersion seems to be quite similar in NR- and NR/BR-based composites (figure 6.4) one can conclude that differences in the chemical composition of the glassy rubber bridges are main reason for the observed differences in reinforcement and dissipation related to the filler network.

Starting from the natural assumption that the NR/BR ratio in the glassy rubber bridges between filler particles is 70/30 in accordance with the overall NR/BR blend ratio changes in the filler network properties are expected. In this context, an explanation for the differences between the NR-CB and NR/BR-CB

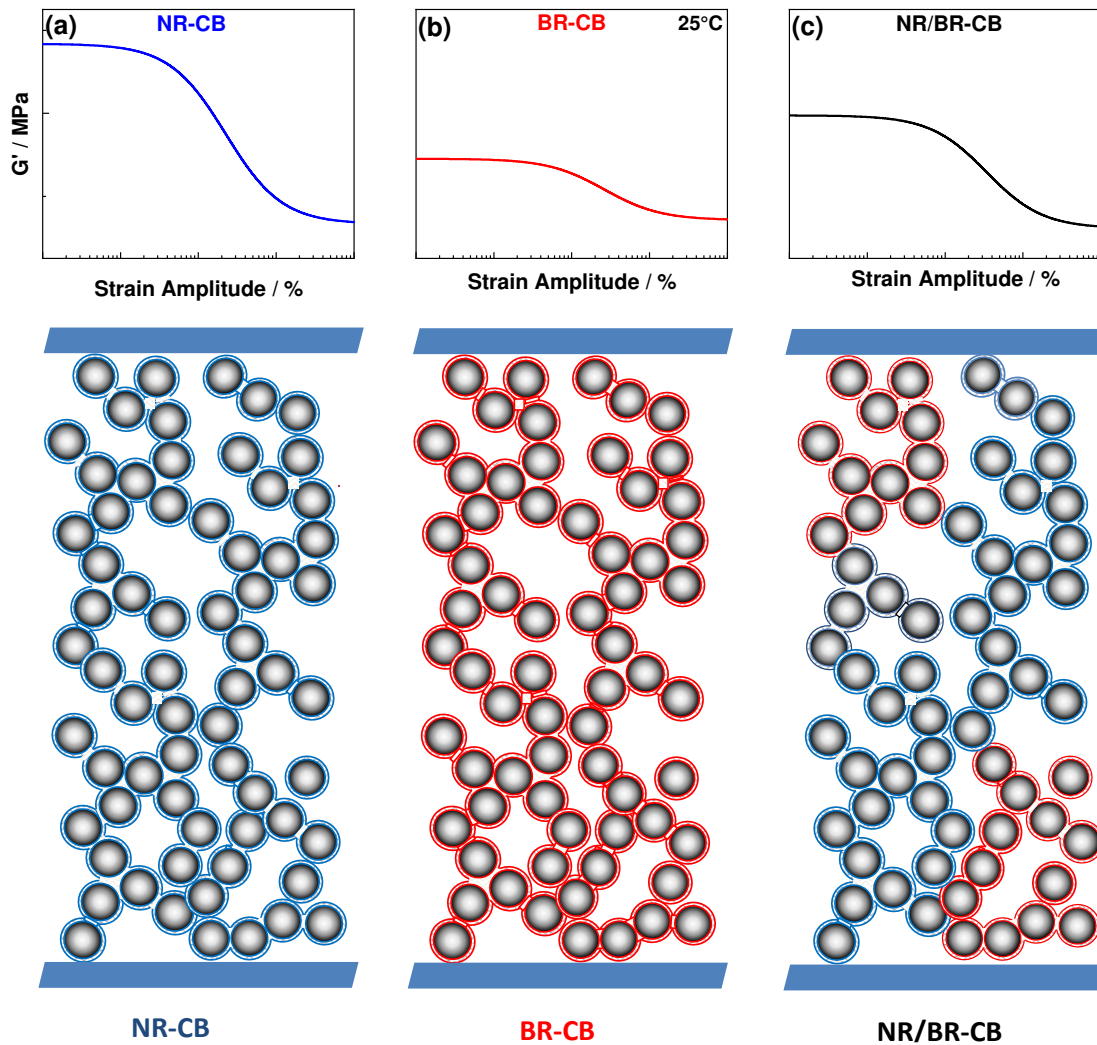


FIGURE 6.4

Scheme to describe the difference between NR-CB and NR/BR-CB by considering identical topology of filler network. The magnitude of the Payne effect for (a) NR-CB, (b) BR-CB and (c) NR/BR-CB can be related to the chemical composition of the glassy rubber bridges. It is considered that at a given temperature, the strength of glassy NR bridge (blue) is relatively higher than that of glassy-BR bridges (red).

composites is the presence of glassy BR bridges along with glassy NR bridges. Glassy bridges containing NR as well as BR should be different since NR and BR are immiscible. Figure 6.4 illustrates the expected situation in NR-CB, BR-CB and NR/BR-CB composites at an identical filler loading and temperature. For the sake of simplicity, microdispersion of carbon-black in both NR-CB and NR/BR - CB is assumed as similar, i.e., the topology of the filler network in both the composites would be the same, as the preparation of these composites is made under identical processing conditions. Correspondingly, the total

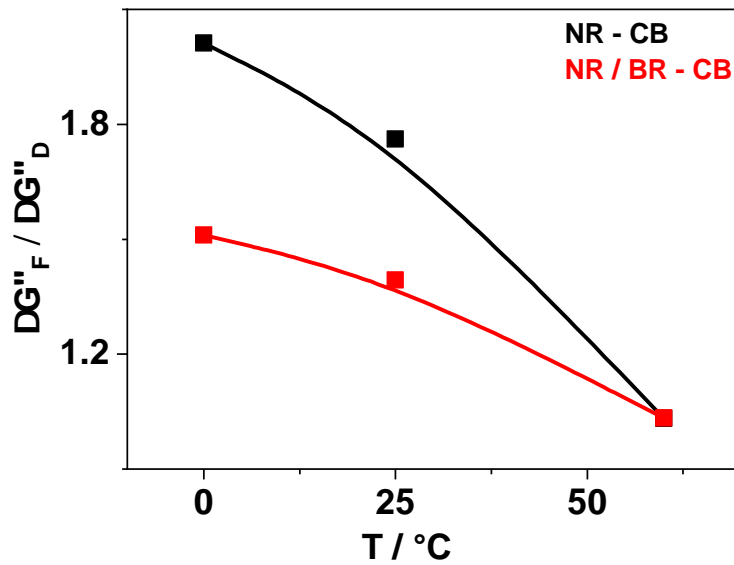


FIGURE 6.5

Ratio of $\Delta G_F''$ to $\Delta G_D''$ with respect to temperature for NR-CB (black) and NR/BR-CB (red). As both the parameters are proportional to initial number of contacts N_0 , which is considered to be constant in both of these composites as the micro-dispersion for TEM image analysis is same, the ratio represents the ratio of proportionality constant q_F to q_D indicating that glassy rubber bridge composition matters and defines the temperature dependence of the dissipative parameters.

number of glassy bridges in the initial state, N_0 would be identical. Clear is that glassy NR bridges are stronger and dissipate more energy as compared to glassy BR bridges under identical conditions. Hypothetically this might be related to a larger volume fraction of immobilized rubber in NR-CB composites compared to the immobilized-BR fraction in the BR-CB composites, due to a larger difference to the bulk rubber T_g resulting in higher load carrying capacity of the NR-CB composite. The proposed argument holds not only for the strength of the filler network but also for filler-network related contribution to dissipation and can explain why, the temperature dependence of $\Delta G_D''$ and $\Delta G_F''$ is different in NR/BR-CB composites in comparison with NR-CB. The quantities are consistently lower if a BR fraction is present in the rubber matrix, similar to observations in reinforcement data. Although $\Delta G_D''$ and $\Delta G_F''$ for both investigated rubber composites are proportional to each other and are related to the initial number of contacts, their ratios are different, as observed in

figure 6.5. This trend indicates that the glassy bridge's chemical composition also defines both the quantum of heat released due to the fracture of glassy bridges (q_F) and heat due to dissipation in intact glassy bridges (q_D). Note that the temperature dependence of NR-CB composite is also more pronounced in comparison to that of NR/BR-CB composite. Only at the highest investigated temperature (60°C), where the number of truly intact glassy rubber bridges is really small, the $\Delta G_F''/\Delta G_D''$ ratio for both composites is comparable.

Influence of the filler incorporation method. The discussion about differences between the filler network in NR-CB and NR/BR-CB composites in the recent paragraph is resulting in the conclusion that main reason for differences is the glassy rubber bridge's chemical composition. In this respect, the results of NR/BR-CB composites prepared by changing the method of filler introduction are also very interesting since the use of masterbatches should influence the type of rubber at the surface of the filler particles significantly. It is reasonable to assume that the immobilized rubber's chemical composition is basically defined by the type of rubber which comes in contact with the filler first. Probably the glassy bridge composition would not be altered by thermodynamically driven preference of the filler for a specific rubber-type due to low mobility of the immobilized rubber layers attached to the filler and limited time during the mixing process and before vulcanization. If this assumption is valid the masterbatch matrix defines the chemical composition of the glassy bridges and could also influence filler localization in the rubber phases driven by thermodynamic parameters.

From the TEM images and unfilled area analysis (figure 5.15), it is inferred that the micro and nano dispersion of the carbon-black in the blend composites is only moderately influenced by the usage of masterbatch. The average sizes of the unfilled domains for NR/BR composites prepared by masterbatches vary only by 10%, and their distribution are relatively similar to

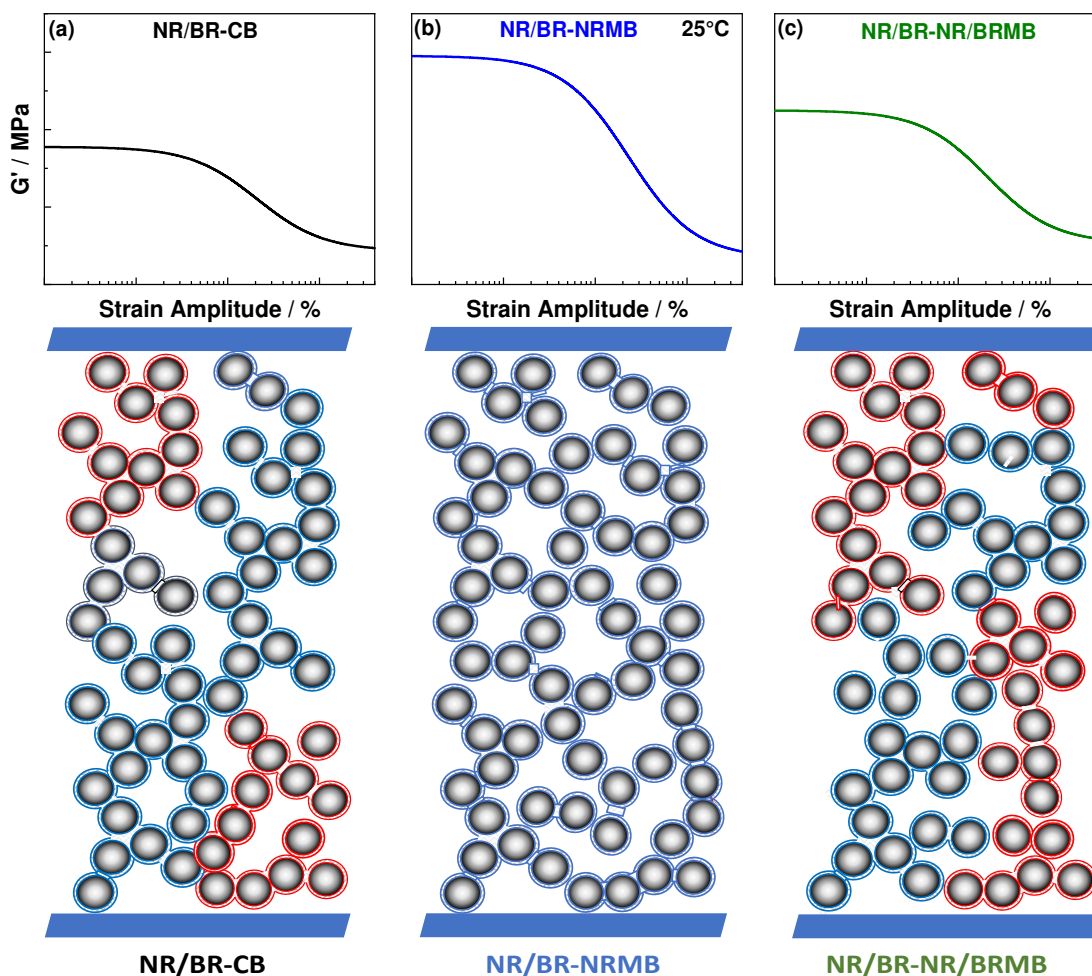


FIGURE 6.6

Scheme to describe NR/BR-CB prepared by different filler incorporation methods. The situation of conventionally mixed NR/BR-CB composites is compared with those where a NR-masterbatch or NR and BR masterbatches are used, respectively. (A detailed description about influence of filler network topology and chemical composition of glassy bridges is given in the main text).

that of the composite prepared by the conventional method. Together with chemical composition of the glassy bridge, the topology of the filler network could influence the mechanical properties significantly. Simplifying the situation, the schematic picture in figure 6.6 helps in understanding the experimental data for filler network contribution to reinforcement 5.12 and dissipation 5.14, respectively. Higher reinforcement and dissipative contributions are observed for NR/BR-NRMB composites (figure 6.6a) in comparison with NR/BR-NR/BRMB composites (figure 6.6b), that are prepared by both NRMB and BRMB in a ratio of 50 : 50, but is lowest for freshly mixed NR/BR-CB

(figure 6.6c) in which carbon-black particles are directly introduced during mixing. The proposed picture (figure 6.6) implies that nearly all intact glassy bridges (N_0) in NR/BR-NRMB composites are composed of immobilized NR. Since, in NR/BR-NRBRMB composites the chemical composition of the immobilized rubber fractions would be similar to the masterbatch ratio, i.e.,(NR:BR, 50:50). The reduced strength and volume for BR bridges are considered as potential reason for lower reinforcement and dissipation in case of NR/BR-NR/BRMB. The fact that NR/BR-CB composite, show a relatively lesser reinforcement and dissipation compared to composites prepared by masterbatch indicates (shown in scheme 6.6) that there are more glassy BR bridges in the filler network, due to affinity of the carbon black particles to the BR phase. This seems to be a bit surprising but is in accordance with literature results and preliminary results from own studies supporting a high affinity of carbon black to BR.[93, 165] Although a certain additional influence of the filler network topology may exist all major effects in the mechanical properties can be obviously explained by differences of the chemical composition of the glassy bridges in case of different filler incorporation methods.

6.3 Consequences for a rational design of tire tread compounds

From detailed and systematic studies on various types of rubber composites, the final conclusion is that the chemical composition and the number of glassy rubber bridges in the filler network influence the application relevant properties of viscoelastic filler network the most. This insight can be potentially used for a rational design of tire tread compounds. Applying the understanding achieved in this work could contribute to innovative solutions.

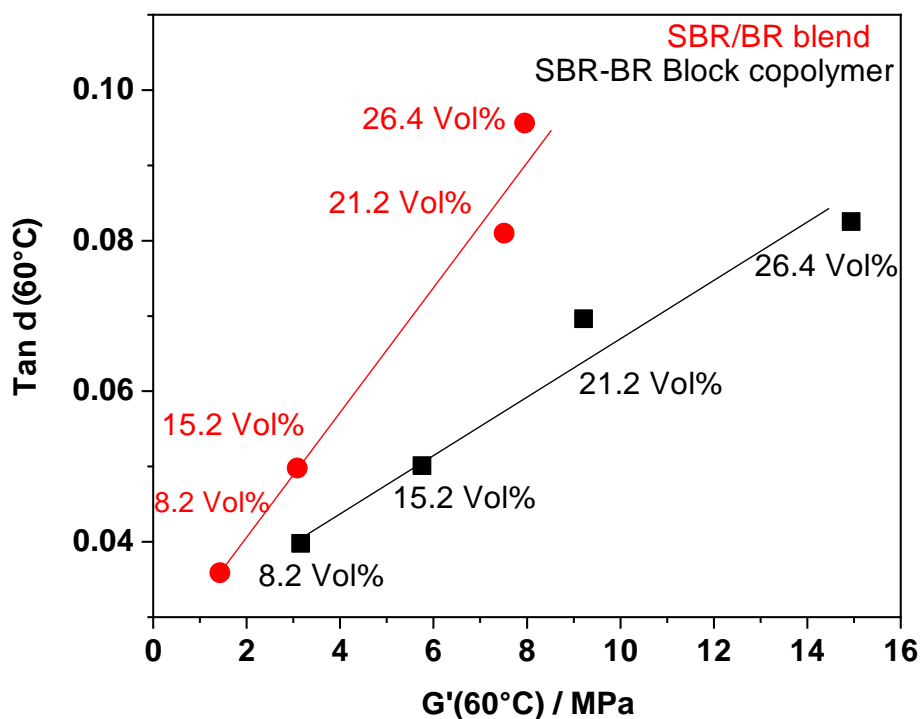


FIGURE 6.7

Rolling resistance indicator $\text{Tan } \delta$ at 60°C with reinforcement at the same temperature for SBR/BR blend composites (Square) and BR-SBR block copolymer (Circle) filled with silica. Adapted with permission from reference [160]. Copyright (2018) American Chemical Society

An interesting approach is to modify the topology of the filler network, i.e. by using the selectivity of fillers for a special phase in self-assembled rubbery block copolymers. BR-SBR block copolymers filled with silica particles are a

special example in this respect. Figure 6.7 shows clearly that $\text{Tan } \delta_0(60^\circ\text{C})$ and $G'_0(60^\circ\text{C})$ are also proportional for silica filled BR/SBR block copolymers as well as BR/SBR blends individually. The main difference compared to Silica-filled SBR/BR blends is that the rolling resistance indicator $\text{Tan } \delta_0(60^\circ\text{C})$ is comparatively lower in case of composites with block copolymer matrix for a given reinforcement (or hardness) often used as primary criterion for tire tread compound optimization. For application relevant G'_0 values of about 8 to 10 MPa, $\text{Tan } \delta_0(60^\circ\text{C})$ is reduced by about 25% compared to related blend based composites. Main difference between block copolymer and blend reference from the structural point of view is the filler network topology. Since the silica prefers the SBR phase, which is continuous in the investigated BR-SBR block copolymer with lamellar morphology, the percolation threshold related to the formation of a filler network can be achieved at lower filler loading. Note that the unfilled BR domains have nanoscopic dimensions and macrodispersion is not influenced. This is an advantage compared to blends, since larger unfilled/underfilled regions are avoided and fillers are selectively incorporated. Another important difference is for sure that the extremely high selectivity of the filler incorporation in the SBR phase in block copolymers resulting in a much higher percentage of glassy SBR bridges compared to related blends. The results shows that by tuning the filler network, comparable reinforcement property can be achieved at lower dissipation in the frequency-temperature range which is relevant for the optimization of rolling resistance of tires.

Alternative approach considered in this work is to use masterbatches. There are clear indications that the reinforcement in blend-based composites can be controlled by the filler incorporation method as seen in figure 6.6 i.e. that the reinforcement G'_0 varies for a given filler content. A main reason might be that the glassy rubber bridges are primarily composed of that rubber which

comes first in contact with the filler due to limited mobility of the once immobilized rubber layer. By using this concept the filler network strength can be influenced without changing the rubber matrix composition as well as filler content although the filler network topology might be influenced to a minor extent in parallel.

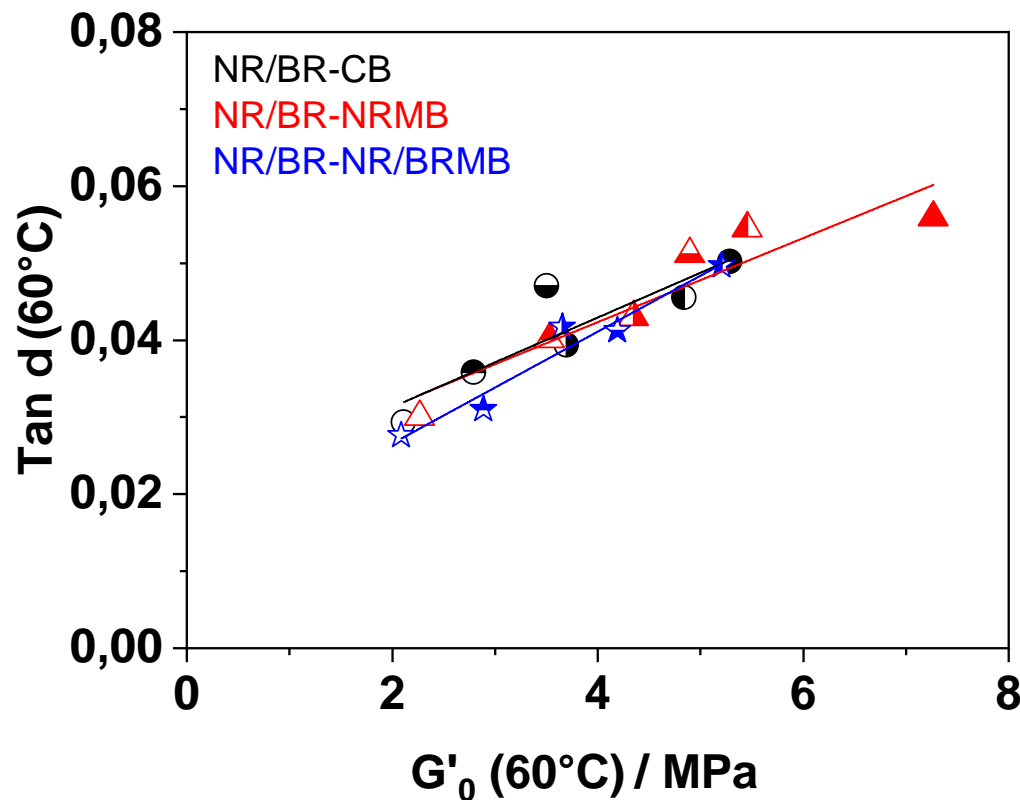


FIGURE 6.8

Rolling resistance indicator $Tan\delta_0$ ($60^\circ C$) Vs reinforcement G'_0 ($60^\circ C$) for NR/BR-CB prepared by different filler incorporation methods. Conventional method (Circles), through NR masterbatch (Triangles) and 50:50 ratio of NR and BR masterbatch (Stars) are compared. Different volume fractions of carbon black are incorporated in the plot: 15% (filled), 13.7% (left half filled), 12.5% (bottom half filled), 11.2% (right half filled), 10% (upper half filled), 7% (open).

Figure 6.8 shows that one can achieve higher reinforcement with lower filler content by using the masterbatch technique. However, it also shows that the ratio of rolling resistance indicator $Tan\delta_0$ ($60^\circ C$) to reinforcement is not influenced by the use of masterbatches indicating that reinforcement and dissipation are similarly influenced, if the glassy bridge composition varies in the

investigated NR/BR composites. This means, we can reduce the filler content to achieve certain G' value by using masterbatches. However, the $\text{Tan } \delta_0(60^\circ\text{C})$ dependence on G' is same for all NR/BR based composites. Requirement for improving the performance of tire tread compounds is reduced rolling resistance (indicator) for a given reinforcement level since the latter is always needed as precondition for rubber composites used in tire treads. Hence, the masterbatch concept can be used for a systematic variation of mechanical parameters of two-phasic rubber composites and a reduction of the filler content in tread compounds resulting in tires with lower weight but is not suitable to improve the performance of tire tread composites regarding rolling resistance directly.

An important message of this work, which can be used for tread compound optimization, is that tuning the chemical composition of the glassy rubber bridges and filler network topology determine to a large extent reinforcement and dissipation of rubber composites as commonly used in tires.

7 Conclusions

Central goal of this work was to quantify the filler network-related contributions to dissipation and reinforcement in highly filled rubber composites and to contribute to a better understanding of their molecular origin. Therefore, relevant mechanical properties of various rubber composites was investigated by dynamic mechanical analysis. The particular focus were strain amplitude-dependent measurements, which are highly sensitive to the filler network, are performed at different temperatures. The results for different series of rubber composites are compared in order to study the influence of (i) rubber matrix composition, (ii) filler incorporation method and (iii) rubber matrix morphology on dissipation and reinforcement.

The analysis of the strain sweep data for $G'(\gamma)$ shows that the Kraus equation is commonly approximating the experimental data well and able to quantify the filler network-related contributions to reinforcement. The strength of the filler network, represented by $\Delta G'$ confirms quite clearly that the filler network is viscoelastic in nature, due to the existence of glassy rubber bridges, which softens sequentially several 10 K above the bulk rubber glass transition temperature as earlier concluded from the reinforcement studies of SSBR filled with silica.

For identifying the filler network contributions to dissipation, the strain amplitude dependent loss modulus is evaluated using a specially modified Kraus equation incorporating the peak like contribution $\widetilde{G}''_{\gamma,F}$ proposed already by Kraus, but also an additional sigmoidally decreasing contribution $\widetilde{G}''_{\gamma,D}$ as

know from the strain amplitude dependent storage modulus $G'(\gamma)$. This approach is successfully applied to quantify different contributions to dissipation. Two of the three contributions to dissipation are dependent on filler loading and measurement temperature and are obviously related to the viscoelastic filler network. An interpretation is provided associating the identified dissipation contributions to different molecular mechanisms, i.e.

- $\widetilde{G''}_{\gamma,D}$: Dissipation due to oscillatory deformation of intact glassy rubber bridges in filler network dominating at small strain amplitudes.
- $\widetilde{G''}_{\gamma,F}$: Heat produced due to fracturing of glassy rubber bridges dominating at intermediate strain amplitudes.
- G''_{∞} : Contributions to dissipation, which are filler network independent remaining at very large strain amplitudes.

An increase in dissipation contributions, $\widetilde{G''}_{\gamma,D}$ and $\widetilde{G''}_{\gamma,F}$, with increasing filler fraction and decreasing temperature indicates that the number of glassy bridges / the volume of immobilized rubber in these bridges increases. Since the strength of the filler network $\Delta G'$ shows similar trends, the molecular origin for dissipation and reinforcement for all investigated rubber composites can be explained based on a common principle. The proposed physical picture has been successfully applied for various types of rubber composites that are quite different from each other underlining its general relevance.

In a further step the influence of (i) rubber matrix composition, (ii) filler incorporation method and (iii) rubber matrix morphology on filler network and its contributions to dissipation and reinforcement has been studied in more detail. In order to investigate changes caused by the rubber composition (i) NR/BR-CB and NR-CB composites that are prepared under identical conditions. Differences in reinforcement and dissipation, suggest that the filler network in the

biphasic system is different from that of single phase rubber composites. Potential reasons for the observed differences could be (1) filler network topology or (2) chemical composition of the glassy rubber bridges. A detailed analysis of TEM images of both the composites showed that the distribution of the unfilled areas is quite similar. Hence, it is hypothesized that the fraction of glassy BR bridges is causing a reduction in dissipation and reinforcement. A possibly explanation is that the T_g of bulk BR is evidently much lower than that of bulk NR.

Studies focusing on the influence of the filler incorporation method (ii) support the importance of the glassy rubber bridge chemical composition the if masterbatch technique is used for incorporating the filler particles in NR/BR-CB composite. The results show that filler network contributions to dissipation and reinforcement are higher for composites prepared by masterbatch techniques compared to conventionally mixed NR/BR-CB composites. Additional TEM images show that the microdispersion and unfilled area size distribution are not much affected by the filler incorporation method used. This indicates that the properties of the viscoelastic filler network are mainly changed by the composition of the glassy rubber bridges, which should be affected by the masterbatch concept since the rubber which come first in touch with the filler is immobilized and part of the resulting filler network. Following this idea the trends in NR/BR-CB composites prepared by different filler incorporation methods can be rationally explained by the changing number of BR bridges in the investigated composites. The effect of the filler network topology seems to be weak in this case.

In the final part of this work the influence of the rubber matrix morphology (iii) on dissipation and reinforcement is considered. It could be demonstrated that selective incorporation of silica particles in self-assembled BR-SBR block

copolymers with lamellar morphology leads to strong changes regarding dissipation and reinforcement as compared to BR/SBR blends with very similar composition and filler content. This can be interpreted as a combined effect caused by the guidance of the filler network by the rubber matrix morphology and a dominance of glassy SBR bridges. Both effects lead to higher reinforcement and dissipation compared to SBR/BR blends. Most interesting is, however, that the ratio of $Tan\delta$ ($60^{\circ}C$) and $G'(60^{\circ}C)$ is compared to related blends. This observation and the findings of this work regarding molecular origin of dissipation and reinforcement in general can be understood as contributions towards a rational design of the tire tread compounds. In this context it will be also interesting to see to what extent related composite design strategies can also help to match the rising demands for optimized tires showing lower rolling resistance with compromising and abrasion resistance being a requirement for a more ecological mobility in the future.

Bibliography

1. Goodyear, C. *US Patent 3633* (1844).
2. Benz, C. *German pat. DRP 37435* (1886).
3. Boyd dunlop, J. *US Patent US435995A* (1890).
4. Dünnebeil, F. & Keller, H. *GHG Mitigation Potential of European Rolling Resistance Labelling and Phase-out Scheme for Heavy Duty Truck Tyres* tech. rep. (Institute for Energy and Environmental Research Heidelberg, (2015)).
5. Dünnebeil, F. & Keller, H. *Monitoring Emission Savings from Low Rolling Resistance Tire Labelling and Phase out Schemes* tech. rep. (Institute for Energy and Environmental Research Heidelberg, (2015)).
6. *Low emission mobility with a focus on freight transport* (2016).
7. Parliament, E. On the Labelling of Tyres with Respect to Fuel Efficiency and other Essential Parameters. *Official Journal of the European Union* (2009).
8. Parliament, E. Setting Emission Performance Standards for New Passenger Cars as Part of the Communitys Integrated Approach to Reduce CO₂ Emissions from Light-duty Vehicles. *Official Journal of the European Union* (2009).
9. Payne, A. R. Dynamic Properties of Heat Treated Butyl Vulcanizates. *J App Polym Sci* **7**, 873–885 (1963).
10. Kraus, G. *Reinforcement of Elastomers* (Interscience Publishers, 1965).
11. Vilgis, T. A., Heinrich, G. & Klüppel, M. *Reinforcement of Polymer Nanocomposites* (Cambridge University Press, 2009).

12. Zhang, P., Morris, M. & Doshi, D. Materials Development for Lowering Rolling Resistance of Tires. *Rubber Chemistry and Technology* **89**, 79–116 (2016).
13. Heinrich, G. & Klüppel, M. Recent Advances in The Theory of Filler Networking in Elastomers. *Ad Polym Sci* **160**, 1–44 (2002).
14. Kohls, D. & Beaucage, G. Rational Design of Reinforced Rubber. *Current Opinion in Solid State and Materials Science* **6**, 183–194 (2002).
15. *Science and Technology of Rubber* (eds Mark, J. E., Ergan, B. & Eirich, F. R.) (Elsevier 3rd Edition, 2005).
16. Leblanc, J. L. *Filled polymers: Science and Industrial Applications* ISBN: 978-1-4398-0042-3 (Boca Raton: CRC Press, 2010).
17. Gerspacher, M. & O'Ferrell, C. P. Tire Compound Materials Interaction. *KGK Kautschuk Gummi Kunststoffe* **54**, 153–158 (2001).
18. Wang, M. J. Effect of Polymer-filler and Filler-filler Interactions on Dynamic Properties of Filled Vulcanizates. *Rubber Chemistry and Technology* **71**, 520–589 (1998).
19. Fröhlich, J., Niedermeier, W. & Luginsland, H.-D. The Effect of Filler–filler and Filler–elastomer Interaction on Rubber Reinforcement. *Composites Part A: Applied Science and Manufacturing* **36**, 449–460 (2005).
20. Ramier, J., Gauthier, C., Chazeau, L., Stelandre, L. & Guy, L. Payne Effect in Silica Filled Styrene-butadiene Rubber: Influence of Surface Treatment. *Journal of Polymer Science Part B: Polymer Physics* **45**, 286–298 (2007).
21. Valentin, J. L. *et al.* Novel Experimental Approach To Evaluate Filler–Elastomer Interactions. *Macromolecules* **43**, 334–346 (2010).
22. Heinrich, G. The Dynamics of Tire Tread Compounds and Their Relationship to Wet Skid Behavior. *Prog. Colloid Polym. Sci.* **90**, 16–26 (1992).
23. Herrmann, V. & Niedermeier, W. Interpretation of Filler Networking of Loaded Rubbers via Mastercurves. *KGK Kautschuk Gummi Kunststoffe* **63**, 559–564 (2010).

24. Heinrich, G. & Vilgis, T. Why Silica Technology Needs S-SBR in High Performance Tires? The Physics of Confined Polymers in Filled Rubbers. *KGK Kautschuk Gummi Kunststoffe* **61**, 368–376 (2008).
25. Mujtaba, A. *et al.* Mechanical Properties and Cross-link Density of Styrene Butadiene Model Composites Containing Fillers with Bimodal Particle Size Distribution. *Macromolecules* **45**, 6504–6515 (2012).
26. Mujtaba, A. *et al.* Detection of Surface-immobilized Components and Their Role in Viscoelastic Reinforcement of Rubber?Silica Nanocomposites. *ACS Macro Lett* **3**, 481–485 (2014).
27. Kumar, S. K., Benicewicz, B. C., Vaia, R. A. & Winey, K. I. 50th Anniversary Perspective: Are Polymer Nanocomposites Practical for Applications? *Macromolecules* **50**, 714–731 (2017).
28. Angell, C. Formation of Glasses from Liquids and Biopolymers. *Science* **267**, 1924–1935 (1995).
29. Donth, E. Characteristic Length of the Glass Transition. *J Polym Sci B: Polym Phys* **34**, 2881–2892 (1996).
30. Ngai, K. *Relaxation and Diffusion in Complex Systems* (Springer, Heidelberg, 2011).
31. McKenna, G. B. Glass dynamics - Diverging views on glass transition. *Nature Physics* **4**, 673–674 (2008).
32. Dutcher, J. & Ediger, M. Materials science - Glass surfaces not so glassy. *Science* **319**, 577–578 (2008).
33. Baeza, G. P. *et al.* Network Dynamics in Nanofilled Polymers. *Nature Communications* **7** (2016).
34. Long, D. & Lequeux, F. Heterogeneous Dynamics at the Glass Transition in van der Waals Liquids, in the Bulk and in Thin Films. *Euro Phys E* **4**, 371–387 (2001).
35. Klüppel, M. The Role of Disorder in Filler Reinforcement of Elastomers on Various Length Scales. *Adv Polym Sci* **164**, 1–86 (2003).

36. Klüppel, M. Evaluation of Viscoelastic Master Curves of Filled Elastomers and Applications to Fracture Mechanics. *Journal of Physics-Condensed Matter* **21** (2009).
37. Jouault, N. *et al.* Well-dispersed Fractal Aggregates as Filler in Polymer-silica Nanocomposites: Long-range Effects in Rheology. *Macromolecules* **42**, 2031–2040. ISSN: 0024-9297 (2009).
38. Lindemuth, B. E. *An Overview of Tire Technology in The pneumatic tire* (eds A.N, G. & J.D, W.) (U.S. Department of Transportation, National Highway Traffic Safety Administration, 2006), 475–532.
39. Grosch, K. A. The Rolling Resistance, Wear and Traction Properties of Tread Compounds. *Rubber Chemistry and Technology* **69**, 495–568 (1996).
40. Grosch, K. A. *Rubber Friction and Tire Traction in The pneumatic tire* (eds A.N, G. & J.D, W.) (U.S. Department of Transportation, National Highway Traffic Safety Administration, 2006), 1–27.
41. LaClair, T. J. *Rolling Resistance in The pneumatic tire* (eds A.N, G. & J.D, W.) (U.S. Department of Transportation, National Highway Traffic Safety Administration, 2006), 421–474.
42. Chandra, A. K. *Current topics in Elastomer Research* (ed Bhowmick, A. K.) (CRC Press, 2008).
43. *Rubber Technologist's Handbook* (ed J. R. White Sadhan Kumar De, K. N.) (Smithers Rapra Technology, 2009).
44. Persson, B. On the Theory of Rubber Friction. *Surface Science* **401**, 445–454 (1998).
45. Tolpekina, T. V. & Persson, B. Adhesion and Friction for Three Tire Tread Compounds. *Lubricants* **7**, 2075–4442 (2019).
46. Mujtaba, A. *Viscoelasticity of Filled Elastomers - Determination of Surface-immobilized Components and Their Role in the Reinforcement of SBR-silica Nanocomposites* PhD thesis (Martin-Luther-Universität Halle-Wittenberg, 2014).

47. Byers, J. T. Fillers for Balancing Passenger Tire Tread Properties. *Rubber Chemistry and Technology* **75**, 527–548 (2002).
48. Vleugels, N., Pille-Wolf, W., Dierkes, W. & Noordermeer, J. Understanding the influence of oligomeric resins on traction and rolling resistance of silica-reinforced tire treads. *Rubber Chemistry and Technology* **88**, 65–79 (Mar. 2015).
49. Araujo-Morera, J., Hernández Santana, M., Verdejo, R. & López-Manchado, M. A. Giving a Second Opportunity to Tire Waste: An Alternative Path for the Development of Sustainable Self-Healing Styrene–Butadiene Rubber Compounds Overcoming the Magic Triangle of Tires. *Polymers* **11** (2019).
50. Brüning, K. *In-situ Structure Characterization of Elastomers during Deformation and Fracture* PhD thesis (Technische Universität Dresden, 2014).
51. *Advances in Elastomers and Rubber Elasticity* (ed Mark, J. L. E.) (Springer, Boston, MA, 1986).
52. Schnecko, H. Polymer systems for tires. *Die Angewandte Makromolekulare Chemie* **202**, 87–102 (1992).
53. Aguiar da Silva, C. *Influence of Morphology on the Relaxation Behavior of Vulcanized PB-SBR Diblock Copolymers* PhD thesis (Martin-Luther-Universität Halle-Wittenberg, 2016).
54. Heinrich, G. & Dumler, H. B. WET Skid Properties of Filled Rubbers and The Rubber - Glass Transition. *Rubber Chemistry and Technology* **71**, 53–61 (1998).
55. Roland, C. M. *Immiscible Rubber Blends* in *Advances in Elastomers I* (Springer, Berlin, Heidelberg, 2013), 167–181.
56. Sakurai, S., Izumitani, T., Hasegawa, H., Hashimoto, T. & Han, C. C. Small-angle Neutron Scattering and Light Scattering Study on the Miscibility of Poly(styrene-ran-butadiene)/Polybutadiene Blends. *Macromolecules* **24**, 4844–4851 (1991).

57. Payne, A. R. The Dynamic Properties of Carbon-black Loaded Natural Rubber Vulcanizates. Part-1. *J App Polym Sci* **6**, Issue. **19**, 57–63 (1962).
58. Medalia, A. Effect of Carbon-black on Dynamic Properties of Rubber Vulcanizates. *Rubber Chemistry and Technology* **51**, 437–523 (1978).
59. Heinrich, G., Klüppel, M. & Vilgis, T. A. Reinforcement of Elastomers. *Curr Opin Solid State Mater Sci* **6**, 195–203 (2002).
60. Fritzsche, J. & Klüppel, M. Structural Dynamics and The Interfacial Properties of Filled Reinforced Elastomers. *J of Phys: Cond. Matter* **23** (2011).
61. Robertson, C. *et al.* Flocculation, Reinforcement, and Glass Transition Effects in Silica-Filled Styrene-butadiene Rubber. *Rubber Chemistry and Technology* **84**, 507–519 (2011).
62. Guy, L., Daudey, S., Cochet, P. & Bomal, Y. New Insights in the Dynamic Properties of Precipitated Silica Filled Rubber Using a New High Surface Silica. *KGK Kautschuk Gummi Kunststoffe* **62**, 383–391 (2009).
63. Guth, E. Theory of Filler Reinforcement. *J. App. Phys.* **16**, 20–25 (1944).
64. Niedermeier, W. & Schwaiger, B. Performance enhancement in rubber by modern filler systems. *KGK Kautschuk Gummi Kunststoffe* **60**, 184–187 (Apr. 2007).
65. Payne, A. R. & Watson, W. F. Carbon-black Structure in Rubber. *Rubber Chemistry and Technology* **36**, 147–155 (1963).
66. Robertson, C., Lin, C., Rackaitis, M. & Roland, C. Influence of Particle Size and Polymer Filler Coupling on Viscoelastic Glass Transition of Particle Reinforced Polymers. *Macromolecules* **41**, 2727–2731 (2008).
67. Donnet, J.-B. & Custodéro, E. *Carbon Black Surface Studied by Scanning Tunneling Microscopy in Carbon black* (ed Jean-Baptiste Donnet Roop Chand Bansal, M.-J. W.) (CRC Press, 1993), 221–228.
68. Schröder, A., Klüppel, M. & Schuster, R. H. Characterisation of Surface Activity of Carbon-black and its Relation to Polymer-filler Interaction. *Macromolecular Materials and Engineering* **292**, 885–916 (2007).

69. A. Schröder M. Klüppel, R. H. S. Energetic Surface Heterogeneity of Carbon-black. *KGK Kautschuk Gummi Kunststoffe* **5**, 260–266 (2001).
70. Hess, W. M. & Herd, C. R. *Microstructure, Morphology and General Physical Properties in Carbon black* (ed Jean-Baptiste Donnet Roop Chand Bansal, M.-J. W.) (CRC Press, 1993), 175–220.
71. Klüppel, M., Schuster, R. H. & Heinrich, G. Structure and Properties of Reinforcing Fractal Filler Networks in Elastomers. *Rubber Chemistry and Technology* **70**, 243–255 (1997).
72. Medalia, A. I. Morphology of Aggregates: I. Calculation of Shape and Bulkiness Factors; Application to Computer-simulated Random Flocs. *J Colloid Interface Sci* **24**, 393–404 (1967).
73. Medalia, A. I. Effective Degree of Immobilization of Rubber Occluded within Carbon-black Aggregates. *Rubber Chemistry and Technology* **45**, 1171 (1972).
74. Herd, C., McDonald, G. & Hess, W. M. Morphology of Carbon-black Aggregates : Fractal Versus Euclidean Geometry. *Rubber Chemistry and Technology* **65**, 107–129 (1992).
75. Herd, C., Smith, G. M. R. & Hess, W. M. The Use of Skeletonization for the Shape Classification of Carbon-black Aggregates. *Rubber Chemistry and Technology* **66**, 491–509 (1993).
76. Hewitt, N. in *Compounding Precipitated Silica in Elastomers* (ed Hewitt, N.) 1–23 (William Andrew Publishing, Norwich, NY, 2007). ISBN: 978-0-8155-1528-9.
77. Rauline, R. *European pat.* EP0501227A1 (1992).
78. Wang, M.-J. & Wolff, S. *Surface Energy of Carbon Black in Carbon black* (ed Jean-Baptiste Donnet Roop Chand Bansal, M.-J. W.) (CRC Press, 1993), 230–244.

79. Jiao Wang, M., Wolff, S. & Donnet, J. Filler Elastomer Interactions. Part III. Carbon-black Surface Energies and Interactions with Elastomer Analogs. *Rubber Chemistry and Technology* **64**, 714–736 (1991).
80. Papirer, E., Balard, H. & Vidal, A. Inverse Gas Chromatography: A Valuable Method for the Surface Characterization of Fillers for Polymers (glass fibres and silicas). *European Polymer Journal* **24**, 783–790 (1988).
81. Jiao Wang, M., Wolff, S. & Donnet, J. Filler Elastomer Interactions. Part I. Silica Surface Energies and Interactions with Model Compounds. *Rubber Chemistry and Technology* **64**, 559–576 (1991).
82. Bansal, R. C. & Donnet, J.-B. *Surface Groups on Carbon Blacks* in *Carbon black* (ed Jean-Baptiste Donnet Roop Chand Bansal, M.-J. W.) (CRC Press, 1993), 90–174.
83. Ephraim Feinblum Raissa Kosso, D. W. S. & Kohls, D. J. *Silica Fillers for Elastomer Reinforcement* in *Current Topics in ELASTOMERS RESEARCH* (ed Bhowmick, A. K.) (CRC Press, 2008), 14.
84. Jacques Noordermeer, W. D. *Rubber–Silica Mixing* in *Current Topics in ELASTOMERS RESEARCH* (CRC Press, 2008), 15.
85. Thiele, S. & Rulhoff, S. *US Patent* US8895684B2 (2014).
86. Robert, P. & Mathieu, S. *US Patent* US7649042B2 (2010).
87. Garance Lopitiaux Didier Vasseur, F. V. *US Patent* US20120259043A1 (2012).
88. Georges Marcel Victor Thielen, F. S. *US Patent* US7671128B1 (2010).
89. Schuster, R. in *Mixing of Rubber Compounds* (ed Limper, A.) 173–236 (Hanser, 2012).
90. Tauban, M. *Impact of Filler Morphology and Distribution on the Mechanical Properties of Filled Elastomers : theory and simulations* PhD thesis (The Université de Lyon, 2016).
91. Limper, A. in *Mixing of Rubber Compounds* (ed Limper, A.) 47–69 (Hanser, 2012).

92. Klockmann, O. in *Mixing of Rubber Compounds* (ed Limper, A.) 95 –105 (Hanser, 2012).
93. Callan, J., Hess, W. M. & Scott, C. Elastomer Blends. Compatibility and Relative Response to Fillers. *Rubber Chemistry and Technology* **44**, 814–837 (1971).
94. Dong, A. *et al.* Effect of Carbon-black Nature on Dynamic Mechanical Properties and Reinforcement of NR Vulcanization by Latex Techniques. *Rubber Chemistry and Technology* **90** (Jan. 2017).
95. Wunde, M. & Klüppel, M. Influence of Phase morphology and Filler Distribution in NR/BR and NR/SBR Blends on Fracture Mechanical Properties. *Rubber Chemistry and Technology* **89**, 588–607 (2016).
96. Berkemeier, D. in *Mixing of Rubber Compounds* (ed Limper, A.) 1 –46 (Hanser, 2012).
97. Keuter, H. & Ryzko, P. in *Mixing of Rubber Compounds* (ed Limper, A.) 107 –171 (Hanser, 2012).
98. Wang, M.-J., Lu, S. X. & Mahmud, K. Carbon-silica Dual Phase Filler. *J Polym Sci B: Polym Phys* **38**, 1240–1249 (2000).
99. Klüppel, M. & Heinrich, G. Physics and Engineering of Reinforced Elastomers: From Mechanical Mechanisms to Industrial Applications. *KGK Kautschuk Gummi Kunststoffe* **58**, 217–224 (2005).
100. Smallwood, H. M. Limiting Law of the Reinforcement of Rubber. *J App Phys* **15**, 758–766 (1944).
101. Einstein, A. Eine neue Bestimmung der Molekül dimension. *Ann. Physics*, 289–306 (1906).
102. Guth, E. & Gold, O. On the Hydrodynamical Theory of the Viscosity of Suspensions. *Phys. Rev.* **53**, 322 (1938).
103. Vilgis, T. & Heinrich, G. Disorder-induced enhancement of polymer adsorption- A model for the rubber-polymer interaction in filled rubbers. *Macromolecules* **27**, 7846–7854 (1994).

104. Thomas, D. G. Transport characteristics of suspension: A note on the viscosity of Newtonian suspensions of uniform spherical particles. *J Colloid Sci* **20**, 267–277 (1965).
105. Hinkelmann, B. The analytical description of the filler influence on the flow behaviour of the polymer melt. *Rheol Acta* **21**, 491 (1982).
106. Wolff, S. & Donnet, J.-B. Characterization of fillers in vulcanizates according to the Einstein-Guth-Gold equation. *Rubber Chemistry and Technology* **63**, 32–45 (1990).
107. Karasek, L., Meissner, B., Asai, S. & Sumita, M. Percolation Concept: Polymer-filler Gel Formation, Electrical Conductivity and Dynamic Mechanical Properties of Carbon-black Filled Rubbers. *Polymer* **28**, 121–126 (1995).
108. Kraus, G. Mechanical Losses Carbon-black Filled Rubbers. *App. Polym. Sci.: App. Polym. Symp.* **39**, 75–92 (1984).
109. Ulmer, J. D. Strain Dependence of Dynamic Mechanical Properties of Carbon-black Filled Rubber Compounds. *Rubber Chemistry and Technology* **69**, 15–47 (1996).
110. Ulmer, J., Hergenrother, W. & Lawson, D. F. Hysteresis Contributions in Carbon-black Filled Rubbers Containing Conventional and Tin End-modified Polymers. *Rubber Chemistry and Technology* **71**, 637–667 (1998).
111. Clement, F., Bokobza, L. & Monnerie, L. Investigation of the Payne Effect and its Temperature Dependence on Silica-Filled PDMS Networks. Part I: Experimental Results. *Rubber Chemistry and Technology* **78**, 211–231 (2005).
112. Clement, F., Bokobza, L. & Monnerie, L. Investigation of the Payne Effect and its Temperature Dependence on Silica-Filled PDMS Networks. Part II: Test of Quantitative Models. *Rubber Chemistry and Technology* **78**, 232–244 (2005).

113. Huber, G., Vilgis, T. A. & Heinrich, G. Universal Properties in the Dynamical Deformation of Filled Rubbers. *Journal of Physics: Condensed Matter* **8**, L409–L412 (1996).
114. Heinrich, M. K. G. Fractal Structures in Carbon-black Reinforced Rubbers. *Rubber Chemistry and Technology* **68**, 623–651 (1995).
115. Le Gal, A., Yang, X. & Klüppel, M. Evaluation of Sliding Friction and Contact Mechanics of Elastomers Based on Dynamic-mechanical Analysis. *The Journal of Chemical Physics* **123**, 014704 (2005).
116. Vieweg, S., Unger, R., Hempel, E. & Donth, E. Kinetic Structure of Glass Transition in Polymer Interfaces Between Filler and SBR Matrix. *J.non-cryst.solids* **235-237**, 470–475 (1998).
117. Vieweg, S., Unger, R., Schröter, K. & Donth, E. Frequency and Temperature Dependent of the Small-strain Behaviour of Carbon-black Filled Vulcanizates. *Polym Net Blends* **5**, 199–204 (1995).
118. Robertson, C. G., Bogoslovov, R. & Roland, C. M. Structural Arrest and Thermodynamic Scaling in Filler-Reinforced Polymers. *Rubber Chemistry and Technology* **82**, 202–213 (2009).
119. Richter, S., Kreyenschulte, H., Saphiannikova, M., Götze, T. & Heinrich, G. Studies of the So-called Jamming Phenomenon in Filled Rubbers Using Dynamical-Mechanical Experiments. *Macromolecular Symposia* **306-307**, 141–149 (2011).
120. Tunnicliffe, L. *et al.* Flocculation and Viscoelastic Behaviour in Carbon Black-Filled Natural Rubber. *Macromolecular Materials and Engineering* **299** (Dec. 2014).
121. Tunnicliffe, L., Thomas, A. & Busfield, J. Effects of Surface Deactivation of Carbon Black on Thermomechanical Sensitivity of Filler Networks in Rubber Compounds. *Macromolecular Materials and Engineering* **301** (June 2016).

122. Wolff, S. & Wang, M. J. Filler Elastomer Interactions. Part 4. The Effect of the Surface Energies of Fillers on Elastomer Reinforcement. *Rubber Chemistry and Technology* **65**, 329–342 (1992).
123. Warasitthinon, N., Genix, A.-C., Sztucki, M., Oberdisse, J. & Robertson, C. The Payne Effect: Primarily Polymer-Related or Filler-Related Phenomenon? *Rubber Chemistry and Technology* **92**, 599–611 (2019).
124. Song, Y. & Zheng, Q. Concepts and conflicts in nanoparticles reinforcement to polymers beyond hydrodynamics. *Progress in Materials Science* **84**, 1–58 (2016).
125. Sternstein, S. S. & Zhu, A.-J. Reinforcement Mechanism of Nanofilled Polymer Melts As Elucidated by Nonlinear Viscoelastic Behavior. *Macromolecules* **35**, 7262–7273 (2002).
126. Chazeau, L., Brown, J. D., Yanyo, L. C. & Sternstein, S. S. Modulus Recovery Kinetics and Other Insights into the Payne Effect for Filled Elastomers. *Polymer Composites* **21**, 202–222 (2000).
127. Maier, P. G. & Göritz, D. Molecular Interpretation of the Payne Effect. *KGK Kautschuk Gummi Kunststoffe* **49**, 18–21 (1996).
128. Fukahori, Y. New Progress in the Theory and Model of Carbon-black Reinforcement of Elastomers. *J App Polym Sci* **95**, 60–67 (2005).
129. Ouyang, G. Network Junction Model for Carbon-black Reinforcement. *KGK Kautschuk Gummi Kunststoffe* **59**, 454–458 (Sept. 2006).
130. Dannenberg, E. M. The Effects of Surface Chemical Interactions on the Properties of Filler Reinforced Rubbers. *Rubber Chemistry and Technology* **48**, 410–444 (1975).
131. Mostafa, A., Abouel-Kasem, A., Bayoumi, M. & El-Sebaie, M. Rubber-filler Interactions and Its Effect in Rheological and Mechanical Properties of Filled Compounds. *Journal of Testing and Evaluation* **38** (ed M. R. Mitchell, R. E. L.) 347–359 (2010).

132. Litvinov, V. M. & Steeman, P. A. M. EPDM-Carbon-black Interactions and The Reinforcement Mechanisms, as Studied by Low-resolution ^1H NMR. *Macromolecules* **32**, 8476–8490 (1999).
133. Dannenberg, E. M. Bound Rubber and Carbon-black Reinforcement. *Rubber Chemistry and Technology* **59**, 512–524 (1986).
134. Tunncliffe, L., Thomas, A. & Busfield, J. Energy losses at small strains in filled rubbers. *Constitutive Models for Rubber VII - Proceedings of the 7th European Conference on Constitutive Models for Rubber, ECCMR*, 63–67 (Jan. 2012).
135. Litvinov, V. M., Orza, R. A., Klüppel, M., van Duin, M. & Magusin, P. C. M. M. Rubber - Filler Interactions and Network Structure in Relation to Stress Strain Behavior of Vulcanized, Carbon Black Filled EPDM. *Macromolecules* **44**, 4887–4900 (2011).
136. Hess, W. M. Characterization of Dispersions. English. *Rubber chemistry and technology* (1991).
137. Le, H. H., Ilisch, S, Prodanova, I & Radusch, H. Online electrical conductivity as a measure to characterize the rheological and thermodynamic effects on the carbon black dispersion in rubber compounds. *KGK Kautschuk Gummi Kunststoffe* **57**, 388–395 (July 2004).
138. Papon, A. *et al.* Solid Particles in an Elastomer Matrix: Impact of Colloid Dispersion and Polymer Mobility Modification on the Mechanical Properties. *Soft Matter* **8**, 4090–4096 (2012).
139. Baeza, G. P., Genix, A. C. & Oberdisse, J. Multiscale filler structure in simplified industrial nanocomposite silica/SBR systems studies by SAXS and TEM. *Macromolecules* **46**, 317–329 (2012).
140. L. Conzatti G. Costa, L. F. & Turturro, A. *Microscopic Imaging of Rubber Compounds* in *Rubber Technologist's Handbook* (ed J. R. White Sadhan Kumar De, K. N.) **2** (Smithers Rapra Technology, 2009), 1–29.

141. Huang, M., Tunnicliffe, L., Thomas, A. & Busfield, J. The glass transition, segmental relaxations and viscoelastic behaviour of particulate-reinforced natural rubber. *European Polymer Journal* **67** (June 2015).
142. Baeza, G. P. *et al.* Effect of Grafting on Rheology and Structure of a Simplified Industrial Nanocomposite Silica/SBR. *Macromolecules* **46**, 6621–6633 (2013).
143. Musino, D. *et al.* Synergistic Effect of Small Molecules on Large-Scale Structure of Simplified Industrial Nanocomposites. *Macromolecules* **50**, 5138–5145 (2017).
144. Ramier, J., Chazeau, L., Gauthier, C., Guy, L. & Bouchereau, M. N. Influence of Silica and its Different Surface Treatments on The Vulcanization Process of Silica Filled SBR. English. *RUBBER CHEMISTRY AND TECHNOLOGY* **80**, 183–193. ISSN: 0035-9475 (2007).
145. Ten Brinke, J. W., Litvinov, V. M., Wijnhoven, J. E. G. J. & Noordermeer, J. W. M. Interactions of Stöber Silica with Natural Rubber under the Influence of Coupling Agents, Studied by ¹H NMR T2 Relaxation Analysis. *Macromolecules* **35**, 10026–10037 (2002).
146. Vieweg, S. *Einfluss von Polymeren Füllstoffen auf den Glasübergang und die Gummiplateauzone von SBR 1500 Vulkanisaten* PhD thesis (Martin Luther Universität Halle Wittenberg, 1997).
147. Fragiadakis, D., Bokobza, L. & Pissis, P. Dynamics near the filler surface in natural rubber-silica nanocomposites. *Polymer* **52**, 3175–3182 (2011).
148. Klonos, P. A. *et al.* Glass Transition and Molecular Dynamics in Core-Shell-Type Nanocomposites Based on Fumed Silica and Polysiloxanes: Comparison between Poly(dimethylsiloxane) and Poly(ethylhydrosiloxane). English. *The Journal of Physical Chemistry C* **123**, 28427–28436 (2019).

149. Merabia, S., Sotta, P. & Long, D. R. A Microscopic Model for the Reinforcement and the Nonlinear Behavior of Filled Elastomers and Thermoplastic Elastomers (Payne and Mullins Effects). *Macromolecules* **41**, 8252–8266 (2008).
150. Berriot, J., Montes, H., Lequeux, F., Long, D. & Sotta, P. Evidence for the Shift of the Glass Transition near the Particles in Silica-filled Elastomers. *Macromolecules* **35**, 9756–9762 (2002).
151. Berriot, J., Montes, H., Lequeux, F., Long, D. & Sotta, P. Gradient of Glass Transition Temperature in Filled Elastomers. *Europhys Lett* **64**, 50–56 (2003).
152. Gusev, A. A. Micromechanical mechanism of reinforcement and losses in filled rubbers. *Macromolecules* **39**, 5960–5962 (2006).
153. Zhu, A.-j. & Sternstein, S. S. Nanofiller-Polymer Interactions At and Above the Glass Transition Temperature. *MRS Proceedings* **661**, KK4.3 (2000).
154. Robertson, C. & Roland, C. Glass Transition and Interfacial Segmental Dynamics in Polymer-particle Composites. *Rubber Chemistry and Technology* **81**, 506–522 (2008).
155. Jouault, N. *et al.* Bound polymer layer in nanocomposites. *Macro Lett* **2**, 371–374 (2013).
156. Jimenez, A. M., Zhao, D., Misquitta, K., Jestin, J. & Kumar, S. K. Exchange Lifetimes of the Bound Polymer Layer on Silica Nanoparticles. *ACS Macro Letters* **8**, 166–171 (2019).
157. Popov, I. *et al.* Strong Reduction in Amplitude of the Interfacial Segmental Dynamics in Polymer Nanocomposites. *Macromolecules* **53**, 4126–4135 (2020).
158. Cheng, S. *et al.* Focus: Structure and Dynamics of the Interfacial Layer in Polymer Nanocomposites with Attractive Interactions. *The Journal of Chemical Physics* **146**, 203201 (2017).

159. Nagaraja, S. M., Mujtaba, A. & Beiner, M. Quantification of different contributions to dissipation in elastomer nanoparticle composites. *Polymer* **111**, 48–52 (2017).
160. Aguiar da Silva, C., Nagaraja, S. M., Weydert, M. & Beiner, M. Diblock-Copolymer-Based Composites for Tire-Tread Applications with Improved Filler Network Topology. *ACS Applied Nano Materials* **1**, 1003–1008 (2018).
161. Stauch, C. *et al.* Silanization of Silica Nanoparticles and Their Processing as Nanostructured Micro-Raspberry Powders - A Route to Control the Mechanical Properties of Isoprene Rubber Composites. *Polymer Composites* **40**, E732–E743 (2019).
162. Bernal-Ortega, P. *et al.* New insight into structure-property relationships of natural rubber and styrene-butadiene rubber nanocomposites filled with MWCNT. *Polymer* **201**, 122604 (2020).
163. Rubinstein, M. & Colby, R. H. *Polymer Physics* (Oxford University Press, Oxford, 2003).
164. Hess, W. M., Vegvari, P. C. & Swor, R. A. Carbon Black in NR/BR Blends for Truck Tires. *Rubber Chemistry and Technology* **58**, 350–382 (1985).
165. Klüppel, M., Schuster, R. H. & Schaper, J. Carbon black distribution in rubber blends: A dynamic-mechanical analysis. *Rubber Chemistry and Technology* **72**, 91–108. (1999).

8 Appendix

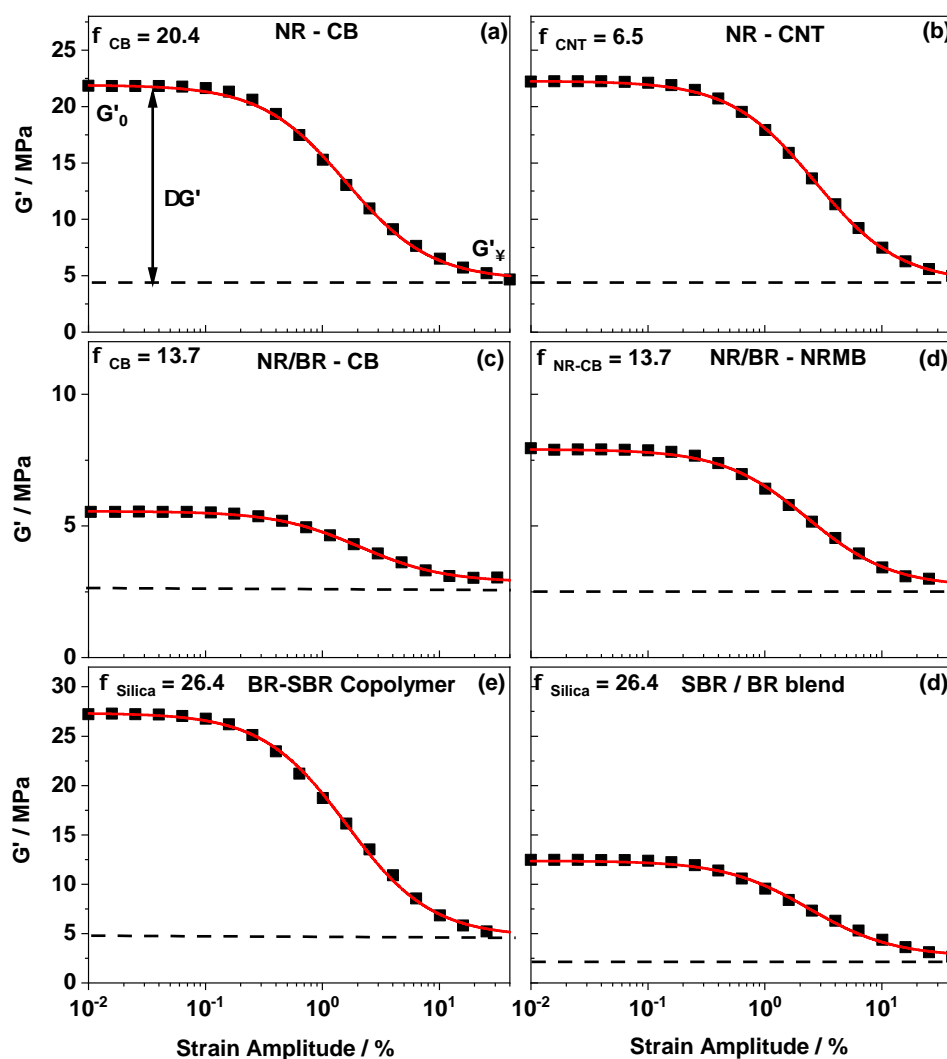


FIGURE 8.1

Strain amplitude dependent dynamic shear loss modulus $G'(\gamma)$ measured at ($T=25^\circ\text{C}$ and $\omega=10\text{ rads}^{-1}$) for (a) NR containing 20.4 Vol% of CB and (b) NR with 6.5 vol% CNT (c) NR/BR blend filled with 13.7 Vol% CB, (d) NB/BR blend with 13.7 Vol% CB introduced via master batch, (e) a BR-SBR block copolymer filled with 26.4 vol% silica as well as (f) a SBR-BR blend containing 26.4 vol% silica. Further details about these samples are discussed later in this section. The data fitting of $G'(\gamma)$ by equation 5.1 according to the Kraus model, are represented in red line.

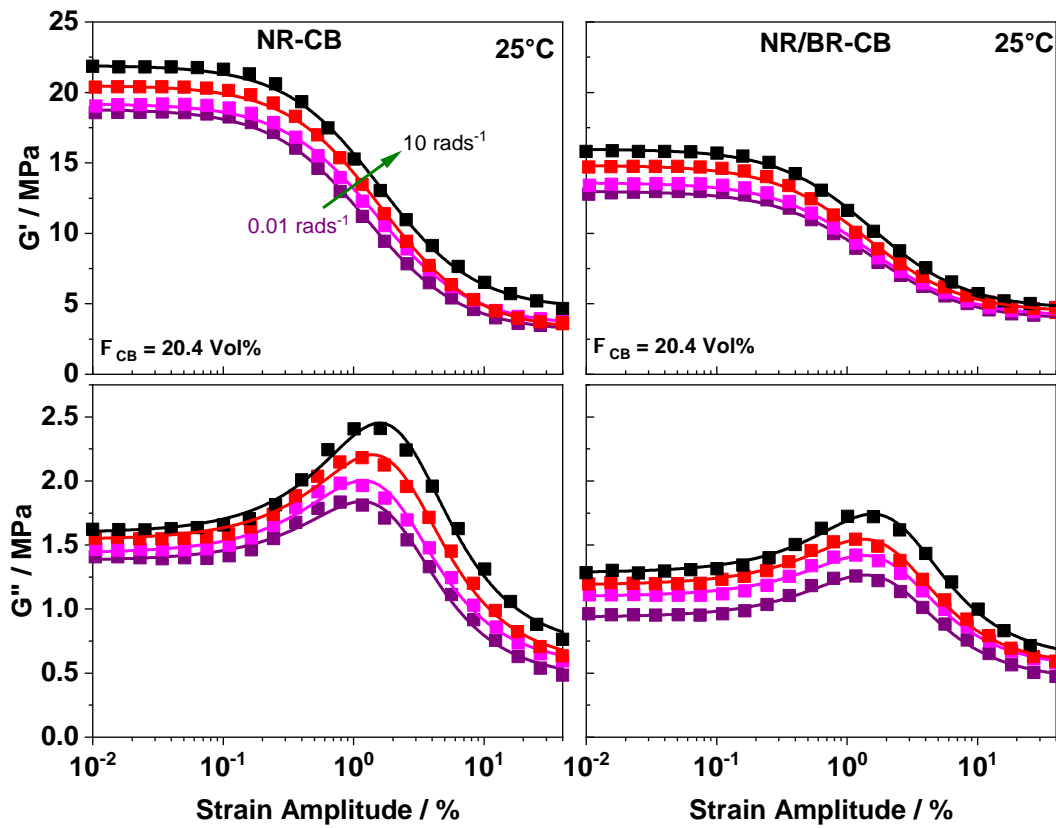


FIGURE 8.2

Strain amplitude dependent (Top) storage modulus $G'(\gamma)$ and (bottom) loss modulus $G''(\gamma)$ measured at 25°C and four different angular frequency (0.01, 1, 10 and 100 rads^{-1}) for (left) NR-CB and (right) NR/BR-CB containing 20.4 vol% of carbon black (Φ_{CB}). The data points are approximated by Kraus equation 5.1 for $G'(\gamma)$ and $G''(\gamma)$ are approximated by equation 5.1 and 5.3, respectively.

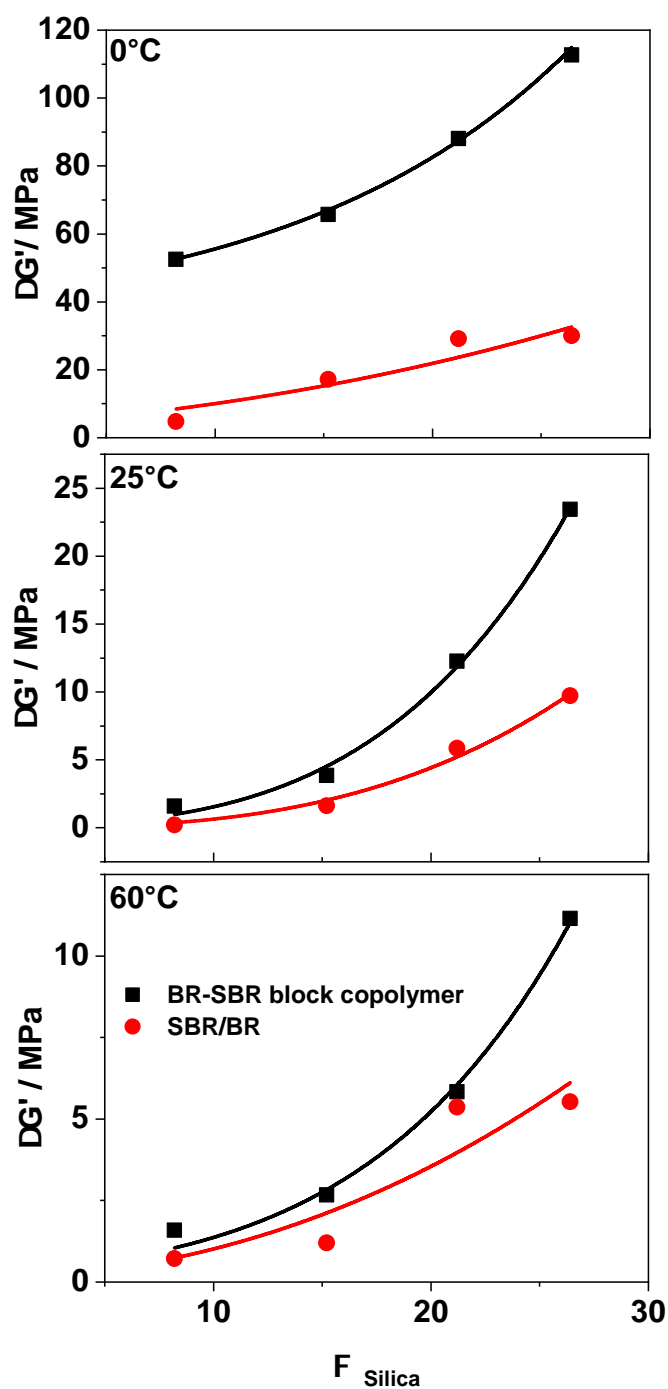


FIGURE 8.3

Strength of filler network $\Delta G' = G'_0 - G'_\infty$ from equation 5.1 with respect to silica loading Φ_{Silica} compared between SBR/BR composite (circle) and BR-SBR block copolymer (square) at three different temperatures 0°C, 25°C and 60 °C.

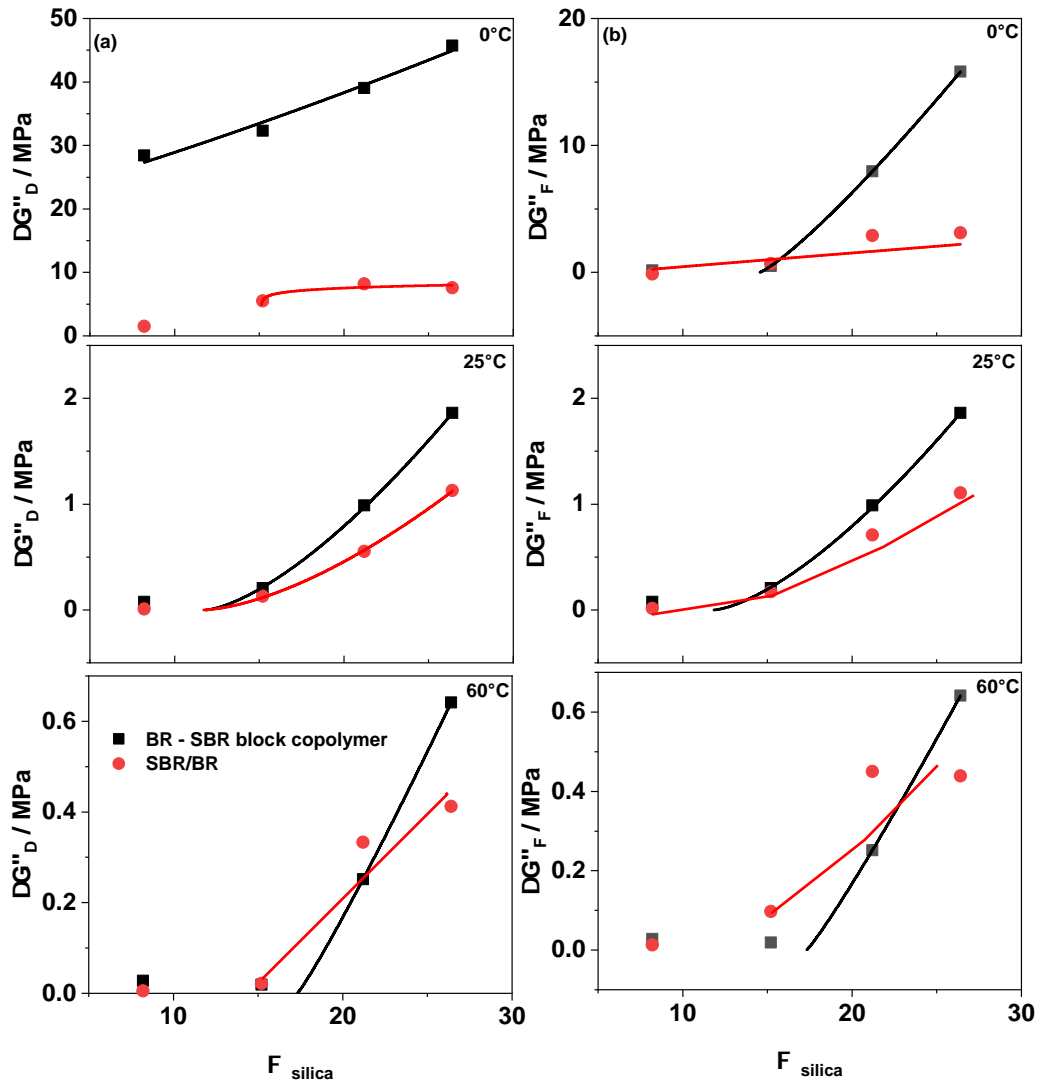


FIGURE 8.4

(a) $\Delta G''_F$, (b) $\Delta G''_D$ are modified Kraus fitting parameters from equation 5.3 with respect to silica loading Φ_{silica} for BR-SBR block copolymer and SBR/BR composites at three different temperatures 0°C, 25°C and 60 °C.

Acknowledgements

I wish to extend my gratitude to my supervisor Prof. Mario Beiner for his constant support, encouragement, and motivation throughout the course of my doctoral research. His positivity and enthusiasm always helped me. I sincerely thank him for investing his time in me and our discussions which sometimes extended well into the late evening hours. I am also thankful to him for providing several opportunities to attend different conferences. I appreciate Dr. Anas Mujtaba for his support with the DMA instrument, as well as discussions at the initial stages which helped me get acquainted to the thesis topic. I am also grateful to Dr. Sven Henning for their support with TEM images. In the end, I thank all my colleagues at Fraunhofer IMWS and friends in Halle for their help and make my stay here memorable. I enjoyed working with all the former and present members of my team. I am grateful for the financial support from Fraunhofer IMWS, its partners, and Martin Luther Universität-Halle Wittenberg.

Eidesstattliche Erklärung

Hiermit versichere ich, Sriharish Malebennur Nagaraja die vorliegende Arbeit selbständig und ohne fremde Hilfe verfasst und keine anderen als die von mir angegebenen Quellen und Hilfsmittel verwendet zu haben. Die den benutzten Werken wörtlich oder inhaltlich entnommenen Stellen habe ich als solche kenntlich gemacht.

Ich erkläre, keine anderweitigen Promotionsversuche unternommen und die vorliegende Dissertation weder in der jetzigen noch in einer anderen Fassung einer anderen wissenschaftlichen Einrichtung vorgelegt zu haben.

Signed:

sriharish m.n

Place, Date: 20.12.2021

Curriculum Vitae

Personal Information

First Name: Sriharish
Last Name: Malebennur Nagaraja
Date of Birth: 6 Sep 1985
Place of Birth: Harihar
Nationality: Indian

Education

Oct 2015 - present: Doctoral studies
Martin Luther University Halle-Wittenberg
Fraunhofer Institute for Microstructure of
Materials and Systems IMWS
Supervisor: Prof. Dr. Mario Beiner

Oct. 2012 - Feb 2015:- Master of Science in Polymer Material Science
Martin Luther University Halle-Wittenberg
Thesis: Influence of Filler-network Topology and Immobilized Rubber
on Reinforcement In Natural Rubber Composites
Containing Different Nanoparticles

Dec.2008 - Dec 2009 Post graduate diploma in Rubber technology
Joint program by Indian Rubber Institute-Karnataka
and Indian Institute of Technology – Kharagpur, India.

July 2005 - July 2009:- Bachelor of Polymer Science and Technology
Sri Jayachamarajendra College of Engineering, India
Thesis: Preparation and characterization of rubber filled with
thermoset industrial scrap

Halle (Saale), March 2021

List of Publications

- S.M. Nagaraja, A.Mujtaba, M.Beiner, Quantification of Different Contributions to Dissipation in Elastomer Nanoparticle Composites, *Polymer*, 111(2017) 48-52.
- C. Aguiar da Silva, S. M. Nagaraja, M. Weydert, and M. Beiner, Diblock-Copolymer-Based Composites for Tire-Tread Applications with Improved Filler Network Topology, *ACS Applied Nano Materials*, 1(2018),1003-1008.
- C. Stauch, T. Ballweg, K.H Haas, R. Jaeger, S. Stiller, A. Shmeliov, V. Nicolosi, S.M. Nagaraja, J. Wötzel, M. Beiner, R. Luxenhofer, K. Mandel, Silanization of Silica Nanoparticles and their Processing as Nanostructured Micro-raspberry powders - a Route to Control the Mechanical Properties of Isoprene Rubber Composites, *Polymer Composites*, 40(2019) E732-E743.
- S.M Nagaraja, S.Henning, S.Ilsch and M.Beiner, Common Origin of Filler Network Contributions to Reinforcement and Dissipation in Rubber Composites, *Polymers*, 13(2021), 2534.